UNIMORE
UNIVERSITÀ DEGLI STUDI DI MODENA E REGGIO EMILIA

UNIVERSITÀ DEGLI STUDI DI MODENA E REGGIO EMILIA

Dottorato di ricerca in
"Molecular and regenerative Medicine"

Ciclo XXXVIII

CHROMOSOME 9p DUPLICATION ENHANCES HEMATOPOIETIC STEM CELLS' CLONOGENIC POTENTIAL AND PROMOTES IMMUNE ESCAPE IN JAK2-MUTANT MYELOPROLIFERATIVE NEOPLASMS

Candidato **MATTEO BERTESI**

Relatore (Tutor): Prof. **ROSSELLA MANFREDINI**

Correlatore (Co-Tutor): Dr. **SEBASTIANO RONTAUROLI**

Coordinatore del Corso di Dottorato: Prof. **MICHELE DE LUCA**

INDEX

ABSTRACT

JAK2V617F is the most common mutation involved in Philadelphia-negative Myeloproliferative Neoplasms (MPN), which are characterized by clonal proliferation of mature cells sustained by JAK/STAT pathway hyperactivation. Each patient clonality is additionally shaped by co-occurring mutations and Copy Number Variations (CNV).

Since *JAK2* gene is located on chromosome 9 short arm (9p), and JAK2V617F Variant Allele Frequency has a major impact on disease severity, any copy number alteration involving its locus can be of clinical significance for disease evolution.

This study identified a subgroup of MPN patients with partial or complete chromosome 9 short arm trisomy (+9p) and outlined the biological features of MPN pathology in this setting. The analysed cohort includes JAK2-heterozygous patients (n=10), JAK2-homozygous patients (n=10) and patients carrying the duplication of chromosome 9p alongside *JAK2* driver mutation (n=12).

To investigate the genetic profile of +9p patients, we employed single $CD34^+$ cell-derived colonies cultured in semisolid medium to record *JAK2* copy number and mutational status through ddPCR. Our findings revealed that most colonies exhibited three copies of *JAK2*, with 2 out of 3 alleles harboring JAK2V617F. Moreover, by analyzing the relative abundance of each combination of ploidy-genotype, our data identified the chronological order of molecular events being JAK2V617F mutation happening first, followed by the duplication of chromosome 9p carrying *JAK2* mutation.

Moving on from genomic to functional analysis, both methylcellulose and collagen clonogenic assays revealed a higher colony formation capacity and a more primitive phenotype of +9p patients' $CD34^+$ cells.

Remarkably, located downstream of *JAK2* on 9p is *CD274* gene, coding for the immune checkpoint mediator PD-L1, which was found upregulated in different myeloid cells from +9p patients.

Starting from published evidence that PD-L1 can promote the expression of the pluripotency factors OCT4 and NANOG in breast cancer through AKT activity, we confirmed the upregulation of both transcription factors in +9p patients, outlining an analogous mechanism of multipotency sustainment in these patients.

To validate the higher dependency on AKT signalling of +9p triploid stem and progenitor cells, we tested MK2206 drug, a specific AKT inhibitor, reporting a decreased colony count of +9p patients-derived cells after treatment. The same results were obtained through

simultaneous silencing of OCT4 and NANOG expression by means of siRNA nucleofection of $CD34^+$ cells from homozygous and +9p patients.

Specifically, the correlation between +9p and *CD274*, OCT4 and NANOG deregulation was proved by a new approach of coupled genomic-transcriptomic characterization of $CD34^+$ derived colonies, highlighting how OCT4 and NANOG, induced by PD-L1 expression, mediate clonogenic signal transduction via AKT in $CD34^+$ cells with two out of three mutated *JAK2* alleles.

Furthermore, flow cytometry analysis revealed in +9p group a higher frequency of $PD\text{-}L1^+$ monocytes, which also showed a strong membrane exposure of PD-L1 by in situ immunofluorescence analysis.

Finally, alongside $PD\text{-}L1^+$ monocytes, flow cytometry showed that +9p patients display also a significantly higher frequency of exhausted cytotoxic T cells compared to other patients' groups.

Altogether, these results suggest that JAK2-mutated patients with a duplication of chromosome 9 short arm represent a distinct class of MPN patients, characterized by a deregulated interplay between *JAK2* and PD-L1/PD-1 pathway, which contributes to both multipotency of $CD34^+$ stem and progenitor cells and immune escape of the malignant myeloid clone.

Keywords:

1. MPN
2. Chromosome 9
3. JAK2
4. PD-L1
5. Immune escape

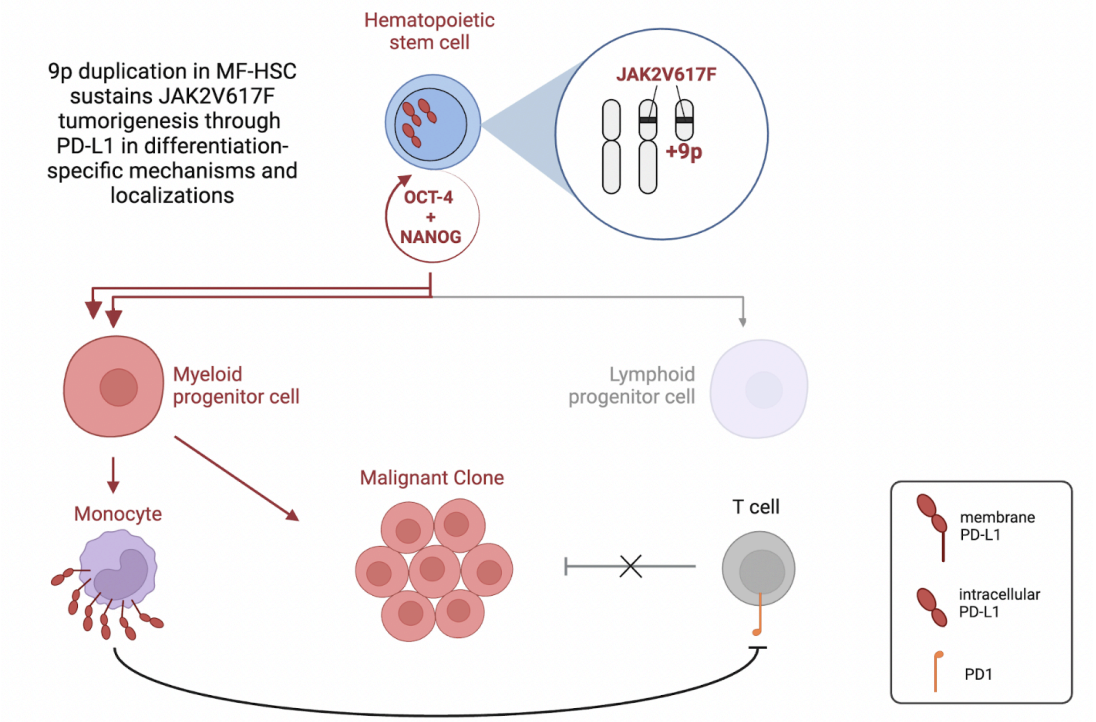

Graphical abstract. Chromosome 9p duplication enhances hematopoietic stem cells' clonogenic potential and promotes immune escape in JAK2-mutant myeloproliferative neoplasms. Abbreviations: +9p, chromosome 9 short arm copy number gain. Created with Biorender.com

SOMMARIO

JAK2V617F è la più comune mutazione coinvolta nelle Neoplasie Mieloproliferative (MPN), disordini ematopoietici con proliferazione clonale di cellule mature sostenuta dall'iperattivazione della via di JAK/STAT. La clonalità di ogni paziente è ulteriormente condizionata da mutazioni co-occorrenti e Variazioni del Numero di Copie (CNV).

Essendo il gene *JAK2* localizzato sul braccio corto del cromosoma 9 (9p), e avendo la Frequenza della Variante Allelica (VAF) di JAK2V617F un impatto rilevante sulla patologia, qualsiasi alterazione del numero di copie che coinvolga il suo locus può essere di rilevanza clinica per l'evoluzione di malattia.

Questo studio ha identificato un sottogruppo di pazienti MPN con trisomia del braccio corto del cromosoma 9 (+9p), permettendo di delineare le proprietà biologiche di questo contesto patologico.

La coorte reclutata include pazienti con mutazione driver di *JAK2*, eterozigoti (n=10), omozigoti (n=10), o con duplicazione del cromosoma 9p (n=12).

Per indagare il profilo genetico dei pazienti +9p, abbiamo impiegato colonie derivate da singole cellule $CD34^+$ cresciute in terreno semisolido, per verificare il numero di copie e lo stato mutazionale di *JAK2* attraverso ddPCR. I nostri risultati hanno rivelato che la

maggioranza delle colonie riporta tre copie di *JAK2*, con due alleli su tre mutati. Inoltre, l'analisi dell'abbondanza relativa di ogni combinazione ploidia-genotipo suggerisce che l'ordine cronologico degli eventi molecolari vede la mutazione driver verificarsi per prima, seguita dalla duplicazione del 9p mutato.

Passando all'analisi funzionale, entrambi i saggi clonogenici in metilcellulosa e collagene hanno riportato una maggior clonogenicità e un fenotipo più primitivo delle cellule $CD34^+$ dei pazienti +9p.

Di rilevante interesse è la localizzazione a valle del locus di *JAK2* del gene *CD274*, codificante per il mediatore del checkpoint immunitario PD-L1, che è risultato upregolato in diversi tipi cellulari mieloidi dei pazienti +9p.

Da evidenze in letteratura, PD-L1 è noto per promuovere l'espressione dei fattori della pluripotenza OCT4 e NANOG in cancro mammario attraverso l'attività della chinasi AKT; da queste premesse, abbiamo confermato l'upregolazione di entrambi i fattori nei pazienti +9p, delineando un meccanismo analogo di sostentamento della multipotenza.

Per validare l'aumentata dipendenza dall'attività di AKT dei pazienti +9p, è stata testata la molecola bioattiva MK2206, inibitore specifico di AKT, riportando una diminuita conta di colonie in seguito al trattamento. Risultati comparabili sono stati ottenuti attraverso il silenziamento simultaneo di OCT4 e NANOG attraverso nucleofezione di siRNA in cellule +9p $CD34^+$.

La correlazione tra +9p e la deregolazione di *CD274*, OCT4 e NANOG è stata poi confermata da un approccio di duplice caratterizzazione genomica-trascrittomica delle colonie, evidenziando come OCT4 e NANOG, indotti da PD-L1, possano mediare il segnale clonogenico attraverso AKT nelle cellule $CD34^+$ con due alleli *JAK2* mutati su tre.

Inoltre, analisi citofluorimetriche hanno rivelato nei pazienti +9p una maggior frequenza di monociti $PD\text{-}L1^+$, caratterizzati anche tramite analisi di immunofluorescenza in situ da una forte esposizione in membrana di PD-L1.

Infine, i pazienti +9p hanno riportato una maggior frequenza di linfociti T esausti, rispetto agli altri gruppi sperimentali.

Questi risultati suggeriscono che i pazienti JAK2V617F +9p rappresentano una classe distinta di pazienti MPN, caratterizzati dalla deregolata interazione tra *JAK2* e la via di PD-L1/PD-1, che contribuisce sia alla multipotenza delle cellule staminali e progenitori $CD34^+$, che all'evasione immunitaria del clone maligno mieloide.

Parole chiave:

1. Neoplasie Mieloproliferative
2. Cromosoma 9
3. JAK2
4. PD-L1
5. Evasione immunitaria

INTRODUCTION

1. Philadelphia-Negative Myeloproliferative Neoplasms

1.1. Classification and Clinical Manifestations

Starting in 1951, from the histological observation of the american clinical hematologist William Dameshek, it was first hypothesized that the heterogeneous pathological conditions under the comprehensive term of "myeloproliferative disorders" were linked by common etiology accounting bone marrow impaired hematopoietic functioning[1]. The description of a common level of neoplastic proliferation affecting either erythroblasts or megakaryocytes led to the definition of Myeloproliferative Neoplasms (MPNs), as used nowadays to define the group of heterogeneous diseases including Polycythemia Vera (PV), Essential Thrombocythemia (ET), Primary Myelofibrosis (PMF), Chronic Myeloid Leukemia and others. All those clinical manifestations share a certain grade of clonal proliferations striking hematopoietic stem and progenitor cells (HSPCs)[2], directly causing the over-expansion of differentiated cells of myeloid lineage in the subject[3].

Besides the MPN chronic phase, a preceding phase of clonal hematopoiesis can be identified. Clonal hematopoiesis is a pre-pathological condition characterized by the expansion of specific clones of HSPCs in the BM, which can be asymptomatic, in case of Clonal Hematopoiesis of Indeterminate Potential, or be associated with altered blood cells count, in case of Clonal Cytopenia of Undetermined Significance[4]. These conditions predispose to the development of MPNs over the years, which in turn can evolve to Acute Myeloid Leukemia after an accelerated phase (**Figure 1**).

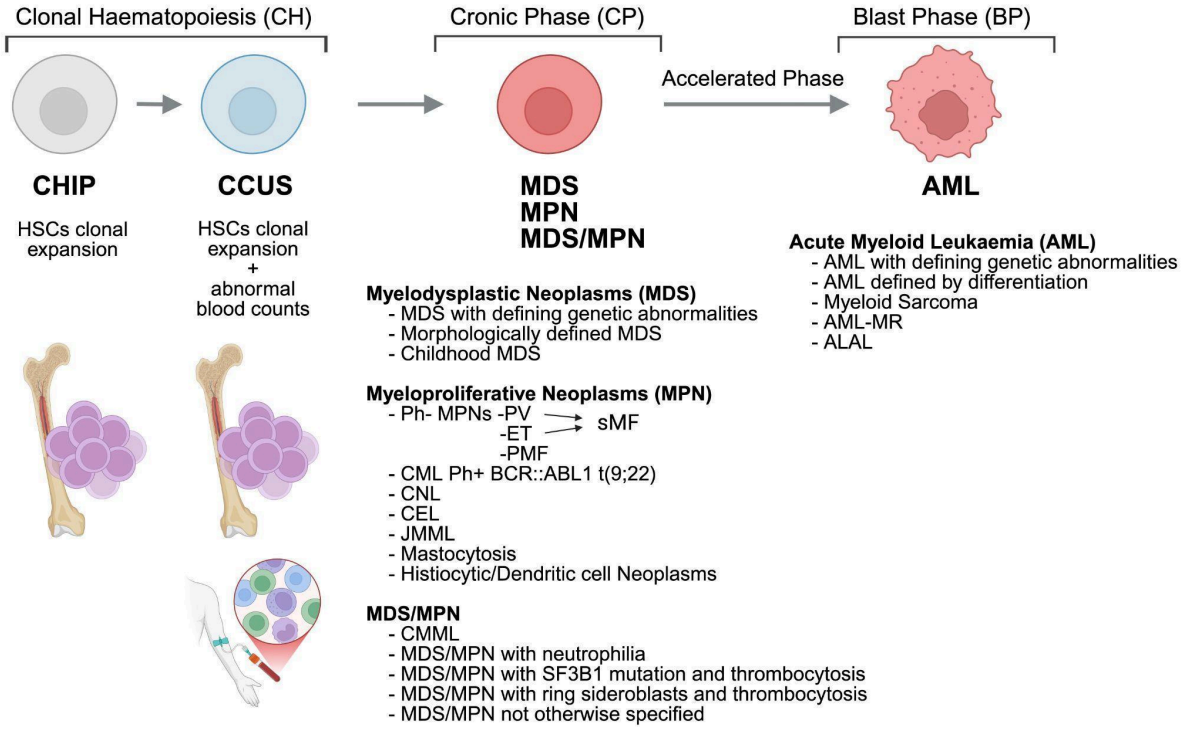

Figure 1. Myeloid Neoplasms classification in accordance with WHO 2022 revision. As defined by World Health Organization (WHO) Classification of Haematolymphoid Tumours released in 2022[5], MPNs are listed into the group of Myeloid Neoplasms alongside Myelodisplastic Neoplasms (MDS) and myelodisplastic/myeloproliferative neoplasms (MDS/MPN); MPNs are preceded by Clonal Hematopoiesis manifestations encompassing Clonal Hematopoiesis of Indeterminate Potential (CHIP) and Clonal Cytopenia of Undetermined Significance (CCUS) and can evolve from chronic phase to blast phase into Acute Myeloid Leukemia (AML) subtypes. Abbreviations: HSCs: Hematopoietic Stem Cells; MDS/MPN: myelodisplastic/myeloproliferative neoplasms; Ph-: Philadelphia-negative; Ph+: Philadelphia-positive; PV: Polycythemia Vera; ET: Essential Thrombocytemia; PMF: Primary Myelofibrosis; sMF: Secondary Myelofibrosis; CML: Chronic Myeloid Leukaemia; CNL: Chronic Neutrophilic Leukaemia; CEL: Chronic Eosinophil Leukaemia; JMML: Juvenile Myelomonocitic Leukaemia; CMML: Chronic Myelomonocitic Leukaemia; AML-MR: AML myelodisplasia-related; ALAL: Acute Leukaemia of Ambiguous lineage. Created with Biorender.com

MPNs lacking the Philadelphia chromosomal anomaly of t(9;22) translocation are defined Philadelphia-negative (Ph-) MPNs, and the classical forms include PV, ET and PMF. Incidence of Ph- MPNs is rare, with an estimated rate of 2,17 cases in 100.000 persons per year, with little variation between PV (0,84 cases / 100.000), ET (1,03 cases / 100.000) and PMF (0.47 cases / 100.000)[6].

Survival outcomes in patients with MPNs are poor and differ by disease subtype. In a large cohort of 1,581 patients analyzed by Tefferi *et al.*, median survival was set at 13.5 years for PV, 19.8 years for ET, and 5.9 years for PMF[7]. MPNs onset is correlated to different factors, such as sex, age, ethnicity and MPN family history. Diagnosis often comes in elderly age, with mean age at diagnosis of 52.9 years for ET, 59.2 years for PV, and 60.6 years for PMF

patients[8]. Additionally, gender affects onset, symptom burden, and disease course in MPNs: women represent the higher fraction of ET cases with a frequency of 68% of cases from an Italian patients database, while only 46% of PV cases, and 32% of PMF diagnosis[7].

1.2. Pathogenesis and symptomatology

MPNs are rare chronic hematological cancers arising in HSC after the acquisition of specific somatic mutations, which confer hypersensitivity or independence from cytokine-mediated signaling. The consequent excessive proliferation of myeloid precursors and overproduction of mature blood cells, primarily affects the bone marrow but the involvement of extramedullary secondary hematopoietic organs, such as spleen and liver, is frequent. MPNs pathogenesis is additionally associated with a general condition of chronic inflammatory microenvironment, generated directly by the malignant clone through the interaction with resident marrow cell types, or indirectly by the excessive proliferation of the neoplastic cells, compromising hematopoietic stem niche fine regulation.

The constant production of inflammatory cytokines leads to the impairment of bone marrow physiology and architectural histology, resulting in collagen fibers deposition and widespread bone marrow fibrosis. The maintenance of blood cell differentiation pool is then shifted towards extramedullary districts, most frequently the spleen with consequent establishment of splenomegaly. Chronic inflammation is also the primary cause of constitutional symptoms that impair patients' quality of life and a leading factor in disease progression[9].

The mutational landscape of MPNs pathology had come into focus after the discovery of the recurrent mutations affecting Janus Kinase 2 (*JAK2*, located on 9p24 chromosome) in 2005, than of Myeloproliferative Leukemia Virus Oncogene (*MPL* or Thrombopoietin Receptor, TPO-R, located on 1p34 chromosome) in 2006, and finally, in 2013, with the discovery of Calreticulin gene mutations (*CALR*, located on 19p13.2 chromosome). Notably, these mutations are mutually exclusive and do not present simultaneously. One mutation among these three can be found in 95% of MPNs cases, and all of them are strictly connected with MPN etiology and clinical phenotype. For those peculiarities, *JAK2*, *CALR* and *MPL* mutations are defined "Drivers Mutations"[10]. Despite this, a limited number of MPN diagnoses do not present any mutation in one of the three driver mutations, characterizing themselves as "triple-negative" MPN. For this reason, clinical features and histology remain an important tool for the diagnosis of MPN cases alongside patient genotyping for driver mutations (**Figure 2**). In this framework, *JAK2*, *MPL* and *CALR* genetic alterations, as well as peculiar clinical features, are differentially associated with PV, ET and PMF.

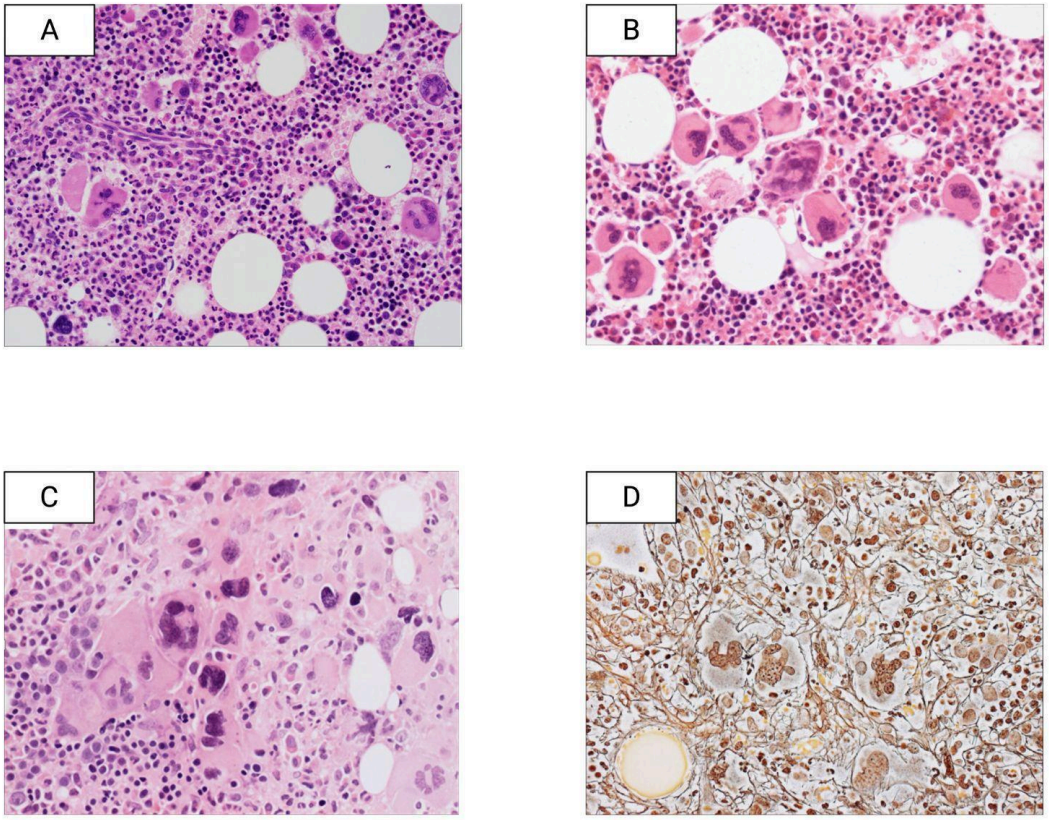

Figure 2. Morphology of myeloproliferative neoplasms bone marrow biopsies. (A-C) Hematoxylin & Eosin staining of bone marrow biopsies from MPN patients. (A) JAK2V617F-mutant PV; hypercellular bone marrow showing pan-myelosis. (B) ET; diffused megakaryocytic hyperplasia. (C) PMF; megakaryocytic hyperplasia with prominent pyknotic hyperchromatic nuclei. (D) Gordon &Sweet's staining of grade-2 PMF bone marrow biopsy. Widespread deposition of reticulin fibers, increased thickness and intersections. Adapted from Ng *et al*[11]. Created with Biorender.com

1.2.1. Polycythemia Vera

PV is one of the three classical forms of MPNs. In 2005 the sequencing of the *JAK2* gene in patients linked the newly described Val617Phe mutation to MPNs, with a stronger association with PV, and described the acquired ability to constitutively activate the EPO downstream signaling pathway[12]. As a matter of fact, 96% of PV cases presents with the gain-of-function somatic mutation JAK2V617F in the HSC compartment[7]. The resulting hyperactivation of the JAK/STAT pathway leads to the overproduction of erythrocytes, and associated thrombotic risk[13]. This marked increase in erythropoiesis was firstly described as independent from Erythropoietin (EPO) levels in patients with PV[14], and bone marrow cells from the same patients exhibited an EPO-independent growth *in vitro*, while in healthy condition EPO binding to cell membrane-exposed erythropoietin receptor (EPO-R) regulates

the differentiation feedback signal in bone marrow (**Figure 2 panel A**). Notably, JAK2 is the kinase associated with EPO-R that transduces the EPO signal to following kinase effectors[15]. Starting from this evidence, the genotyping of JAK2V617F became a fundamental practice for PV diagnosis. PV is defined by an acquired increase of hematocrit level above 16.5 g/dL (49%) in men and 16 g/dL (48%) in women, in association with JAK2 mutation and typical bone marrow morphology. Clinically, an increased erythrocytes count is associated with additional symptoms such as hypertension, elevated blood viscosity with microcirculatory symptoms, pruritus, and vessel thrombosis, occurring as the first manifestation in approximately 20% of PV patients[16].

A potential natural evolution of PV disease is secondary myelofibrosis (sMF), which brings fibrotic bone marrow transformation occurring with a mean frequency of 10% of PV cases in the first decade[17].

1.2.2. Essential Thrombocythemia

ET is characterized by abnormal thrombopoietin-independent megakaryocytes production, resulting in a consequent persistent thrombocytosis ($\geq 450 \times 10^9$/l)[18] (**Figure 2 panel B**). Up to 90% of patients with ET present genetic alterations activating JAK–STAT signaling pathway. Secondary symptoms include a spectrum of microcirculatory manifestations, such as fatigue, headache, visual disturbances, chest pain, splenic discomfort sometimes associated with splenomegaly, and thrombotic or hemorrhagic symptoms[19]. Epidemiology studies reported that ET patients have a life expectancy slightly inferior to sex- and age- matched population, while superior to the one associated with PV and PMF[19]. Concerning transformation to sMF, post–ET sMF occurs less frequently than post–PV cases, with a reported incidence of 3.9% at 10 years, increasing to 9.3% at 15 years from diagnosis[17]. Interestingly, comparing ET cases phenotype to driver mutations, it was reported that JAK2-mutated cases were associated with both higher hemoglobin levels and leukocyte counts, whereas CALR-mutated and triple-negative cases exhibited higher platelet counts[19].

1.2.3. Primary Myelofibrosis

PMF is the third classical form of Ph- MPNs. Among MPNs, PMF has the worst-outcome and also represents the most aggressive form. JAK2V617F is the most prevalent mutation in PMF, occurring in approximately 55–60% of cases, followed by *CALR* mutations as the second most frequent driver (~40%), while *MPL* mutations are relatively less common (~5%)[20].

The search for profibrotic mediators involved in the cumulative deposition of extracellular matrix fibers in PMF bone marrow niche led to the identification of various molecules with fibrogenic activity, such as Transforming Growth Factor-Beta (TGF-β), Platelet-Derived Growth Factor (PDGF), Vascular-endothelial Growth Factor (VEGF), Interleukin-8 (IL-8), and Osteopontin (OPN)[21–23]. These molecules are potentially secreted by cells belonging to the neoplastic clone such as dysplastic megakaryocytes, as well as by wild-type activated monocytes[21]. Several studies sustain that fibrogenic cells in PMF are derived from mesenchymal stromal lineage[24,25]; others, suggest a cross-talk between megakaryocytes, granulocytes, and inflammation-primed wild type fibroblasts and mesenchymal stromal cells[26]. Interestingly, rather than mesenchymal stromal cells, Verstovsek *et al*. suggested that megakaryocytes-derived cytokines in PMF patients' bone marrow could induce the differentiation of clonal neoplastic monocytes into fibrocytes, which would mediate fibrosis development[27]. Nevertheless, even if the molecular drivers of PMF fibrotic process remain to be fully understood, its diagnosis also relies on BM fibrosis' evaluation. The European Consensus on BM fibrosis grading described its histological features through four stages: grade 0, with linear and scattered reticulin fibres lacking intersections; grade 1, with a loosely arranged pattern of intersecting reticulin fibers, specifically present in perivascular areas; grade 2, with concentrated reticulin fibers, highly intersected and possible bundles of collagen fibers depositions; and grade 3, with dense and diffused fibers of reticulin, highly intersected and with broad bundles of collagen[28]. Myelofibrotic BM histopathology is further characterized by megakaryocyte proliferation and osteosclerosis in advanced stages. Overt PMF, the state with the highest level of bone marrow fibrosis (grade 2-3), may be preceded by a prefibrotic Early PMF stage, which shares clinical features with ET but is distinguished from it by the presence of splenomegaly, increased bone marrow cellularity with dysplastic megakaryocyte proliferation, and eventual development of low-grade fibrosis (grade 0) (**Figure 2 panel C**).

Beside BM fibrosis, PMF distinctive traits include myeloid lineage clonal expansion, the presence of megakaryocytes with hyperplastic and dysplastic features in BM, high peripheral granulocytes count, a widespread pro-inflammatory state mediated by cytokines production, and extramedullary hematopoiesis associated with secondary hematopoietic organs, such as spleen and liver.

Disease severity is mainly driven by a high risk of leukemic transformation (14–25%) and severe cytopenias, alongside a broad spectrum of complications including thromboembolic, hemorrhagic, infectious, and cardiovascular events, as well as cachexia[29].

Another feature of PMF is the presence of high levels of circulating $CD34^+$ blasts, with increasing levels accompanying disease progression. Blast counts of 10–19% are associated with the accelerated phase preceding leukemic evolution, whereas levels exceeding 20% define leukemic transformation[30]. Moving from these observations, circulating $CD34^+$ cells level has been established as a useful marker for distinguishing PMF from other Ph-MPNs[31–33].

1.2.4. Secondary Acute Myeloid Leukemia

The stratification of additional mutations alongside the driver mutation and the chromosomal abnormalities induced by such increased replication stress can result in the evolution of MPNs into secondary Acute Myeloid Leukemia (sAML) (**Figure 3**). WHO guidelines indicate a level of 20% of blasts in peripheral blood or bone marrow to differentiate the diagnosis from MPNs to sAML, while more recent references theorize the need for a less strict threshold, considering the complex interaction between circulating blasts and each patient's immune system, the type of driver mutation, and pharmacological treatments[34].

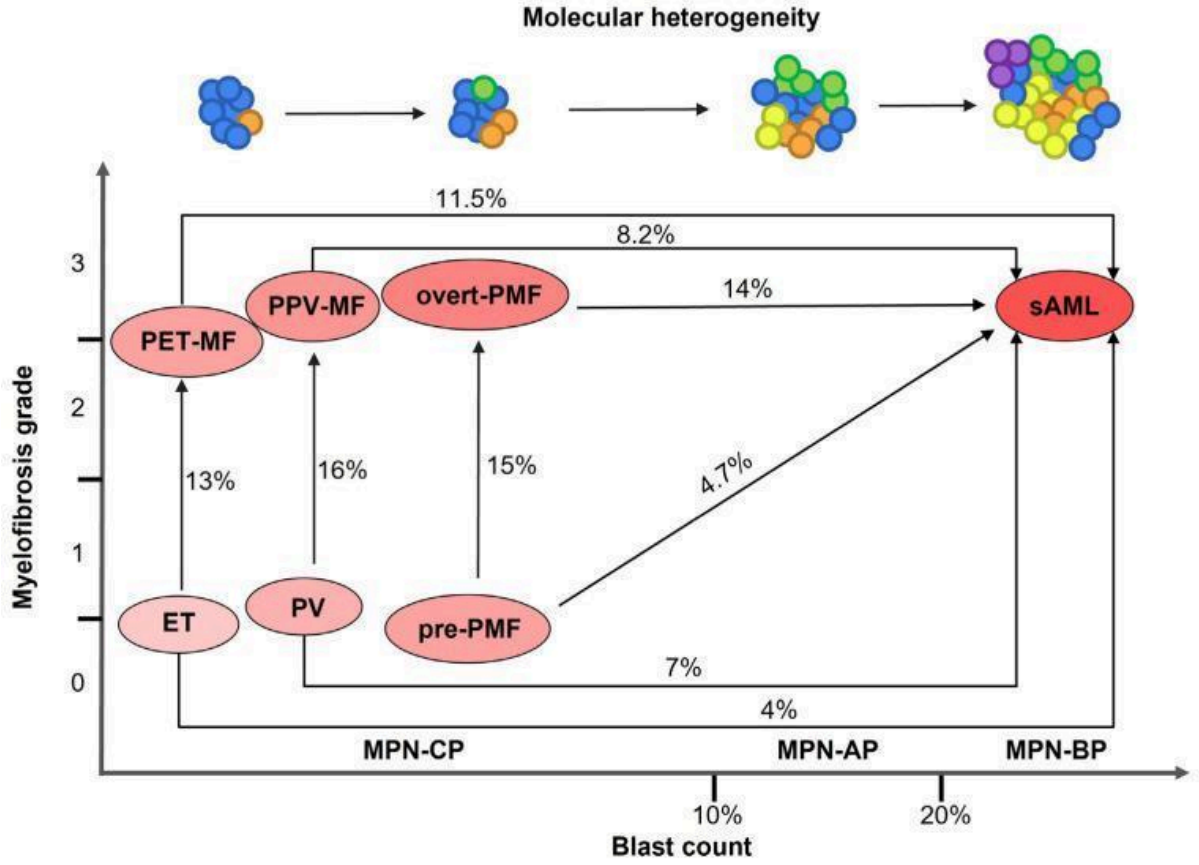

Figure 3. Different paths of MPN progression towards sAML. Steps of disease progression and evolution of MPNs. State transitions can be defined based on two clinical variables, the degree of bone marrow fibrosis and the frequency of blasts in peripheral blood and bone marrow. An increasing molecular heterogeneity is associated with disease evolution. Percentages reported on the arrows represent the observed frequency of disease progression in MPN patients. Shades of red indicate disease aggressiveness increase. Abbreviations: ET, Essential Thrombocythemia; PV, Polycythemia Vera; pre-PMF, pre-fibrotic Primary Myelofibrosis; PET-MF, post-ET Myelofibrosis; PPV-MF, post-PV Myelofibrosis; sAML, secondary Acute Myeloid Leukemia; MPN, Myeloproliferative Neoplasm; MPN-CP, MPN chronic phase; MPN-AP, MPN accelerated phase; MPN-BP, MPN blast phase. Adapted from Rontauroli *et al*[35].

The genetic landscape underlying leukemogenesis in post-MPN sAML differs from that of *de novo* AML. Comparative analyses of mutation frequencies in genes commonly implicated in myeloid malignancies demonstrate a significant association of *TP53* mutations with sAML, whereas alterations in *IDH1/2*, *NRAS*, *RUNX1*, and *CBL* appear to contribute equally to leukemogenesis of *de novo* AML and sAML. Conversely, the mutual exclusivity of certain mutations supports the involvement of distinct transformation pathways towards AML subtypes. Cytogenetic analyses further reveal that a greater karyotypic complexity is correlated with sAML compared with *de novo* AML, along with differential distributions of specific chromosomal abnormalities between the two groups[36].

Additionally, *TP53* mutations in sAML represent a strong independent predictor of poor survival, underscoring the critical role of DNA damage response pathway in sAML

pathogenesis. In this light, de novo AML and sAML can be considered biologically distinct tumoral forms, both at the cytogenetic and molecular level[36].

The most relevant risk factors for AML progression from chronic phase MPNs have been identified in advanced age (≥60–65 years), leukocytosis (≥15–30 × 10^9/L), the level of circulating blasts (≥3–10%), and progressive cytopenias including thrombocytopenia and/or erythropenia[37].

Treatment-related acute myeloid leukemias are associated with an unfavorable prognosis, with an estimated overall survival of 7 months[38].

1.3. Diagnosis

WHO subsequent revisions of the classification guidelines of myelodysplastic and myeloid neoplasms progressively refined the clinical variables and symptomatology for the diagnosis of MPNs subtypes. The latest edition released in 2022 maintained the overall criteria proposed in the previously 2016 version; yet, acknowledging the significant advancements in genetic and molecular biomarker identification to improve diagnostic and prognostic criteria, underlined the necessity to integrate new clinical, morphologic, immunophenotypic, cytogenetic, and genetic data for more accurate disease definitions. Criteria identified for diagnostic determinations are reported in **Figure 4**.

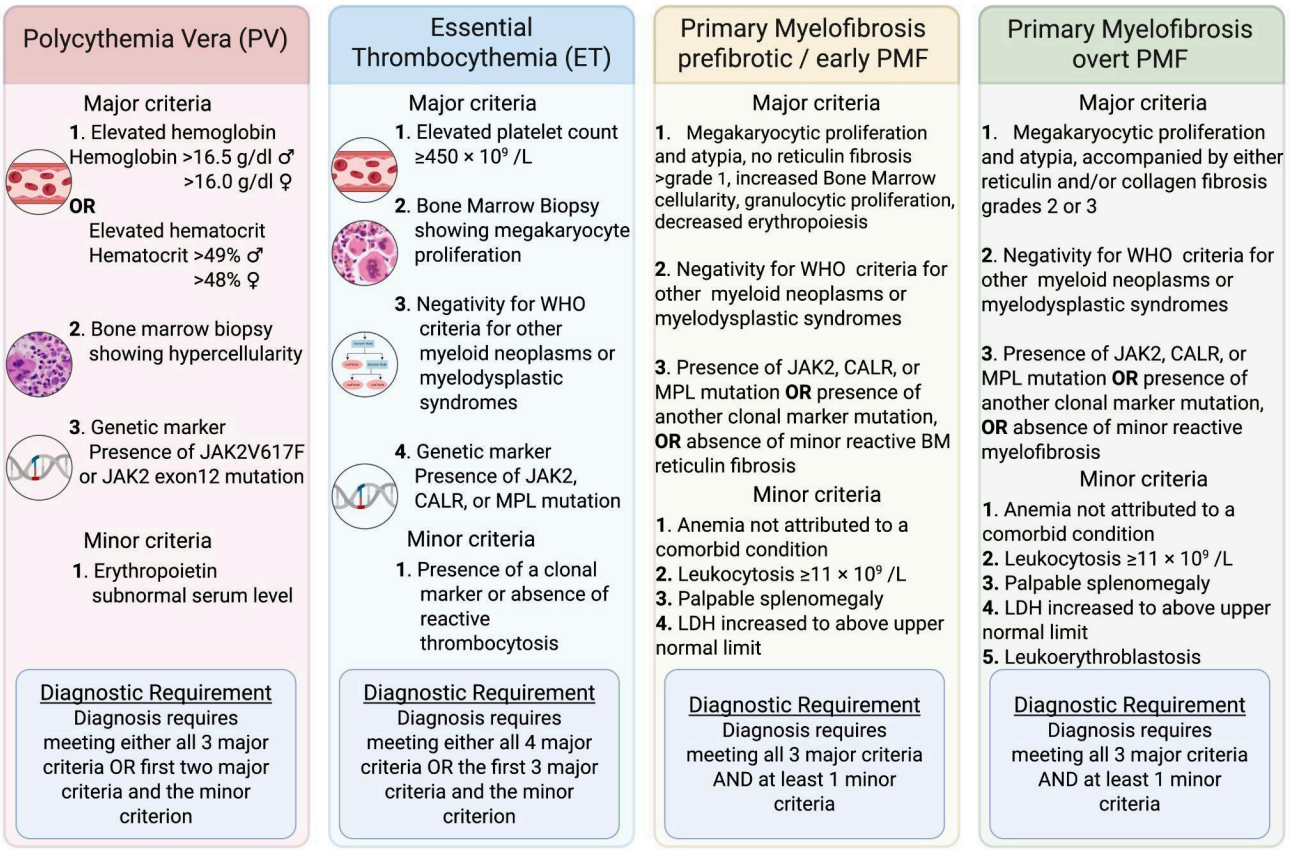

Figure 4. Current MPN diagnostic criteria as listed by WHO (2022).
The figure summarizes the differential diagnostic criteria of MPNs outlined by WHO in 2022, making distinctions among PV, ET, and both early- and overt- PMF. The classification largely relies on diagnostic criteria established in earlier editions, with minor refinements. Differentiation among MPNs entities requires an integrated assessment of peripheral blood parameters, genetic molecular markers, and bone marrow morphologic features. Adapted from Khoury *et al*[5]. Created with Biorender.com

1.4. Prognosis

MPNs patients' prognosis can be highly variable, being affected by several risk factors, including thrombosis predisposition, leukocytosis, age of onset, cytopenias, circulating blasts level, complex karyotypes, and constitutional symptoms. Reported median survivals are also variable among PV, ET and PMF. PMF is characterized by the most unfavorable prognosis with reported median survival times ranging from approximately 4 to 7 years from diagnosis. Starting from the need for an instrument to evaluate the likeness of better or worse prognosis outcome regarding PMF and to support difficult therapeutic decisions (for example regarding stem cell transplantation and new pharmacological treatments), a large scale multicenter clinical study published in 2009 outlined the International Prognostic Scoring System (IPSS), a prognostic accurate tool enabling the risk stratification of patients with myelofibrosis[39]. Clinicians and researchers identified five key variables able to act as independent predictors

of reduced survival, used to stratify patients into four distinct risk categories with clearly separated outcomes: Low risk (0 factors present), Intermediate Risk-1 (1 factor present), Intermediate Risk-2 (2 factors present), and High risk (from 3 to 5 risk factors detectable). Those five risk indicators are the age at diagnosis >65 years, the presence of constitutional symptoms, anemia, leukocytosis, and circulating blasts level[39].

The following year, a new study integrated the IPSS guidelines with a cytogenetic risk categorization. The aim of the work by Hussein *et al.* was that of evaluating the prognostic value of cytogenetic anomalies, not considered during the outlining of the IPSS system. Remarkably, it was reported how cytogenetic evaluation can facilitate treatment decision making alongside IPSS prediction, proving its additional value in risk assessment among patients with PMF[40].

IPSS system was subsequently refined into the Dynamic International Prognostic Scoring System (DIPSS), a model that accounts for changes in risk factors over time rather than just at diagnosis, using data from a large cohort of PMF patients; DIPSS allowed risk stratification through a calculated score based on disease progression during follow-up[41].

More recently, a new series of scoring systems was developed implementing different evaluation criteria on the basis of the previously proposed models. A first pair, named MIPSS70 (Mutation-enhanced International Prognostic Scoring System) and MIPSS70 plus (Karyotype Enhanced MIPSS70+) scoring systems was generated to assess the prognostic evaluation of patients eligible for bone marrow transplant under the age of 70. The first, besides the criteria of the previous IPSS, takes into account platelets count, bone marrow fibrosis grade, the presence of *CALR* type 1 driver mutation, and the presence of specific non-driver "high molecular risk" mutations: *ASXL1*, *EZH2*, *SRSF2* or *IDH1/2* genes[42,43]. MIPSS70+ system then distinguishes itself for evaluating the additional layer of cytogenetic alterations[44].

Moving further, three more systems were designed. In 2017 it was published MYSEC-PM (Myelofibrosis Secondary to PV and ET-Prognostic Model), a system specific for patients with sMF with a past diagnosis of PV or ET who added a focus upon *CALR* mutations prognostic significance[45]. GIPSS (Genetically Inspired Prognostic Scoring System), released in 2018, was built only upon the genetic asset of the PMF patient to predict the associated risk score[46]. Finally, MTSS prognostic system presented in 2019, aimed at developing a tool to assess post-transplant outcomes by integrating clinical, molecular and transplant-specific variables, among which bone marrow donor HLA-match and patients' mutational profile[47].

As regards PV and ET patients, different prognostic scoring systems have been outlined based on risk factors associated with each pathology. For PV, classical evaluated variables are age at diagnosis and thrombosis history[48], which are maintained in the Molecular International Prognostic Scoring System for polycythemia vera (MIPSS-PV), which evaluates thrombosis history, white blood cell count, age >67 years, and presence of *SRSF2* mutations. Based on the weight of each risk factor present, PV patients are subsequently stratified into Low risk, Intermediate risk, and High risk[49,50]. On the other hand, Molecular International Prognostic Scoring System for Essential Thrombocythemia (MIPSS-ET) relies on the evaluation of leucocytosis, age >60 years, gender, and the presence of adverse mutations in SRSF2, SF3B1, U2AF1, and TP53[49,50].

In the end, the new diagnostic and prognostic approaches developed in recent years have allowed a growing understanding of molecular pathophysiology of MDS and MPN. In this light, the increasingly precise international classification of MPN entities aims to include classes of disease molecularly defined at the mutational and cytogenetic level[51].

2. MPNs mutational landscape

2.1 Driver Mutations

As previously mentioned, Ph- MPNs are a group of hematological malignancies that includes three different but related clinical manifestations usually presenting mutually exclusive 'Driver mutations' with the common effect of the hyperactivation of the JAK/STAT signalling pathway, strongly guiding oncogenic proliferation of HSPCs (**Figure 5**). Many authors throughout the last two decades have extensively described how the establishment of a hierarchical clonal architecture composed of dominant clones and genetically distinct subclones with variable competitive fitness takes place within individual patients, usually starting from the selective advantage conferred by the driver mutation. More recently, single-cell analyses have further revealed complex clonal hierarchies, with dominant and subclonal populations exhibiting distinct genomic and transcriptomic profiles within individual patients. This heterogeneity arises from subsequent clonal evolution, as cells accumulate additional genetic alterations that promote divergence from the founding clone, ultimately reshaping the clonal landscape. The guiding force of this evolutionary process is selective advantage, which in MPNs is primarily led by JAK/STAT pathway[35,52,53].

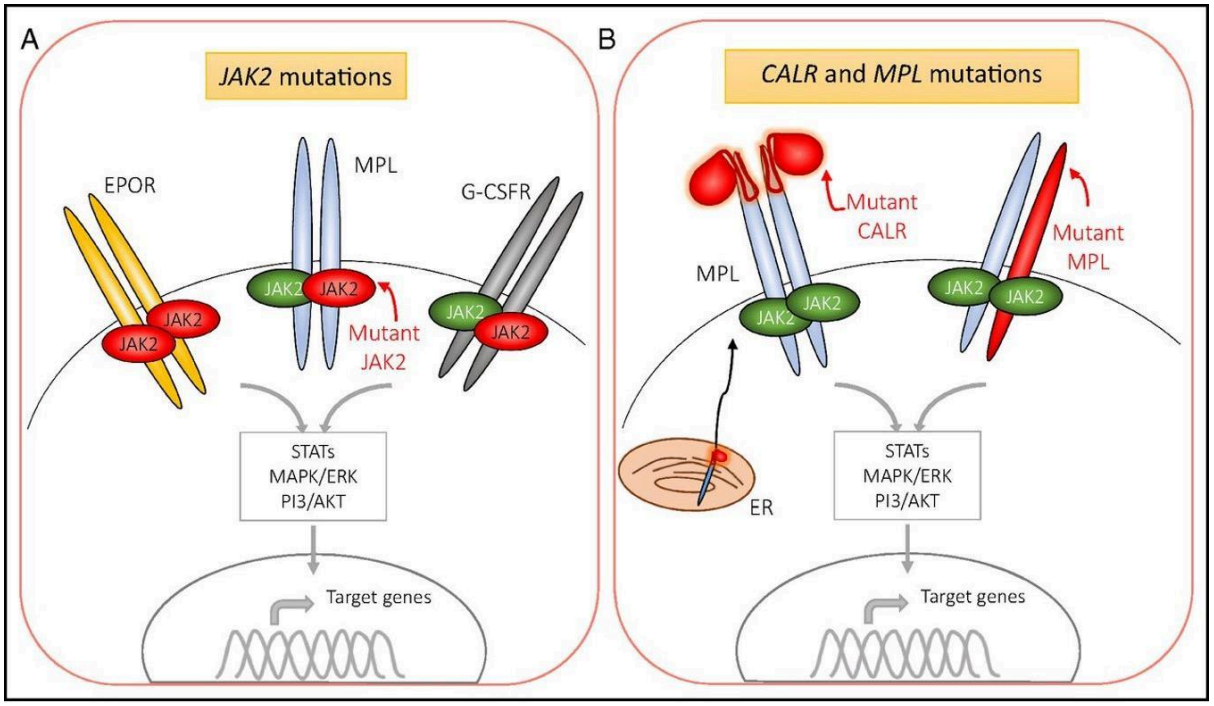

Figure 5. Overview of MPN driver mutations induced myeloproliferative effect.
Constitutively active signaling downstream of JAK2 is triggered by any of *JAK2*, *CALR*, or *MPL* mutation. (A) JAK2 associates with the cytoplasmic domain of various cytokine receptors. Mutant JAK2, depicted in red, is constitutively active and drives variable degrees of erythroid and megakaryocytic proliferation and differentiation, with effects also on the granulocytic lineage. (B) Mutations in *CALR* and *MPL* both lead to aberrant activation of MPL receptor signaling. Mutant CALR forms a complex with MPL binding site; both *CALR* and *MPL* mutations promote receptor dimerization and constitutive JAK2 activation, resulting in downstream signaling through the MAPK/ERK, PI3K/AKT, and STAT pathways. Abbreviations: JAK2, Janus kinase 2; EPOR, Erythropoietin Receptor; MPL, Thrombopoietin Receptor; STAT, Signal Transducer and Activator of Transcription; MAPK, mitogen-activated protein kinase; ERK, Extracellular signal-regulated kinases; PI3, phosphatidylinositide 3-kinase; AKT, protein kinase B; CALR, Calreticulin; ER, endoplasmic reticulum. Adapted from Nangalia *et al.*[54].

2.1.1 JAK2

Janus kinases are a family of tyrosine kinases associated with cell surface receptors and involved in multiple intracellular signaling pathways. The *JAK2* gene is located on chromosome 9p24 and it's composed of 25 exons. Structurally, JAK2 presents a C-terminal catalytically active kinase domain (JH1) and an adjacent pseudokinase domain (JH2), which negatively regulates kinase activity and ensures cytokine-dependent activation. The N-terminal FERM-like domain facilitates receptor association, while the SH2-like domain mediates binding of JAK2 to the cytoplasmic tails of various cytokine receptors[55].

JAK2 activation is triggered upon cytokine binding to its associated receptor, inducing conformational changes that bring the receptor-bound JAK2 molecules into proximity, allowing trans-phosphorylation and activation. Activated JAK2 subsequently phosphorylates tyrosine residues on the receptor's cytoplasmic tail, creating docking sites for downstream

adaptor proteins and signaling effectors containing phosphotyrosine-recognition domains, such as SH2 domains[56]. Among those secondary signal transducer proteins are STAT (Signal Transducer and Activator of Transcription), whose phosphorylation promotes homodimerization followed by nuclear translocation and retention, where STATs function as transcription factors[57].

In 2005, somatic *JAK2* exon 14 mutation c.1849G>T (p.V617F) was firstly identified and shown to confer constitutive activation of the JAK2 kinase domain[12,58–60]. JAK2V617F, a gain-of-function mutation located within the pseudokinase domain, is the most prevalent MPN driver mutation occurring in approximately 55–60% of patients with PMF. It promotes autonomous dimerization of mutant pseudokinase domains, stabilizing the active JAK2 dimer conformation and turning off inhibitory control of the kinase domain[10].

JAK2V617F induces constitutive downstream signaling of the three main homodimeric receptors for myeloid cytokines (EPOR, G-CSFR, and MPL), therefore accounting for its association with multiple MPN phenotypes. Aberrant signaling primarily involves activation of the STAT pathway (including STAT1, STAT3, and STAT5, depending on receptor context), as well as the PI3K/AKT/mTOR and RAS/MAPK pathways. Beyond promoting proliferation of HSPCs, JAK2V617F confers a strong growth advantage to differentiating myeloid precursors and primes mature cells toward an inflammatory phenotype, largely mediated by STAT3 activation and contributing to constitutional symptomatology and thrombotic risk[20].

Phylogenetic reconstruction of clonal evolution in JAK2V617F-positive MPNs indicates that the mutation can arise decades before clinical disease onset or even *in utero*, highlighting a potential window for early therapeutic intervention[61].

Beyond its canonical kinase function, two studies have demonstrated that JAK2 also exhibits an ‘epigenetic writer’ activity, directly acting on chromatin accessibility by phosphorylating tyrosine 41 of histone H3 (H3Y41), a marker associated with transcriptionally active chromatin[62,63].

Soon after the discovery of JAK2V617F mutation, its oncogenic activity was studied through new developed mouse models. Remarkably, in 2008 Tiedt *et al.* pointed out that JAK2-V617F knock-in transgenic mice’s myeloproliferative phenotype was dependent on the allele burden of the JAK2 mutation. Specifically, the expression of JAK2V617F/wtJAK2 at a ratio of 1:1 resulted in an ET–like phenotype, characterized by elevated hemoglobin, thrombocytosis, and neutrophilia. On the other hand, higher levels of retrovirally transduced JAK2V617F in murine bone marrow induced a PV-like phenotype in the absence of thrombocytosis, similar to what can be observed in patients[64]. Successively, another

JAK2-mutated mouse model developed by Mullally *et al.* proved that, alongside the expansion of myeloid progenitor populations and skewed erythroid differentiation, mutated stem cells have the ability to initiate the disease in serial transplantation cycles[65].

JAK2V617F variant allele frequency (VAF) is associated with advanced disease features and clinical complications in MPNs, and given its pivotal role in guiding disease pathogenesis, VAF represents a valuable biomarker for assessing treatment response and minimal residual disease[66].

2.1.2 MPL

MPL, or Thrombopoietin receptor, is the second most frequently mutated gene involved in MPN pathogenesis; its chromosomal localization is 1p34 and it's composed of 12 exons. Starting from evidences of JAK2-negative MPN cases, in 2006 it was identified as an alternative driver mutation besides *JAK2*[67]. As reported, MPL is one of the possible receptorial partners of JAK2 kinase, and gain-of-function mutations result in a constitutively stimulated JAK/STAT pathway. Commonly, mutations involve codon 515 of MPL protein primary structure and result in the substitution of a crucial tryptophan residue belonging to the juxtamembrane domain, causing a ligand-independent receptor activation[68,69].

Despite the close molecular relation between MPL and JAK2, their mutation-correlated phenotype is not superimposable, since MPLW515L/K results in thrombocytosis rather than in erythrocytosis. A murine model of myelofibrosis generated with the retroviral knock-in of MPLW515L in bone marrow cells demonstrated its oncogenic potential and recapitulated many traits of ET and PMF, among which thrombocytosis, megakaryocytic hyperplasia, bone marrow fibrosis, and splenomegaly associated with extramedullary hemopoiesis[67].

2.1.3 CALR

The latest described MPN driver mutation involves *CALR*, a gene encoding a highly conserved protein with functions in the endoplasmic reticulum, cytoplasm and cell surface. Physiologically, CALR presents a chaperone activity involved in protein glycosylation and Ca^{2+} homeostasis to ensure a correct protein folding[70]. Various types of *CALR* gene insertions or deletions were detected in MPN, all involving exon 9 and generating a +1 base-pair frameshift in the resulting translated protein. Among all the molecular alterations, the two most represented are a 52 bp-long deletion (referred as "type 1" mutation, c.1092_1143del), and a 5 bp insertion ("type 2" mutation, c.1154_1155insTTGTC)[10].

The resulting mutated CALR protein shows a novel C-terminal domain with gain-of-function oncogenic activity. CALR mutated C-terminus domain exhibits the loss of all negatively charged aminoacidic residues included in wt protein, acquiring new pathogenic characteristics. Structure-function studies reported that mutant CALR acquires the capacity to physically interact with MPL extracellular domain, placing *CALR* driver mutation into the signalling paradigm of JAK/STAT MPNs etiology[71–73]. The proposed model of CALRmut pathogenicity assumes that CALR positively-charged mutant C-terminus is required for ER and cell membrane subcellular localization, where the oligomerization of mutant CALR proteins mediates MPL binding and activation of the downstream signal cascade[74,75].

Among patients with ET or PMF with non-mutated *JAK2* or *MPL*, *CALR* mutations were identified in 67% of ET cases and 88% of PMF cases. Consistently, CALRmut patients showed higher platelet count and lower hemoglobin levels compared with JAK2-mutant cases[76,77].

It was reported by Pietra *et al.* that patients with ET harboring type 1 *CALR* mutations exhibited a significantly higher risk of progression to myelofibrosis compared with both those carrying type 2 *CALR* mutations and those with JAK2V617F mutation[78].

Clinical manifestations observed in CALRmut patients were then confirmed in mouse models of type 1 and 2 mutated *CALR* and linked to its specific molecular domains and receptor partner[79].

2.2 Chromosomal alterations in MPNs

Beside DNA point mutations and small insertion/deletion events, chromosome rearrangements are large-scale alterations that can still influence the fitness of a cell and result in clone proliferation. Those alterations usually result in the acquisition or loss of extended chromosomal regions that vary the ploidy of the cell, causing aneuploidies.

A simple example of chromosomal alteration which does not result in a CNV is acquired Uni-Parental Disomy (UPD), a process that can lead to loss of heterozygosity of specific mutations following chromosomal recombination[80] as depicted in **Figure 6**. These events are therefore classified as Copy-Neutral Loss of Heterozygosity (CN-LOH).

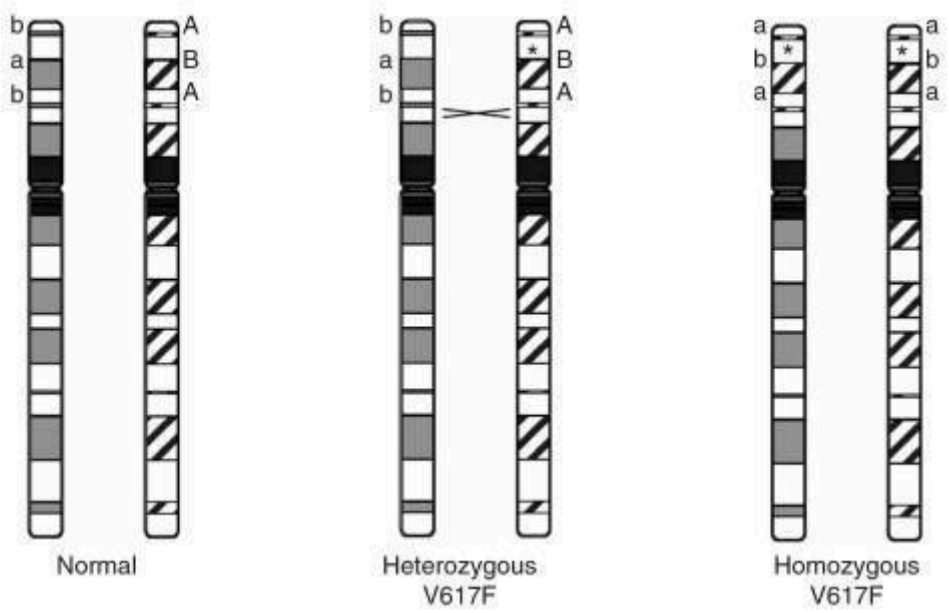

Figure 6. Acquired UPD steps of chromosome 9p involving JAK2V617F. JAK2V617F mutation, indicated by an asterisk, and flanking SNPs can be reduced to homozygosity following copy-neutral mitotic recombination**.** Adapted from Jones *et al*[80].

Hematological neoplasms are often defined by recurrent chromosomal abnormalities, even if not always associated with specific clinical outcomes. Unlike solid tumors, blood cancers show on average an equal occurrence of events of gain and loss of chromosomal material, as reported in **Table 1**. This feature delineates a landscape in which the selective advantage conferred by chromosomal alterations is not just related to an increased proliferation rate resulting from a reduced amount of genetic material, but can also be associated with specific mechanisms of gene dosage alteration and deregulation[81].

Neoplasm	Cytogenetic alterations	Clinical outcome
Chronic myelomonocytic leukemia (CMML)	–Y	Favorable
	+8, CK	Poor
Myelodysplastic syndromes (MDS)	–Y	Very favorable
	–7[b]	Poor
	CK	Very poor
Acute myeloblastic leukemia (AML)	–5[b], –7, +8, –17 or abn(17p), CK, MK	Poor
Chronic lymphocytic leukemia (CLL)	+12[b], +18	NPA
Multiple myeloma (MM)	+1, +3, +7, +11, +15	NPA
Non-Hodgkin lymphoma (NHL)	+3, +5, +7, +12, +18	NPA
Myeloproliferative neoplasms (MPN)	-7[b], +8[b], +9[b], –Y[b]	NPA
Acute lymphoblastic leukemia (ALL)	+21, hyperdiploidy (>50 chr)[b]	Favorable
	Hypodiploidy (<40 chr)[b]	Poor

Table 1. Main aneuploidy cytogenetic abnormalities in Hematological Neoplasms. Abbreviations: abn, abnormality; chr, chromosomes; CK, complex karyotype; del, deletion; MK, monosomal karyotype; NPA, no prognosis associated. [b] intended as a single abnormality. Adapted from Molina e*t al*[81].

Approximately one-third of patients with PMF present cytogenetic abnormalities in karyotype profiling, the most frequent being del(20q), del(13q), trisomy 8 and 9, and abnormalities of chromosome 1 including 1q duplication[82].

Specifically, chromosome 9 gain in MPN spans between 3% and 33% of cases, with a mean percentage of 12%. Together with −7/del(7q), −5/del(5q), 12p deletion, chr1 abnormalities, and +8, +9 gain was associated with unfavorable prognosis and increased risk of leukemic transformation[83,84].

As JAK2 gene is located on the short arm of chromosome 9, the association between 9p abnormalities and MPNs has been investigated in literature. Patnaik *et al.* reported that even if 9p translocations are frequent in hematological malignancies, the cases described do not always involve JAK2; nevertheless, JAK2-encompassing translocations are typically associated with an MPN diagnosis and frequently carry the JAK2V617F mutation, suggesting a potential cause–effect relationship[85].

Hahm *et al.* employed the tracing of CN-LOH events through a single nucleotide polymorphism array karyotyping, to follow genetic alterations in the chronic phase and during disease progression of MPN and MDS/MPN patients. They reported CN-LOH of JAK2-mutated allele being the most frequent aberration, followed by the copy-number alterations of 5q deletion and 9p gain. In addition, copy number alterations events were more frequently associated with patients who underwent disease progression. Finally, it was shown that most patients harboring 9p CN-LOH or 9p gain had a *JAK2* mutant allele burden greater than 50%[86].

Overall, these findings suggest that chromosome 9 status should be considered when interpreting *JAK2* mutational status, and that additional molecular studies are required to clarify the role of +9 in conferring selective advantage and in driving clonal evolution in *JAK2*mut MPNs.

3. Pharmacological treatment options for MPNs

Considering the great molecular and clinical complexity of MPN manifestations, approaching efficacious and reliable treatment strategies has been a challenging need since the first steps of MPN research. Despite this, treatment management still lacks disease-modifying therapies for MF/MPN patients, with the exception of the limited subset of patients who achieve clinical, molecular, and haematological regression with interferon therapy or bone marrow transplant[87].

Some pharmacological treatments have been established to control constitutional symptoms and risk factors associated with the myeloproliferation, such as hydroxyurea in ET patients and low-dose aspirin in PV cases to relieve thromboembolic complications[88,89]. On the other hand, the development of anti-clonal therapies for MPN patients still faces limitations that preclude targeted approaches against neoplastic cells. The major issue is the inefficient activity of available drugs targeting crucial mutated proteins such as JAK2[90,91]. The second limitation is the unavailability of drug options active on crucial targets, especially for epigenetic mutations such as *TET2* and *ASXL1*. The last obstacle towards optimal MPN pharmacological treatment is each patient's clonal genetic and epigenetic heterogeneity, shaping complex and unique cellular targets[92].

Given the primary relevance of JAK/STAT pathway on the pathogenesis of myeloproliferative diseases, JAK-inhibitor (JAKi) molecules are a prominent pharmacological option. The most employed molecule of this class is Ruxolitinib, a JAK1/2 inhibitor that suppresses the proliferation of hematopoietic precursors and differentiated cells through the targeting of JAK/STAT signaling pathway[93]. Its clinical efficacy was acknowledged in reducing splenomegaly, circulating levels of pro-inflammatory cytokines, blood counts, and in prolonging survival[82,94]. Yet, it is currently well known that MPN clones persist even in presence of chronic JAKi treatment, and JAK2V617F knock-in mouse models provided evidence that disease-initiating cells are resistant to JAK1/2 inhibition[65]. Moreover, JAK/STAT signalling can be affected by other mutated alleles (eg. *TP53*, *ASXL1*, and *TET2*), strongly influencing response to JAKi[95]. For these reasons, a shift towards drugs with a more marked specificity against mutant JAK2 is being pursued.

Epidrugs constitute a different category of molecules for MPN treatment, focused on evidences of how abnormal epigenetic gene regulation potentially contributes to the pathogenesis and the phenotypic diversity of MPNs. Two main classes of epidrugs have been tested throughout the years: DNMT inhibitors and HDAC inhibitors. The former are active on DNMT proteins and mediate the block of DNA methylation in CpG sites, preventing the heterochromatin-mediated repression of onco-suppressor genes. The latter act by preventing the euchromatin availability of oncogenes involved in tumor proliferation and selective advantage, mediated by the binding of acetyl groups on positively-charged aminoacidic residues on histone tails[96].

A third promising approach to MPN pharmacological treatment is immunotherapy, a strategy to counteract tumor-mediated immunomodulatory signals and support the immune system's anti-tumoral activity. Two methods have been proposed to achieve this aim focusing on shutting down either pro-inflammatory cytokines (such as IL-1b, IL-6 and TNFa) or immune escape tumoral behaviour (T cell exhaustion, PD-L1 upregulation)[97].

An overview of MPN therapeutic approaches is reported below in **Figure 7**.

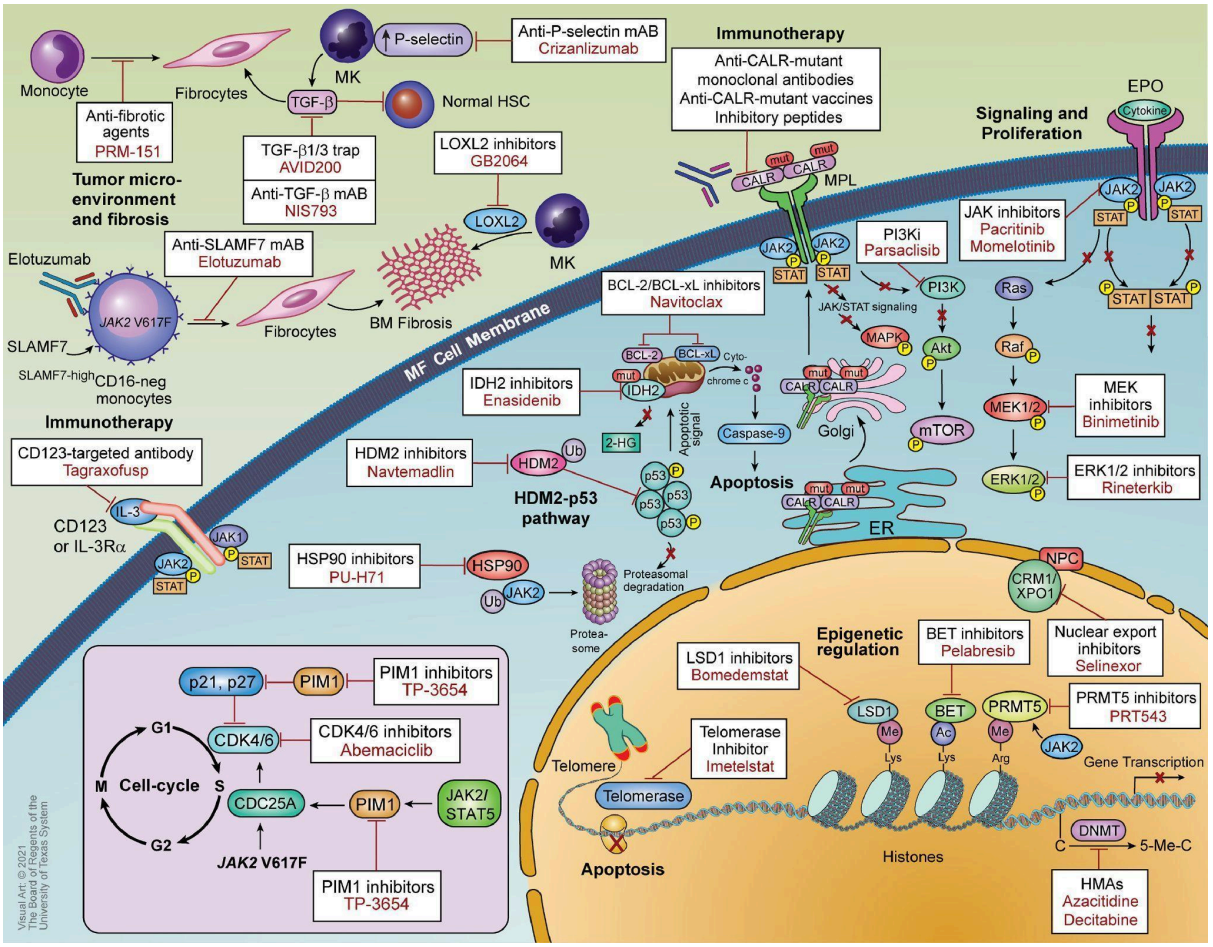

Figure 7. Targets of novel therapeutic agents in clinical development for myelofibrosis: epigenetic regulators, apoptotic and intracellular signaling/proliferation pathways, telomerase, immunogenic antigens, bone marrow microenvironment, and others. Abbreviations: Akt, protein kinase B; BM, bone marrow; CALRmut, mutant calreticulin; C, cytosine; 5-Me-C, 5-methyl-cytosine; CDC25A, Cell division cycle 25A; CDK4/6, cyclin-dependent kinase 4/6; CRM1/XPO1, chromosomal region maintenance 1/exportin 1; DNMT, DNA (cytosine-5)-methyltransferase; EPO, erythropoietin; ER, endoplasmic reticulum; ERK, extracellular signal-regulated kinase; 2-HG, 2-hydroxyglutarate; HMAs, hypomethylating agents; HSC, hematopoietic stem cell; IL-3, interleukin-3; IL-3Rα, interleukin-3 receptor α (CD123); mAB, monoclonal antibody; MAPK, mitogen-activated protein kinase; MEK, mitogen-activated protein/extracellular signal-regulated kinase; MK, megakaryocyte; mTOR, mammalian target of rapamycin; NPC, nuclear pore complex; p21, cyclin-dependent kinase inhibitor 1A; p27, cyclin-dependent kinase inhibitor 1B; PIM1, proviral integration site of Moloney murine leukemia virus serine/threonine-specific kinase 1; Raf, rapidly accelerated fibrosarcoma; Ras, rat sarcoma; Ub, ubiquitin. Adapted from Chifotides *et al*[98]**.**

4. PD-L1 role in cancer

Programmed death ligand 1 (PD-L1), encoded by *CD274*, is a well characterized protein among checkpoint inhibitor molecules. Firstly described in 1999 as a surface antigen present in many tissues, its primary known role is regulating T cells' proliferation and mediating the release of anti-inflammatory cytokines such as IL-10[99]. Soon after its initial identification, PD-L1 relevance in tumor biology became evident when *CD274* was found expressed in cancer cells as a signal molecule able to bind its receptor PD1 on T lymphocytes, causing the inhibition of immune cells activation and ultimately their anergy state. PD-L1 immunological shutdown ability is therefore frequently exploited by neoplastic cells to induce an immune-cold tumor microenvironment[100].

PD-L1 primary structure is formed of 290 amino acids, and its tertiary structure belongs to type 1 transmembrane protein in the immunoglobulin superfamily. It lacks intrinsic kinase activity, but it engages various kinases and protein ligands, such as the costimulatory receptors of T cell activation complex, thus exhibiting an antagonist activity that results in T cell functional deactivation[101].

Throughout the years, several studies of biological activity led to a broad assessment of PD-L1 relevance in cancer immunology. Curiel *et al.* reported how the treatment with a PD-L1 neutralizing antibody was able to improve T cells' activation through the expression of the immune response cytokines interleukin-2 and interferon gamma, and that PD-L1-specific antibody treatment sustained lymphocytes-mediated anti-cancer activity in mouse models[102]. Such evidence led to the development of the class of immune checkpoint blockade agents, which found application in different diseases. Nevertheless, the use of anti-PD-L1 and anti-PD1 treatments often proved to be insufficient for the control of neoplastic pathologies, suggesting a more complex biological mechanism of action.

PD-L1 exhibits a dual signalling role, specifically a cell-extrinsic and a cell-intrinsic effect[100] (**Figure 8**).

Its extrinsic role can be identified in the PD-L1/PD1 interaction, which follows PD1 downstream activation, whose effects are mediated by second messengers within the cellular context of $PD1^+$ immune cells, such as T cells.

On the other hand, PD-L1 intrinsic role is exerted within PD-L1-expressing cells. Consistently, PD-L1 reverse signalling triggered by PD1/PD-L1 interaction has been reported in various tumor types, potentially mediated by its intracellular domain and able to promote PD-L1^{+} cells growth[103–105]. Post-translational modifications such as acetylation mediated mainly by p300 and HDAC2 enzymes have also been described as involved in PD-L1 intracellular relocalization, undermining the efficacy of immunomodulating therapies[106]. When localized in the nuclear space, PD-L1 was found associated with specific promoter regions with a cofactor-like behaviour, and associated with the transcription of oncogenic gene signatures[107].

Finally, as regards PD-L1 role in MPNs, its expression has been positively correlated with JAK2V617F mutational burden, and PV patients displayed the highest mRNA expression levels in neoplastic myeloid cells compared to ET and MF patients. PD-L1 was also shown to be upregulated on MPN HSPC surface, and its exposure was downregulated by JAK inhibitor treatment[108]. This significant correlation between PD-L1 and JAK2V617F corroborates a potential role of PD-L1 in MPN pathogenesis.

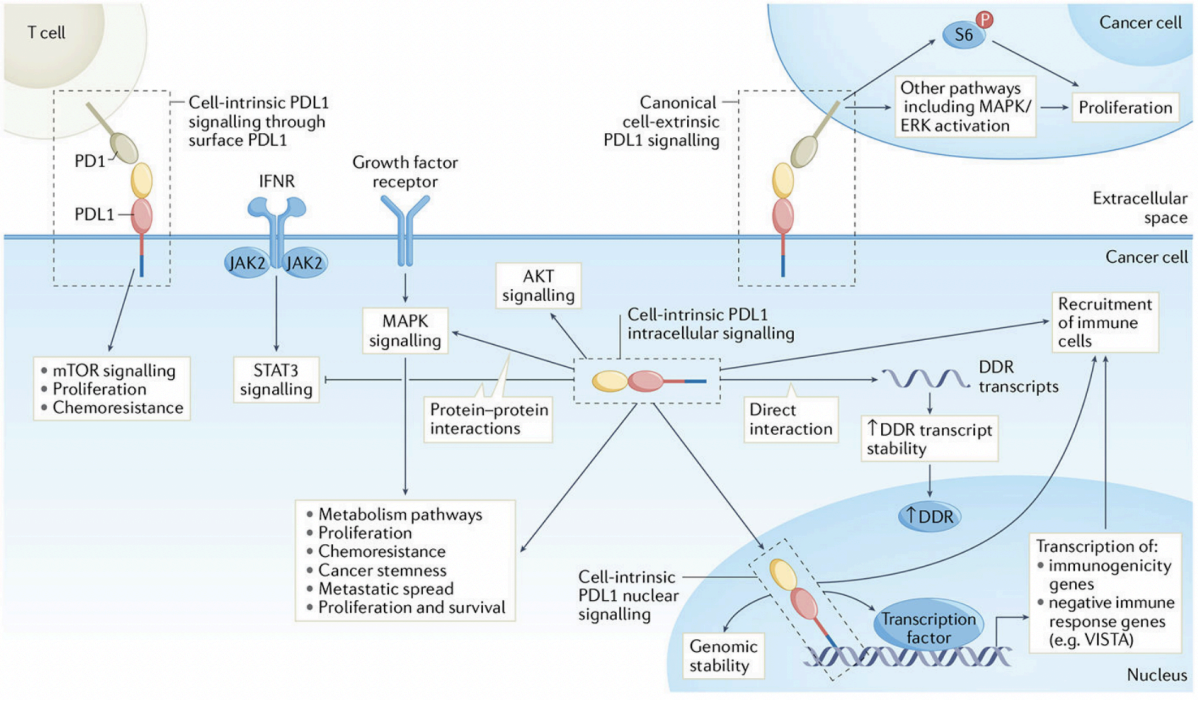

Figure 8. Overview of PD-L1 cell-intrinsic trafficking and signalling in cancer cells. Abbreviations: DDR, DNA Damage Response; IFNR, Interferon Receptor. Adapted from Kornepati *et al.*[100].

EXPERIMENTAL PLAN

Chronic Philadelphia-negative Myeloproliferative Neoplasms (MPNs) are a group of hematological malignancies that includes three different disorders: Polycythemia Vera (PV), Essential Thrombocythemia (ET), and Primary Myelofibrosis (PMF). Among MPNs, PMF represents the pathological condition distinguished by the most aggressive phenotype, inferior survival, and higher risk of Acute Myeloid Leukemia evolution. PV, ET and PMF often present with mutually exclusive 'Driver mutations' affecting *MPL*, *JAK2*, or *CALR* genes, strongly guiding oncogenic proliferation of hematopoietic stem and progenitor cells (HSPCs) through the hyperactivation of the JAK/STAT signalling pathway[3].

Additional genetic alterations affect, among others, epigenetic remodelers, splicing regulators and DNA damage repair genes, and concur to the generation of complex genotypes which negatively affect MPN prognosis and response to treatment[35]. Beside gene point mutations, insertions and deletions, many chromosomal anomalies can arise resulting in inheritable copy number variations and in shaping the fitness of affected neoplastic clones. As a matter of fact, alongside many described characteristic genetic mutations, cytogenetic abnormalities are commonly observed in Myeloproliferative Neoplasms (MPNs), particularly involving chromosome 9[81].

Using an NGS-based genomic analysis on peripheral blood MPN samples, we identified a subset of patients positive for JAK2 driver mutation and reporting a copy number gain involving JAK2 gene itself.

Since JAK2V617F allele frequency most significantly impacts on MPN disease severity and phenotype[109], we investigated the significance of such genomic result by validating *JAK2* gene ploidy status through a Multiplex Ligation-dependent Probe Amplification (MLPA) PCR-based assay; we also outlined that the copy number gain was not restricted to *JAK2* locus, since the minimum common duplicated region always involved the whole chromosome 9 short arm (9p). Considering that *JAK2* gene is located on 9p, we speculated whether 9p copy number abnormalities might represent a disease modifier in JAK2V617F-mutant MPN patients.

Based on these premises, in my PhD project, we sought to characterize the effects of 9p copy number variations on JAK2-mutated hematopoiesis. The starting point was the tracking of 9p copy number gain in HSPCs, as well as in terminally differentiated cells. To reach our aim, we studied the acquisition order of 9p duplication (+9p) and JAK2 mutation, the clonogenic and differentiation potential associated with specific genotypes, and other biological processes influenced by 9p duplication.

We gathered a cohort of 32 MPN patients, split into three experimental groups according to *JAK2*V617F zygosity and 9p copy number status determined through next-generation sequencing and cytogenetics. The groups were identified as JAK2-heterozygous, JAK2-homozygous, and +9p.

To approach the resolution of the clonal hierarchy of the neoplastic fraction, clonogenic assays were set up to retrieve DNA samples from single $CD34^+$ cells-derived colonies; colony genotyping through ddPCR discriminated the presence of 9p amplification and of *JAK2* wild type and mutated alleles, allowing the reconstruction of the evolutionary sequence of molecular events which led to the observed genomic asset. To validate the data observed in colony culture, we performed single-cell genomic analysis of circulating $CD34^+$ HSPCs and CD34- differentiated cells in a MF patient, which allowed the reconstruction of the order of acquisition of molecular alterations using a reliable culture-independent approach (**Figure 9**).

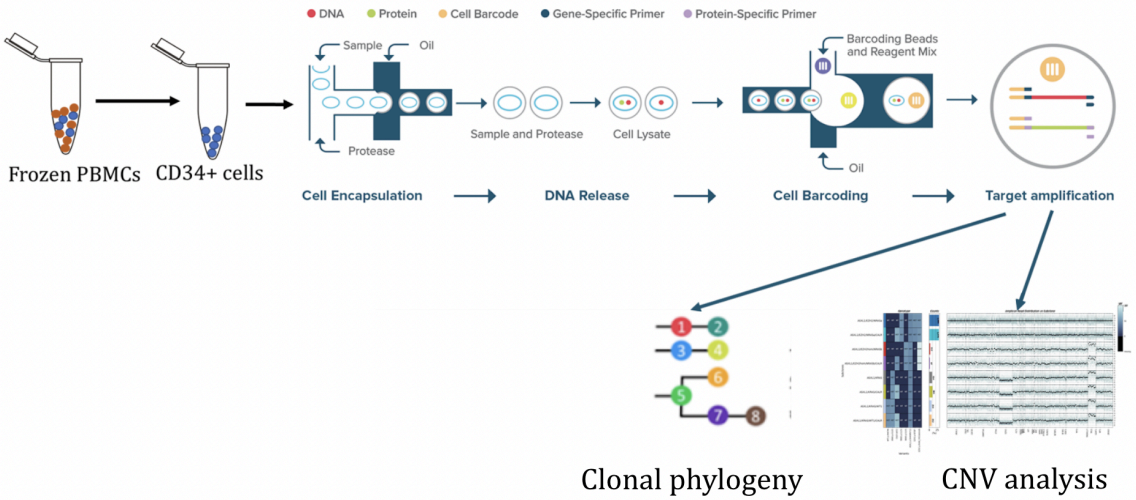

Figure 9. Single-cell genomics workflow. Abbreviations: PBMCs, Peripheral Blood Mononuclear Cells; CNV, Copy Number Variation. Created with Biorender.com

To inspect the functional features of mutated cells, we moved on by analyzing the clonogenic potential and the differentiation capacity of HSPCs from the three classes of patients by means of methylcellulose- and collagen-based clonogenic assays.

Since trisomy involved the entire short arm of chromosome 9, many other genes were amplified besides *JAK2*. We started by investigating the effect of the duplication of *CD274*, which is located downstream *JAK2* and encodes Programmed Death-Ligand 1 (PD-L1). *CD274* expression in blood cell subpopulations from each patient's group was recorded by means of real time qRT-PCR. Of note, a work published by Almozyan *et al*. showed that PD-L1 is able to promote the expression of the pluripotency factors *POU5F1* and *NANOG* in breast cancer through AKT activity[110], and we took the chance to investigate this mechanism also in MF. *POU5F1* (encoding OCT4) and *NANOG* expression levels were then inspected through real time qRT-PCR in bulk $CD34^+$ patients' cells. To provide evidence that the PD-L1/AKT/OCT4 NANOG axis is active in our *CD274* overexpressing samples, we evaluated whether +9p HSPCs displayed a higher dependency on AKT signalling to sustain the observed increased clonogenicity; to this end, we set up clonogenic assays in the presence of an AKT inhibitor.

To link precise cellular genotypes to *CD274*, *POU5F1* and *NANOG* transcripts upregulation, we carried out a combined analysis by means of ddPCR, allowing a coupled genomic-transcriptomic characterization of colonies as reported in **Figure 10**.

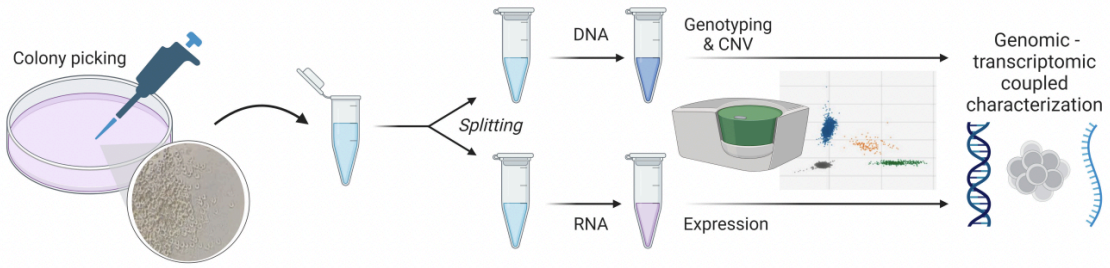

Figure 10. Experimental workflow of genomic/transcriptomic-coupled characterization of single-cell derived colonies by means of ddPCR. Abbreviations: CNV, Copy Number Variation. Created with Biorender.com

To validate the involvement of OCT4 and NANOG in eliciting the observed biological effects, clonogenic assays were set up after silencing the two factors in $CD34^+$ cells through small interfering RNA nucleofection.

Besides the reported cell-intrinsic role of PD-L1, a large body of evidence described the cell-extrinsic role of PD-L1/PD-1 axis in mediating immune evasion of neoplastic clones in MPNs[111]. In addition, more recent studies reported that PD-L1 expression levels are significantly correlated with granulocytic JAK2V617F mutational burden[108].

Starting from these considerations, *CD274* deregulation was also investigated at the protein level in monocytes; cytofluorimetric analysis allowed the measurement of $PD\text{-}L1^+$ fraction within monocytes in each experimental group, while PD-L1 cellular localization was highlighted by *in situ* immunofluorescence. Finally, to understand whether PD-L1 exposure on monocytes' surface could play a role in immune surveillance impairment in line with literature reports, MPN patients' $CD8^+$ T lymphocytes were analyzed by flow cytometry to evaluate the expression of several exhaustion markers.

As a whole, my PhD project aimed at characterizing the biological features of a particular subset of JAK2V617F-positive MPN patients distinguished by 9p trisomy. The study of the deregulated molecular signalling established after +9p contributes to a better understanding of disease pathogenesis in 9p trisomic patients which might be functionally separated from the canonical classification of JAK2 heterozygous and homozygous MPN patients. This work can therefore lay the foundation for further investigations to shape both clinical understanding and therapeutic strategy for +9p MPN patients, taking into account the critical role of PD-L1 deregulation.

MATERIALS AND METHODS

1. Ethics statement

This study was performed on a cohort of 18 healthy donors and 32 patients with a diagnosis of ET, PV, primary or secondary MF, followed by the Hematology department of Azienda Ospedaliera-Universitaria of Modena, Institutional MPN database of the Hematology Unit, University of Insubria (Varese, Italy), or Azienda Ospedaliero-Universitaria Careggi (Florence, Italy). ET, PV, and MF were diagnosed according to 2016 World Health Organization criteria[112], while the International Working Group for Myeloproliferative neoplasms Research and Treatment criteria were used for sMF diagnosis[113].

The study was conducted in accordance with the Declaration of Helsinki under the local Institutional Review Board's approved protocol. All subjects involved in the study provided informed written consent.

2. Purification of cell populations from peripheral blood and culture conditions

Collection and culture of peripheral blood (PB) samples and cell fractions of enrolled patients and healthy donors were achieved as previously described[114,115]. In detail, PB samples were drawn via venipuncture in EDTA-containing tubes, and diluted with PBS +2mM EDTA. Peripheral blood mononuclear cells (PBMCs) were isolated through density gradient centrifugation (Lympholyte H, Cedarlane, Burlington, Canada). $CD34^+$ cells, $CD3^+$ cells and $CD14^+$ cells were positively selected from PBMCs via immunomagnetic separation by using CD34 MicroBead Kit UltraPure, CD3 MicroBead Kit UltraPure and CD14 MicroBead Kit UltraPure, respectively (Miltenyi Biotech, Auburn, CA, USA). Granulocytes were isolated from the cell pellet containing both erythrocytes and granulocytes formed after density gradient centrifugation, by using ammonium chloride-based red blood cell lysis reagent. After immunomagnetic separation, $CD34^+$ cells were cultured at a concentration of 5×10^5 cells/ml in Iscove's modified Dulbecco's medium (IMDM) (ThermoFisher Scientific, Waltham, MA, USA) supplemented with 20% Fetal Bovine Serum (Sigma-Aldrich, St. Louis, Missouri, United States), SCF (Stem Cell Factor, 50 ng/ml), Flt3L (Flt3-ligand, 50 ng/ml), TPO (Thrombopoietin, 20 ng/ml), IL-6 (Interleukin-6, 10 ng/ml) and IL-3 (Interleukin-3, 10 ng/ml) (all cytokines from Miltenyi Biotech, Auburn, CA, USA).

3. Next generation sequencing (NGS)

Targeted DNA sequencing was performed on genomic DNA extracted from whole PB of MPN patients, as detailed in previous work[52]. In detail, targeted DNA sequencing on genomic DNA extracted from whole PB samples of MPN patients was performed through a Capture-based target enrichment kit—CE-IVD Myeloid SolutionTM (Sophia Genetics, Lausanne, Switzerland) on the Illumina MiSeq platform. FASTQ files were processed using SOPHiA DDM platform, based on SOPHiA Artificial Intelligence (version 4.1.1 Build 510, JSI Medical Systems, Ettenheim, Germany). The minimum required coverage rate was set to 1000×. Somatic mutations validity was checked against the publicly accessible COSMIC v69 database (http://cancer.sanger.ac.uk/cancergenome/projects/cosmic), and their functional interpretation was performed using SIFT 1.03 (http://sift.jcvi.org), PolyPhen 2.0 (http://genetics.bwh.harvard.edu/pph2) and MutationTaster 1.0 algorithms (http://www.mutationtaster.org). Single nucleotide polymorphisms were annotated based on NCBI dbSNP (http://www.ncbi.nlm.nih.gov/snp; Build 137) and gnomAD (http://gnomad.broadinstitute.org; gnomAD r2.0.1) databases.

4. Multiplex ligation-dependent probe amplification (MLPA) analyses

MLPA analysis was performed on 50 ng of DNA extracted from whole PB, $CD34^+$ cells, $CD14^+$ cells, $CD3^+$ cells, or granulocytes using P474 MLPA kit (MRC-Holland, Amsterdam, Netherlands), following the manufacturer's instructions. Fragment analysis was performed through the 3130xl Genetic Analyzer instrument (Applied Biosystems), and resulting data were analysed using Coffalyser.net software (MRC-Holland), as previously described[116].

5. Methylcellulose and collagen clonogenic assays

For each patient, 300 $CD34^+$ cells were seeded in triplicate in 1 ml of semisolid methylcellulose-based medium supplemented with cytokines for hematopoietic progenitor growth (MethoCult GF H4434; StemCell Technologies Inc., Vancouver, Canada), as previously described[117]. Colonies were enumerated and scored after 14 days of incubation.

MK colony forming units (CFU-MK) were assayed in collagen-based medium, by seeding 5000 $CD34^+$ cells isolated from PB in each chamber of a double-chamber slide from a commercial MK assay detection kit (MegaCult-C; StemCell Technologies Inc.), as previously reported[118]. Colonies were scored after 11 days of incubation following the manufacturer's protocol.

6. *POU5F1* and *NANOG* silencing in CD34+ cells

Frozen $CD34^+$ cells underwent nucleofection by using 4D-Nucleofector System (Lonza, Basel, Switzerland). Briefly, preserved $CD34^+$ cells from JAK2V617F-homozygous and +9p patients were thawed and, starting from the second day after thawing (+48h), each sample was electroporated twice, with a 24h interval between each reaction. 3 μg of a small interfering RNA (siRNA) targeting human POU5F1 mRNA (ThermoFisher Scientific, siRNA ID s10873) and NANOG mRNA (ThermoFisher Scientific, siRNA ID s36650) were used per sample each nucleofection cycle. To exclude non-specific effects caused by interfering RNA (RNAi) nucleofection, it was included a sample transfected with a Silencer™ Select Negative Control No. 1 siRNA (ThermoFisher Scientific). Methylcellulose-based clonogenic assays were set up 12h after the last nucleofection, seeding 300 $CD34^+$ cells from each condition. Nucleic acids extracted from individual colonies isolated after 14 days of incubation underwent droplet digital PCR (ddPCR) analysis as detailed below.

7. AKT-inhibitor treatment of CD34+ cells in methylcellulose assay

Frozen $CD34^+$ cells from JAK2-homozygous or +9p patients were thawed and maintained in liquid culture as described above. 48h later, 300 cells were seeded in triplicate in 1 ml of semisolid methylcellulose-based medium (MethoCult" GF H4434; StemCell Technologies) supplemented with 1μM MK2206 or DMSO (0.1%) as negative control. Colonies were scored and individually picked after 14 days of incubation. DNA and RNA extracted from isolated colonies was used for ddPCR analysis as detailed below.

8. DNA extraction

For each MPN patient, DNA was extracted from purified $CD34^+$ cells, $CD14^+$ cells, $CD3^+$ cells, and granulocytes by means of DNeasy Blood & Tissue Kit (Qiagen, Hilden, Germany) following the recommended protocol.

Single cell-derived colonies' DNA was extracted using Arcturus PicoPure DNA Extraction Kit (Applied Biosystems, Waltham, Massachusetts, USA), according to manufacturer's instructions.

9. RNA extraction and reverse transcription

Total RNA from Granulocytes, $CD14^+$, or $CD34^+$ cells was extracted using the miRNeasy Micro Kit (Qiagen, Hilden, Germany) as previously reported[119]. Next, reverse transcription was performed on an amount of 100 ng of total extracted RNA, by means of High-Capacity cDNA Reverse Transcription Kit (ThermoFisher Scientific, Waltham, Massachusetts, USA) as previously described[120].

For the extraction from single-cell derived colonies, RNA was isolated and retro-transcribed by means of TaqMan™ Gene Expression Cells-to-CT™ Kit (ThermoFisher Scientific) following the manufacturer's protocol.

10. Quantitative Real-Time PCR (qRT-PCR)

Quantitation of *CD274*, *POU5F1* and *NANOG* gene expression in cDNA from Granulocytes, $CD34^+$ cells or $CD14^+$ cells was carried out by means of qRT-PCR. Amplification reactions were performed in triplicate for each sample, using TaqMan™ Fast Advanced Master Mix and TaqMan probes specific for *CD274* (Hs00204257_m1), *POU5F1* (Hs04260367_gH), NANOG (Hs02387400_g1) or *GAPDH* (Hs03929097_g1) as endogenous control. Reactions were run on Applied BiosystemsTM QuantStudioTM 12K Flex Real-Time PCR System (ThermoFisher Scientific). Gene expression data were analysed using the ΔΔCT method, using healthy donors as calibrators.

11. Droplet digital PCR (ddPCR) assay

For the genotyping of JAK2, 10ng of DNA from each sample were assayed through ddPCR to quantify the copies of JAK2p.G571S (ddPCR Mutation Assay: dHsaMDS2512546; Bio-Rad Laboratories Inc.) and JAK2V617F (ddPCR™ Mutation Assay: dHsaMDV27944642; Bio-Rad Laboratories Inc.). *JAK2* copy number was determined through the quantification of *JAK2* (using ddPCR™ Copy Number Assay: dHsaCP1000500; Bio-Rad Laboratories Inc.) normalized on *AP3B1* gene copies (ddPCR™ Copy Number Assay: dHsaCP2500348; Bio-Rad Laboratories Inc.), according to manufacturer's instructions. *AP3B1* gene was employed as diploid reference for this analysis.

For coupled genomic-transcriptomic assay, isolated colonies were split in half to recover DNA and RNA, as detailed above. JAK2V617F genotyping and *JAK2* copy number analysis were performed as described above. For the quantitation of *CD274*, *POU5F1* and *NANOG* gene expression, amplification reactions were performed on colonies' cDNA by using ddPCR Supermix for Probes (No dUTP) (Bio-Rad Laboratories Inc.) and TaqMan probes specific for *CD274* (Hs00204257_m1), *POU5F1* (Hs04260367_gH), *NANOG* (Hs02387400_g1) or *GAPDH* (Hs03929097_g1) used as endogenous control (all probes from ThermoFisher Scientific). For all ddPCR reactions, droplet generation was achieved through QX200™ Droplet Generator. ddPCR reactions were performed using QX200 Droplet Digital PCR (ddPCR™) System (Bio-Rad Laboratories Inc.), setting 56°C as annealing temperature for genotyping and copy number analysis, and 59°C as annealing temperature for gene expression analysis. Positive droplets measurement was determined using the QX200™ Droplet Reader (Bio-Rad Laboratories Inc.).

12. Single cell DNA library preparation and sequencing

Frozen PBMCs were thawed following 10× Genomics® "Sample Preparation Demonstrated Protocol" (10× Genomics, Pleasanton, CA, USA). PBMCs and purified $CD34^+$ cells were mixed at a 1:1 ratio and then processed through Tapestri™ Platform (Mission Bio, San Francisco, CA, USA) as previously described[53]. Barcoded samples underwent targeted PCR amplification. After emulsion breaking, PCR products were purified with AMPure XP beads (Beckman Coulter, Brea, CA, USA), and Illumina i5/i7 indices were incorporated through PCR. Primer dimers were subsequently removed from the reaction through AMPure XP magnetic beads and the resulting library was quantified via Qubit™ 4 Fluorometer (ThermoFisher Scientific, Waltham, MA, USA) and Agilent 2100 Bioanalyzer (Agilent Technologies, Santa Clara, CA, USA). The obtained genomic library was sequenced with 2x150bp paired-end chemistry on an Illumina NovaSeq platform (service by Macrogen Inc, Seoul, South Korea).

Paired FASTQ files were analyzed using Tapestri Pipeline V2. The software performs an initial quality control, adaptor trimming, reads alignment (hg19 assembly), read-cell barcode association and variant calling through GATK v.3.7 algorithm, generating a VCF file. The output .h5 file created by Tapestri Pipeline was then employed for downstream analyses. Mean panel uniformity among cells was 88%. A total of 8891 cells were sequenced with 38 mean reads/cell/amplicon. Measured allele dropout rate was 12.75%. Mosaic v.3.1.1 algorithm was employed to reconstruct clonal architecture and copy number variations. In order to get an optimal cell genotypization, the following parameters were set: variant genotype quality > 30, at least 10 reads per cell for each variant to define a genotype, and variants genotyped in less than 50% of cells and/or cells with less than 50% of genotyped variants were filtered out. Variants were firstly selected if detected by bulk NGS analysis. Then, germline, intronic and/or synonymous variants were filtered out. The pathogenicity associated with the remaining variants was then assessed by consulting Varsome database (v11.9) to retain potentially pathogenic and reportedly pathogenic variants. Next, we defined genetic clones harboring the previously identified variants. Clones were retained if present in >1% cells and harboring an allele dropout rate score <0.8. As regards CNV analysis, the amplicons were filtered in order to retain only those genotyped in >50% cells. Then, reads normalization was performed and the wild-type clone was set as the diploid reference. To discriminate between diploid and triploid cells, the average ploidy for each amplicon was calculated. Next, 95th percentile of this distribution (2.624748) was set as threshold above which triploid cells were identified. To identify +9p cells, the mean ploidy level of the amplicons spanning across chromosome 9p was computed for each cell (**Table 2**). Cells with mean ploidy > 2.624748 were identified as +9p cells.

Chr	Amplicon_start	Amplicon_end	Forward_seq	Reverse_seq	Target
9	5064833	5065063	TGGAGTTGACTTTCTAAAAGGTGCTATTT	ACTTTTAAGTCTGTATTACTCACGAAATTG	JAK2
9	5069842	5070081	ACACATTTCATTTTACTCCTCTTTGGA	AAGACAGTAATGAGTATCTAATGACTTACA	JAK2
9	5073652	5073881	GGACAACAGTCAAACAACAATTCTTT	CACTGACACCTAGCTGTGATCC	JAK2

Table 2. JAK2 amplicons included in the single cell genomic panel.

To record the number of JAK2 mutated alleles in each cell, the variant allele frequency for JAK2V617F was employed to classify cells in the following classes: for diploid cells, VAF between 0% and 10% identified WT cells, VAF between 10% and 90% defined JAK2V617F heterozygous cells, and VAF>90% identified JAK2V617F-homozygous cells; for +9p cells in turn, a VAF threshold inferior to 10% identified WT cells, a VAF between 10% and 50% defined cells with 1 JAK2V617F-mutated allele, VAF level between 50% and 90% identified

cells with 2 JAK2V617F-mutated alleles, and a VAF exceeding 90% defined triploid JAK2V617F-homozygous cells. The distribution of cells based on JAK2 genotype and copy number was obtained through ggplot2 geom_jitter plotting function.

13. Flow cytometry

To avoid aspecific antibodies' binding, $CD14^+$ and $CD3^+$ cells purified from PB of patients were incubated 10 minutes at 4°C in the dark with "FcR Blocking Reagent, human" (Cat. no. 130-059-901, Miltenyi Biotech, Cologne, Germany) and subsequently stained using anti-PD-L1 (PE, clone 29E.2A3) and anti-$CD14^+$ (APC-Vio770, clone TÜK4) antibodies (1:50 in PBS 1X + 5% FBS) (all from Miltenyi Biotech), then incubated 20 minutes at 4°C in the dark. $CD3^+$ cells isolated from PB of patients were stained using anti-CD3 (APC-Vio770, clone REA613) (Miltenyi Biotech), anti-CD4 (PerCP/Cy5.5, clone A161A1), anti-CD8 (FITC, clone SK1), anti-PD-1 (BV421, clone EH12.1H7), anti-PD-L1 (APC, clone 29E.2A3), anti-CD57 (Alexa Fluor 647, clone HNK-1), anti-CTLA-4 (PE/Cyanine7, clone BNI3), anti-LAG-3 (PerCP/Cy5.5, clone 11C3C65), anti-TIM3 (PerCP/Cy5.5, clone F38-2E2) and anti-CD244 (PE, clone C1.7) antibodies (1:50 in PBS 1X + 5% FBS) (BioLegend, San Diego, California) and incubated 20 minutes at 4°C in the dark. Cell viability of samples was assessed through LIVE/DEAD™ Fixable Aqua Dead Cell Stain Kit (ThermoFisher Scientific), according to manufacturer's instructions. Stained cells were then analysed using BD FACSCanto II (BD Biosciences; San Jose, CA, USA) as previously described[121]. Data was analysed by FlowJo (version 10.7.1).

14. Immunofluorescence staining

Cytospin slides of $CD14^+$ cells were fixed with 4% paraformaldehyde and permeabilized using 0.2% Triton X-100 in PBS for 10 minutes. After blocking with 1% BSA in PBS, slides were incubated for 16 hours at 4°C with rabbit monoclonal anti-human PD-L1 antibody (Cell Signaling Technology, Inc., Danvers, Massachusetts, USA) at a dilution of 1:50. The slides were subsequently incubated with goat anti-rabbit Alexa Fluor 568-conjugated secondary antibody (Invitrogen, Carlsbad, CA) and mouse anti-human CD14 FITC-conjugated antibody (Miltenyi Biotech), each at a dilution of 1:50, leaving the hybridization reaction for 2h at room temperature in the dark. All the aforementioned incubations were followed by 3 washes with PBS solution. Nuclear counterstaining was performed with 49,6-diamino-2-phenylindole (DAPI). Slides were then mounted with Dako Fluorescence Mounting Medium

(Sigma-Aldrich). Finally, fluorescence imaging capture of representative areas was performed using Zeiss LSM 510 Meta Confocal Microscope (Zeiss, Germany).

15. Statistical analysis

Statistical analyses were performed using GraphPad Prism version 8.4.0 (GraphPad Software, San Diego, CA, USA).

After passing a normality test, comparisons between three or more groups of numerical variables with normal distribution were performed using one-way ANOVA test, while Kruskall-Wallis nonparametric test was performed for data with non-Gaussian distribution. Comparisons between two groups of numerical variables were then performed using Uncorrected Fisher's Least Significant Difference (LSD) test after one-way ANOVA test, while Uncorrected Dunn's test was performed for multiple comparisons after Kruskal-Wallis test. Two-tailed Student t-tests were employed for average comparisons in unpaired samples with Gaussian distribution, while nonparametric Mann-Whitney test was performed if samples harbored normal distribution. Categorical variables were compared through Fisher's exact test or χ-square test. Sample size for each experimental condition is provided in the corresponding Figure Legend. p-values <0.05 were considered as statistically significant.

RESULTS

1. Identification of a subset of MPN patients carrying 9p duplication

To characterize the genomic profile of newly diagnosed MPN patients from affiliated hospital hematology clinic, our laboratory routinary performs NGS analysis on patients' whole blood samples collected at diagnosis. To this end, we employ the SOPHiA NGS Myeloid panel which can detect genomic mutations and copy number variations associated with each sample.

The genotype of a fraction of patients notably displayed a JAK2 locus copy number gain (**Figure 11**). Intriguingly, all the identified patients sharing such amplification also presented with JAK2V617F driver mutation.

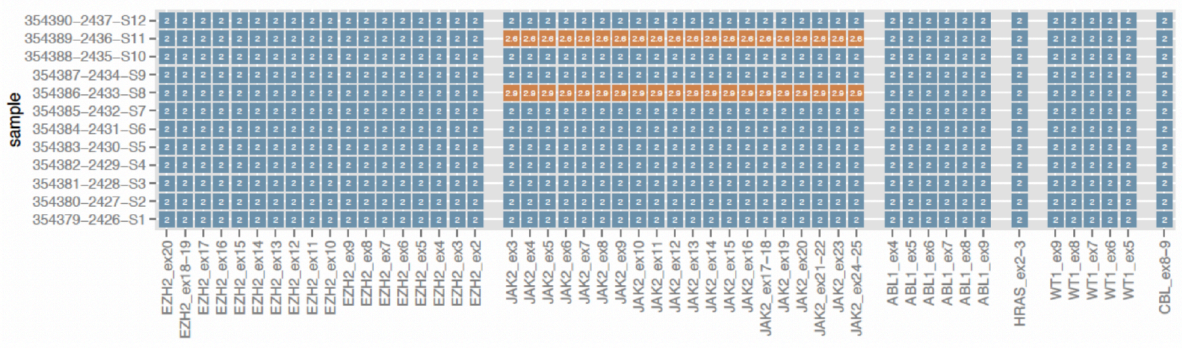

Figure 11. Representative NGS CNV of MPN patients. JAK2 copy number gain detected in two patients with a Next Generation Sequencing panel performed on peripheral blood. On x-axis, panel amplicons reference; on y axis, patients' ID. The first displayed JAK2-amplified patient reported a count of 2,6 copies of JAK2, while a second patient reported a count of 2,9 copies.

Considering that JAK2V617F VAF has a major impact on disease severity and that any copy number alteration involving its locus can be of clinical significance for disease evolution, we validated the copy number count of *JAK2 in these patients* through MLPA (**Figure 12**).

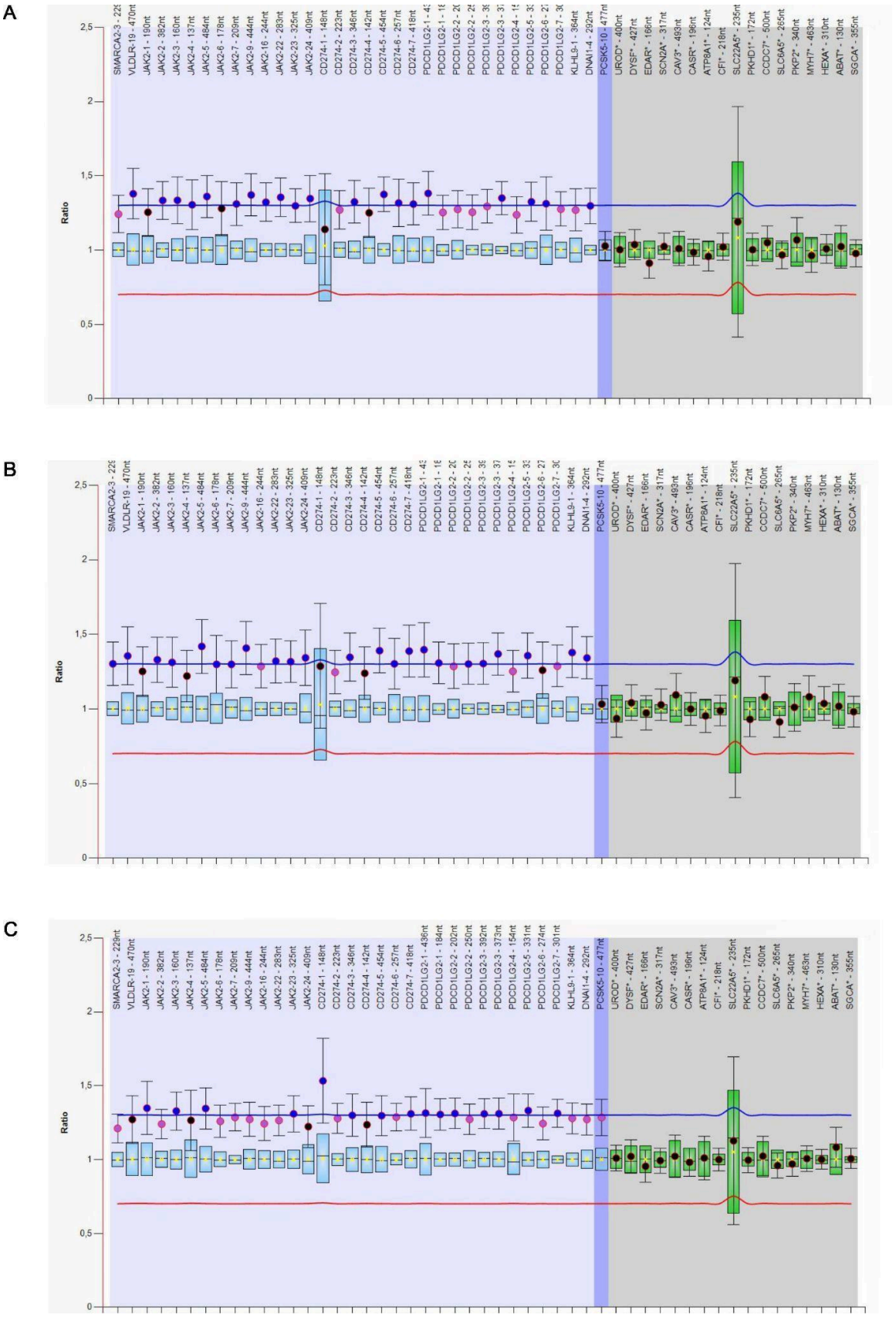

Figure 12. MLPA validation of 9p amplification in patients #1-3. MLPA copy number profiling of chromosome 9 in DNA extracted from Whole Peripheral Blood samples of patients #1 (A), #2 (B), and #3 (C). On the horizontal axis are plotted the genomic regions assayed by MLPA probes; on the vertical axis is shown the ratio between the signal of the patient's probe and the signal of the reference sample. Light blue area comprises the probes mapping on 9p. Probe in purple area maps on

chromosome 9q. Grey area includes reference probes. Blue horizontal line identifies the threshold above which a probe's signal identifies an amplified region, therefore a copy number gain. Red horizontal line identifies the threshold below which a probe's signal identifies a deleted region, therefore a copy number loss. Data analysis was performed with Coffalyser.net software.

The results of MLPA on sequenced patients confirmed the copy number gain of *JAK2* locus. In addition, MLPA probes covering other loci on chromosome 9 short arm resulted amplified as well, providing evidence that the patients shared a higher-order alteration and not just an amplification confined to *JAK2* locus amplification. Concerning the extension of the genomic alteration, we were able to infer that chromosome 9 long arm (9q) was not affected by the copy number alteration thanks to the presence of a MLPA probe mapping in *PCSK5* gene included in 9q (**Figure 12**). According to MLPA, *PCSK5* copy number count was equal to control probes' quantity, thereby demonstrating that the observed chromosomal amplification in this subset of MPN patients does not involve chromosome 9q.

Starting from the description of this cytogenetic alteration, we speculated whether 9p duplication could affect disease pathobiology in terms of functional and biological features of the affected clones, and whether it retains any relation with JAK2V617F allele burden. To this end, gathered a group of 12 JAK2-mutated patients reporting the amplification of chromosome 9, identified using NGS based genotyping, clinical karyotyping, and/or MLPA analysis. Chromosome 9 short arm represented the minimal amplified region as a fraction of patients presented with 9p amplification, while those remaining exhibited the duplication of the entire chromosome 9, as reported in **Table 3**. Two control groups of MF patients were included, a JAK2-homozygous group and a JAK2-heterozygous group. JAK2V617F driver mutation VAF, co-occurring mutations, disease diagnosis and karyotype are detailed in **Table 3**.

PATIENT	GROUP	JAK2V617F VAF (%)	OTHER MUTATIONS	DISEASE	KARYOTYPE
1	+9p	66.7	CSF3R p.(Met696Thr)	PMF	46,XX,add(18)(p?13)[16]/46,XX[4]
2	+9p	57.0	TET2 p.(Asp1788Gly)	PMF	N/A
3	+9p	52.4	RUNX1 p.(Gly69Arg)	PPV	N/A
4	+9p	47.1	JAK2 p.(Gly571Ser)	PMF	47,XX,+9[13]/46,XX[7]
5	+9p	78.3	/	PPV	47,XY,+9[5]/46,XY[20]
6	+9p	2.3	/	PPV	48,XY,+8,+9[2]/46,XY[28]
7	+9p	79.2	JAK2 p.(Ala554Thr), CSF3R p.(Ala119Thr)	MF	46,XX,add(9)(p24)[8]/46,XX[15]
8	+9p	71.9	/	MPN-U	49,XY,t(1;16)(q12;q11.2),+9,+9der(16)t(1;16)(q12;q11.2)[20]/46,XY[2]
9	+9p	25.9	/	PET	47,XX,+9,del(20)(q11.2q13.3)[1]/46,XX[13]
10	+9p	63.7	CSF3R p.(Glu405Lys)	PET	47,XY,t(3;15)(p25;q24),+9,del(17)(q11.2q22)[22]/46,XY,t(3;15)(del(17))[3]

11	+9p	25.9	CEBPA p.(His195_Pro196dup), SRSF2 p.(Pro95His)	PMF	47,XY,+9[4]/46,XY[16]
12	+9p	81.1	/	PMF	47,XX,+9[2]/46,XX[22]
13	JAK2_HET	55	ASXL1 p.(Gly646Trpfs*12), CBL p.(Cys419Phe)	PET	46,XX[20]
14	JAK2_HET	43.7	RUNX1 p.(Leu58Ser)	PMF	46,XX,del(5)(q15q33)[20]
15	JAK2_HET	48.4	U2AF1 p.(Gln157Arg)	PMF	46,XY[20]
16	JAK2_HET	31.6	ASXL1 p.(Pro1097Arg)	PMF	N/A
17	JAK2_HET	54	SRSF2 p.(Pro95His)	PMF	46,XY[20]
18	JAK2_HET	28.7	ASXL1 p.(Gly646Trpfs*12), ASXL1 p.(Ser770Ter), ASXL1 p.(Glu705*), CEBPA p.(His195_Pro196dup), U2AF1 p.(Gln157Pro), EZH2 p.(Arg288Gln)	PMF	46,XY[20]
19	JAK2_HET	48	/	PPV	46,XY[20]
20	JAK2_HET	39.7	/	PPV	46,XY[20]
21	JAK2_HET	38.9	ABL1 p.(Asn336His)	PPV	N/A
22	JAK2_HET	22.9	/	PMF	N/A
23	JAK2_HOM	87.6	CSF3R p.(Glu149Asp)	PPV	46,XY,del(13)(q12q14),del(20)(q12 [14]/46,XY[6]
24	JAK2_HOM	86	ASXL1 p.(Glu635Argfs*15)	PMF	N/A
25	JAK2_HOM	97.9	RUNX1 p.(Arg233Profs*28), TET2 p.(Met638Ilefs*61), TET2 p.(Phe1287Leufs*76), ASXL1 p.(Met1161Thr)	PPV / PMF	46,XX[20]
26	JAK2_HOM	97.7	SF3B1 p.(Lys700Glu), TET2 p.(His1036Thrfs*19)	PMF	N/A
27	JAK2_HOM	84.6	ZRSR2 p.(Trp291*)	PPV	46,XY[20]
28	JAK2_HOM	80.3	TET2 p.(Met695Cysfs*5)	PPV	N/A
29	JAK2_HOM	99.6	TET2 c.4044+1del	PMF	46,XX[20]
30	JAK2_HOM	71.2	/	PPV	46,XX[20]
31	JAK2_HOM	92.5	ZRSR2 p.(Ser447_Arg448dup), ASXL1 p.(Gly704Arg), ASXL1 p.(Ala861Thr)	PPV	46,XX[20]
32	JAK2_HOM	93.5	ASXL1 p.(Ala636Val)	PET	46,XY[20]

Table 3. Genomic features of JAK2-mutated patients. Abbreviations: VAF, Variant Allele Frequency.

To investigate the global mutational framework of our cohort, a waterfall plot was set up, allowing a comprehensive view of the frequency of co-mutated genes in each experimental group of patients and the mutational burden of each patient. As a result we observed that +9p was negatively correlated with the presence of HMR mutations (ASXL1, SRSF2, EZH2, and IDH1/IDH2) and epigenetic factors mutations (ASXL1, EZH2, TET2, IDH1/2 and DNMT3A) (**Figure 13 panel B, C**). Moreover, homozygous patients group displayed a higher JAK2V617F VAF compared to +9p patients (**Figure 13 panel D**).

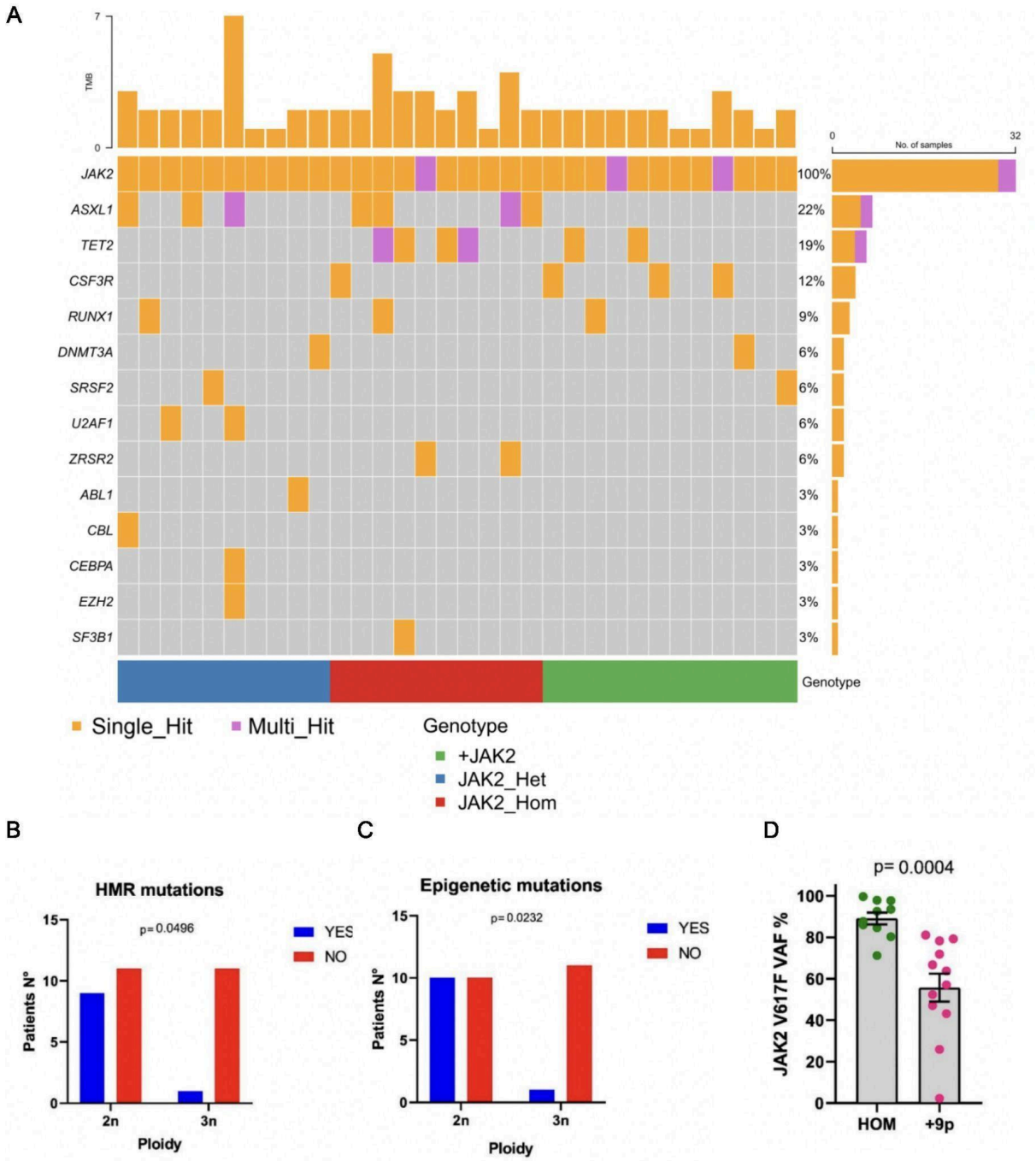

Figure 13. Mutational Profile of enrolled patients and Association of patients' ploidy status with genetic features. (A) Mutational landscape of MPN patients enrolled in the study. The waterfall plot was divided into JAK2-heterozygous patients (blue), JAK2-homozygous patients (red), and patients reporting an amplification of the short arm of chromosome 9 (green). Each column represents the mutational status of a single MPN patient. On the rows are plotted the somatic mutations detected. All patients share JAK2 Driver Mutation. Grey rectangle: absence of corresponding gene mutation in specific patient. Orange rectangle: presence of single-hit mutation of corresponding gene in specific patient. Purple rectangle: presence of multi-hit mutation of corresponding gene in specific patient. Above the plot are depicted the Tumor Mutational Burden (TMB) of each patient. On the right of the plot, the frequencies of each observed mutation in the patients' cohort. Abbreviations: JAK2_Het, JAK2-heterozygous; JAK2_Hom, JAK2-homozygous. (B) Correlation between 9p ploidy status and occurrence of High Molecular Risk (HMR) mutations identified in the study cohort. Abbreviations: 2n = diploid patients; 3n = +9p patients (C) Correlation between 9p ploidy status and occurrence of epigenetic mutations identified in the study cohort. Abbreviations: 2n = diploid patients; 3n = +9p patients. (D) JAK2V617F VAF mean level in HOM patients' group and +9p patients' group. Results

are represented as means ±SEM. Abbreviations: HOM = JAK2-homozygous patients; +9p = JAK2-mutated patients with 9p trisomy.

2. Assessment of chromosome 9 trisomy in hematopoietic cells subpopulations

Next, we sought to determine which cellular types harbors chromosome 9 aneuploidy previously detected in whole blood biopsies. We purified circulating $CD34^+$ hematopoietic stem and progenitor cells, $CD14^+$ monocytes and $CD3^+$ T cells with positive selection by means of immunomagnetic beads, and isolated granulocytes by density gradient. MLPA analysis performed on bulk DNA derived from each cellular population highlighted chromosome 9p copy number gain in three out of four cell types, results from one representative patient are reported in **Figure 14**. Specifically, $CD34^+$ hematopoietic stem and progenitor cells (**Figure 14 panel A**), $CD14^+$ monocytes (**Figure 14 panel B**), and granulocytes (**Figure 14 panel C**) all displayed an increased ratio for probes spanning the entire chromosome 9p, underlining that cells affected by the 9p duplication were of myeloid lineage derivation or hematopoietic stem and progenitor cells. The chromosomal aberration was not found in $CD3^+$ T lymphocytes subpopulation, which present diploid levels of all assayed probes, as reported in **Figure 14**, panel D, denoting a somatic mutational event and excluding the possibility of a germline alteration.

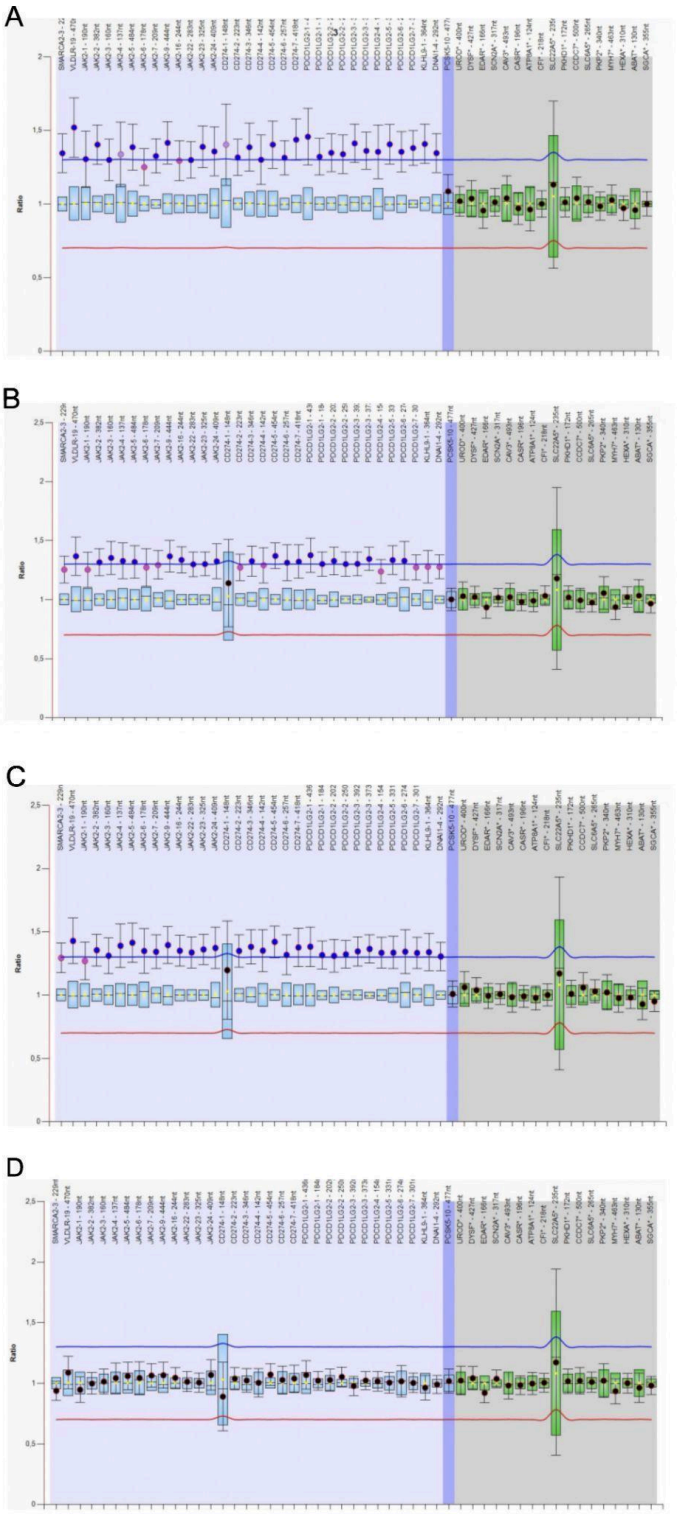

Figure 14. Assessment of chromosome 9 trisomy in sorted blood fractions. MLPA profiling of chromosome 9 copy number status in $CD34^+$ cells (A), $CD14^+$ cells (B), Granulocytes (C), or $CD3^+$ cells (D) purified from patient #2. On the horizontal axis are plotted the genomic regions assayed by MLPA probes; on the vertical axis is shown the ratio between the signal of the patient's probe and the signal of the reference sample. Light blue area comprises the probes mapping on 9p. Probe in purple area maps on chromosome 9q. Grey area includes reference probes. Blue horizontal line identifies the threshold above which a probe's signal identifies an amplified region, therefore a copy number gain. Red horizontal line identifies the threshold below which a probe's signal identifies a deleted region, therefore a copy number loss. Data analysis was performed with Coffalyser.net software.

3. Genetic profiling of +9p patients by means of single-colony ddPCR analysis

Considering the co-occurrence of JAK2V617F and +9p in our cohort of duplicated patients, we investigated the order of acquisition of mutational events leading to the observed genomic asset. Given the broad heterogeneity of each patient's clonal composition, bulk studies would preclude a comprehensive resolution and reconstruction of genetic evolutionary events and relative abundance of resulting cellular clones. For this reason, moving on from the evidence of the presence of +9p in circulating $CD34^+$ stem and progenitor cells identified through MLPA, we exploited methylcellulose-based clonogenic assay to obtain single-HSPC derived colonies. A total of 139 colonies derived from 8 +9p patients included in our cohort were analyzed. By means of ddPCR, we were able to combine two levels of genetic information for each colony. Specifically, JAK2V617F and JAK2wt allele counts were obtained in a first genotyping reaction, while *JAK2* copies count compared to a reference diploid locus was recorded in a second ddPCR run. This approach allowed the dual inference of *JAK2* ploidy and allele burden at the single colony level. **Figure 15 panel A** shows the frequency of colonies harboring each genotype derived from the occurrence of *JAK2* driver mutation acquisition and 9p copy number variation, revealing the absence of +9p colonies lacking JAK2V617F allele and a major representation of 9p duplicated colonies with two mutated *JAK2* copies out of three.

To reconstruct the order of acquisition of *JAK2* mutation and its duplication, colonies were classified based on *JAK2* mutational status and copies and represented in a jitter plot (**Figure 15 panel B**). The most represented genetic asset of +9p patients' colonies was 9p gain with two mutated *JAK2* alleles, while the relative abundance of the other genetically distinct clones provided the most probable chronological sequence of molecular events. Diploid heterozygous colonies appeared as the putative preceding clone, leading to the generation of the most frequent genetic asset through a single duplication event of *JAK2*-mutated chromosome.

Notably, one patient of the +9p group held a non-canonical *JAK2* mutation, specifically JAK2G571S, located upstream of the JAK2V617F driver mutation. This molecular marker enabled the discrimination through ddPCR of an additional step in the acquisition order of mutational events, confirming that the amplification of 9p follows the acquisition of both mutations' (**Figure 15 panel C**).

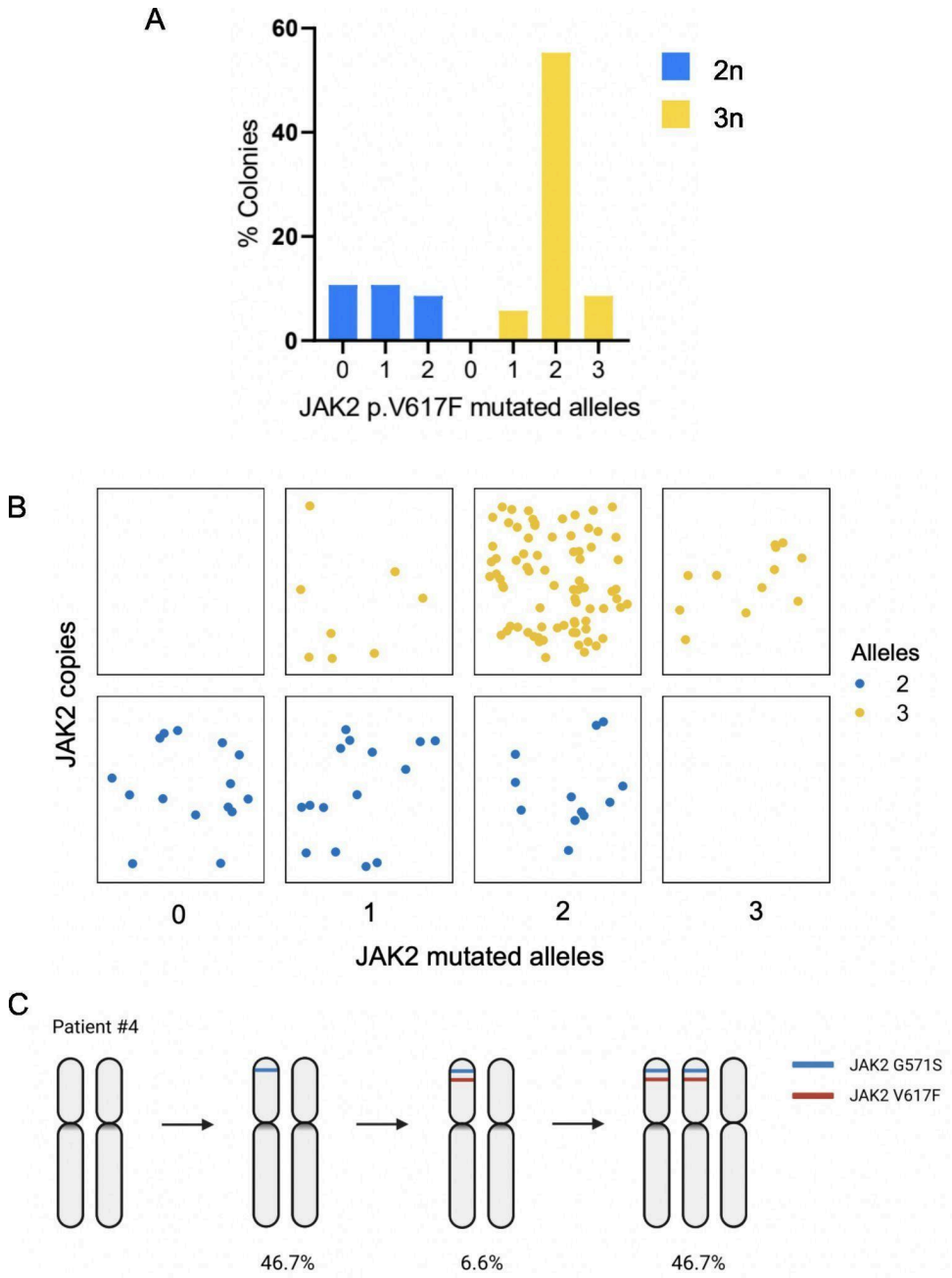

Figure 15. ddPCR analysis of JAK2 mutational burden and copy number on DNA of single HSPC-derived colonies from +9p patients. (A) Frequencies of *JAK2* mutational burden split between diploid and +9p colonies (n = 139 colonies, with 17 average colonies per patient across 8 patients). Abbreviations: +9p, chromosome 9p trisomic colonies. (B) Jitter plot displaying the representation of each combination of *JAK2* copies (y axis) and JAK2 mutational status (x axis) detected in colonies. (C) Graphical representation showing the order of occurrence of molecular events inferred by ddPCR from colonies of patient #4 HSPC (n = 15 colonies). Percentages indicate the frequency of colonies carrying the above setting of 9p ploidy and *JAK2* genotype. Created with Biorender.com

4. Genetic profiling of a +9p patient by means of single-cell genomic analysis

To overcome the possible biases associated with the growth of colonies in methylcellulose-based semisolid medium, such as genotype-linked growth advantage or retromutations, we validated the results obtained with colony genotyping using a single-cell genomic approach. Through Tapestri™ single-cell genomic platform, circulating $CD34^+$ and mononuclear cells from patient #2 were genotyped individually by using a custom panel of amplicons mapping on most frequently mutated genes in MPN. Copy number of specific chromosomal regions frequently affected by aneuploidies in MPN was inferred through read depth of the amplicons included in the panel. Amplicon ploidy was recorded in HSPC and mononuclear cells from Patient #1 (**Figure 16 panel A**), unveiling a marked copy number gain affecting consecutive amplicons located on chromosome 9 in JAK2-mutated clone compared to wt clone. More specifically, three amplicons covering *JAK2* gene reported a ploidy of 2.7 - 2.8, corroborating the data of a 9p copy number gain in this patient (**Figure 16 panel B**).

JAK2 mutational status and ploidy was therefore determined at the single-cell level and shown in Jitter plot, as reported in **Figure 16 panel C**. The distribution of genotyped cells follows the pattern previously seen in colony analysis, with duplicated cells presenting two mutated *JAK2* copies and a single wt allele being the most represented clone in Patient #1, followed by heterozygous diploid clone. This pattern traces the order of acquisition of the molecular alterations, strengthening the hypothesis that the duplication of 9p most frequently affects the *JAK2*-mutated chromosome in the heterozygous clone. JAK2V617F point mutation most likely represents the first molecular event in the pathogenesis of +9p MPN patients. This single-cell analysis independently confirms the results obtained from colony genotyping, outlining the most likely clonal evolutionary dynamic in duplicated patients.

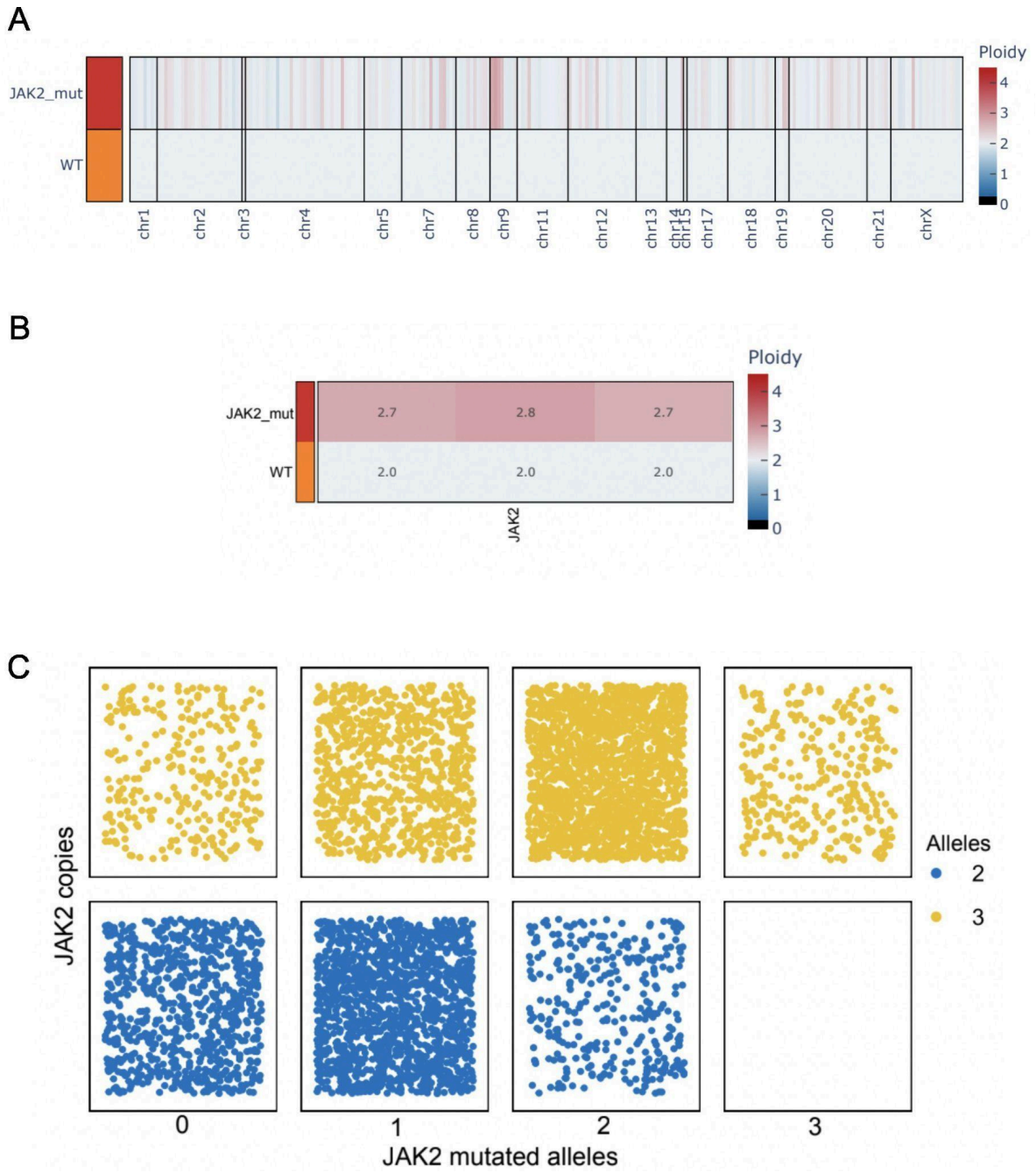

Figure 16. Single-cell genomic analysis of CD34^{+} cells and PBMCs from patient #1. (A) Copy number variation assessment of *JAK2*-mutated clone at the amplicon level, throughout the genome. wt cells clone (bottom row) was used as reference for copy number count, and set as diploid reference. Shades of red and blue reported in the ploidy legend represent the ratio between the median ploidy of each amplicon in JAK2-mutated clone and the median ploidy of the corresponding amplicon of wt clone. (B) *JAK2* locus amplicons ploidy, in JAK2-mutated clone and in the reference JAK2 wt clone, detected by Tapestri single cell CNV analysis. (C) Jitter plot displaying the representation of each combination of *JAK2* mutational status and JAK2 copy number genotype recorded in single cells from JAK2-mutated clone (upper row) and wt clone (bottom row). n=5617 cells.

5. Chromosome 9p trisomy stimulates clonogenic potential of CD34$^+$ cells

The observed different frequencies of colonies and single-cells with a specific genotype led us to investigate circulating CD34$^+$ cells' stemness features across +9p, JAK2-HET and JAK2-HOM patients. Specifically, both methylcellulose and collagen based clonogenic assays were analyzed to characterize the impact of the combination of JAK2V617F and somatic 9p gain on HSPC clonogenic and differentiation potential.

Both methylcellulose-based (**Figure 17 panel A**) and collagen-based assays (**Figure 17 panel B**) revealed that CD34$^+$ cells from duplicated patients generated a significantly higher colony number compared to both heterozygous and homozygous patients.

As regards the effect exerted by +9p and JAK2 driver mutation on cell fate determination, the analysis of colonies' phenotype revealed that differentiation commitment was less marked in colonies originated from +9p patients, which retained a higher frequency of CFU-GEMM colonies in methylcellulose-based clonogenic assay (**Figure 17 panel C**), and CFU-MIX colonies in collagen-based one (**Figure 17 panel D**). As a matter of fact, both these classes constitute the most undifferentiated colony types in each specific clonogenic assay, denoting a higher frequency of primitive progenitors in circulating CD34$^+$ cells from duplicated patients.

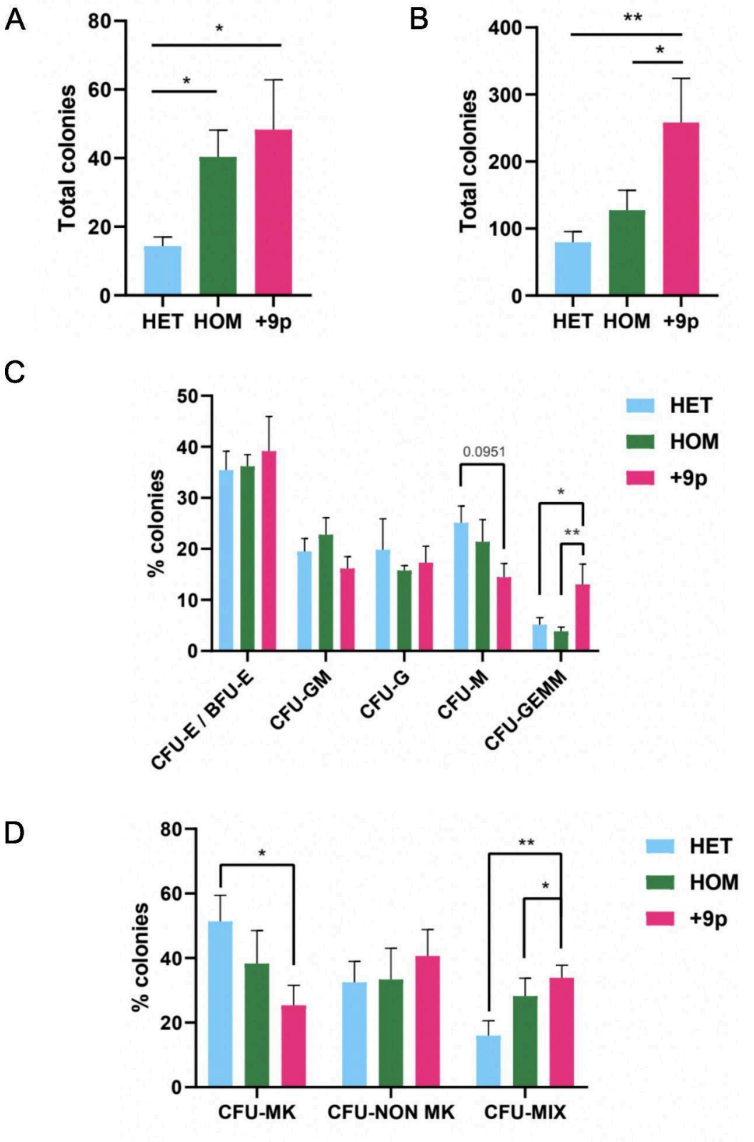

Figure 17. Clonogenic capacity of CD34$^+$ cells in JAK2-mutated MF patients. (A) Total colony counts from CD34$^+$ cells seeded in methylcellulose-based clonogenic assay (n = 7 HET, n = 7 HOM, n = 6 +9p). (B) Total colony counts from CD34$^+$ cells seeded in collagen-based clonogenic assay (n = 7 HET, n = 7 HOM, n = 6 + 9p). (C) Percentage of each Colony-Forming Units (CFUs) type obtained from methylcellulose-based clonogenic assays. (D) Percentage of each CFU type grown in collagen-based clonogenic assays. Results are represented as mean + SEM. Abbreviations: CFU-E/BFU-E, Colony-Forming Unit-Erythroid/Burst-Forming Unit-Erythroid; CFU-GM, Colony-FormingUnit-Granulocyte/Macrophage; CFU-G, Colony-Forming-Unit Granulocyte; CFU-M, Colony-Forming Unit-Macrophage; CFU-GEMM, Colony-Forming Unit-Granulocyte/Erythrocyte/Macrophage/Megakaryocyte; CFU-MK, Colony Forming Unit Megakaryocyte; CFU-NON MK, Colony Forming Unit Non-Megakaryocyte; CFU-MIX, Mixed CFU-Mk/Non CFU-Mk colonies; HET, JAK2-mutated heterozygous patients; HOM, JAK2-mutated homozygous patients; +9p, JAK2-mutated patients with 9p trisomy. *p < 0.05; **p < 0.01.

6. *CD274*, *POU5F1* and *NANOG* axis is engaged in +9p MPN cells

In the attempt to decipher the mechanism responsible for the increased potency exhibited by +9p HSPCs, we focused on other genes involved in 9p duplication which could account for this behaviour. Notably, *CD274*, encoding the immune checkpoint molecule PD-L1, stands among the genes included in the duplicated region since it is located downstream of *JAK2* locus (**Figure 18 panel A**). Interestingly, it has been reported in a work by Almozyan *et al*. that PD-L1 is able to sustain stemness in breast cancer cells[110]. More precisely, *PD-L1* expression was proved to be positively correlated with stemness gene signature in breast cancer (**Figure 18 panel B**). The authors suggested that OCT4 and NANOG, whose expression is maintained by AKT phosphorylation activity, are the biological mediators of such stemness response as summarized in **Figure 18 panel C**.

To validate the hypothesis that PD-L1 sustains +9p HSPC stemness, we first measured *CD274* expression in our patients cohort. We showed that an extra copy of *CD274* generated by 9p duplication is sufficient in inducing its transcriptional overexpression **(Figure 18 panel D - F**). In detail, *CD274* mRNA levels were increased in +9p patients' bulk $CD34^+$ HSPCs (**Figure 18 panel D**), $CD14^+$ cells (**Figure 18 panel E**), and granulocytes (**Figure 18 panel F**) compared to healthy controls, HET and HOM counterparts. Given the assessed overexpression of *CD274* in HSPCs and myeloid lineage cells, we next sought to evaluate the expression of the two pluripotency factors *POU5F1,* encoding OCT4*,* and *NANOG* in the same cells. qRT-PCR confirmed the upregulation of both factors in +9p $CD34^+$ cells, in line with *CD274* trend in the same compartment (**Figure 18 panel G - H**).

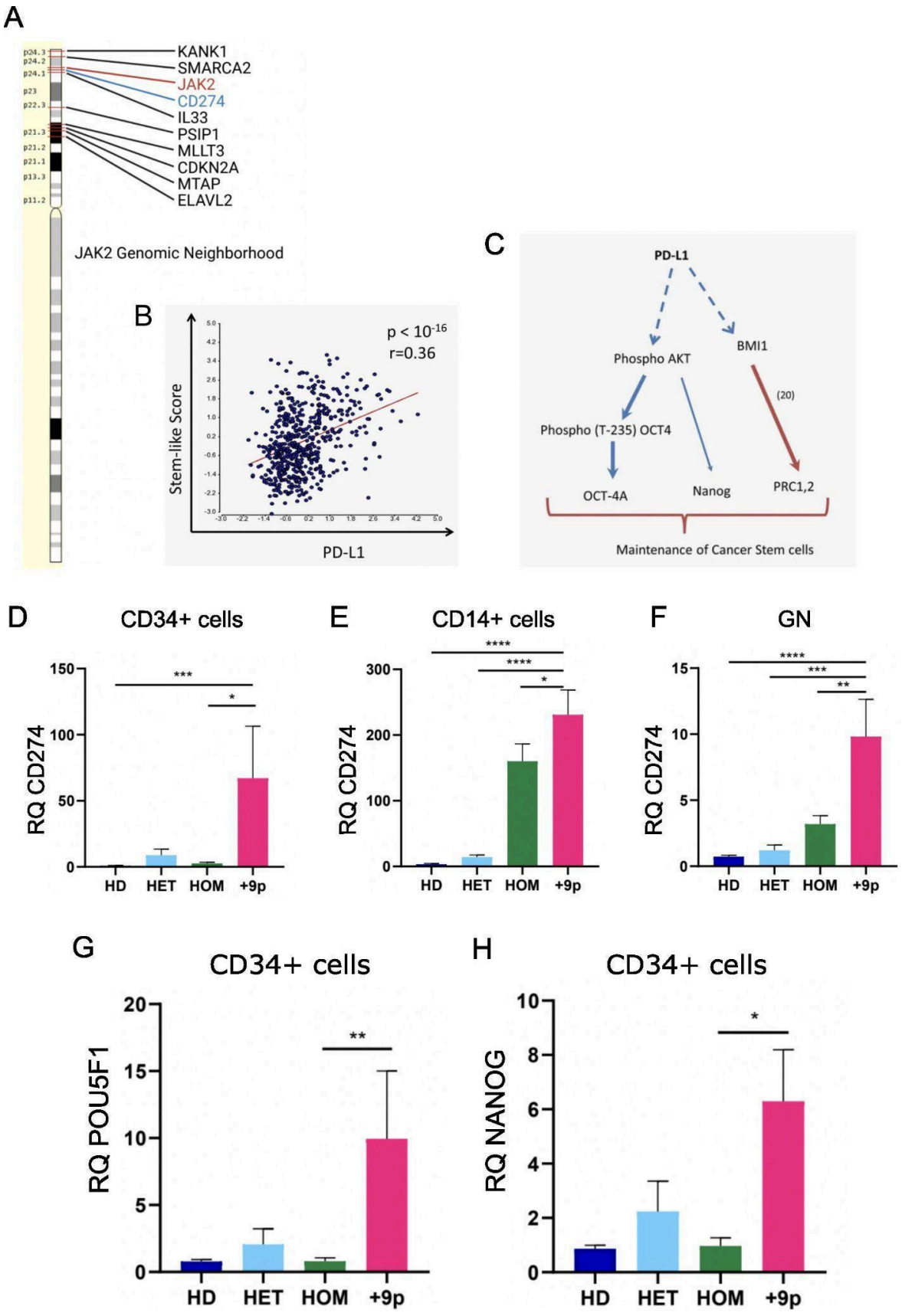

Figure 18. *CD274*, *POU5F1* and *NANOG* axis is established in +9p patients' HSPCs. (A) *JAK2* genomic neighborhood on chromosome 9p. Created with Biorender.com (B - C) PD-L1 involvement in breast cancer stem cells' renewal capacity. Adapted from Almozyan *et al.*[110] (B) Scatter plot showing the positive correlation between transcriptional stem-like score, inferred by mRNA levels of

100 breast stem-cell-associated genes, and *CD274* transcript levels in breast cancer. r: Correlation test's Pearson coefficients. P: correlation test's p values. (C) Schematic diagram showing the interaction between PD-L1, AKT, OCT4 and NANOG, sustaining breast cancer cells' stemness. Continuous blue lines indicate a demonstrated direct effect. Continuous red line indicates a direct effect demonstrated by other studies. Lines thickness discriminate between a strong (thick) or mild (thin) effect. Dotted lines indicate a demonstrated effect, either direct or indirect. (D - F) *CD274* expression levels in haematological cell subpopulations, isolated from healthy donors or MPN patients groups.. (D) *CD274* mRNA levels in $CD34^+$ cells. (E) *CD274* mRNA levels in $CD14^+$ monocytes. (F) *CD274* mRNA levels in granulocytes. (G) POU5F1 transcript levels in bulk $CD34^+$ from healthy donors and MPN patients groups. (H) NANOG transcript levels in bulk $CD34^+$ from healthy donors and MPN patients groups. Abbreviations: RQ, relative quantity. HD, healthy donors.

To investigate if the putative PD-L1/OCT4/NANOG axis could rely on AKT kinase activity, we evaluated if +9p HSPCs displayed a higher dependency on AKT signalling pathway. To assay AKT functional activity, HOM and +9p $CD34^+$ cells were cultured in methylcellulose complete medium, either supplemented with 1μM AKT inhibitor (AKTi) MK2206 or left untreated (UNT), and resulting clonogenicity was compared. Methylcellulose-based clonogenic assay firstly revealed the formation of a larger number of colonies in the homozygous samples compared to +9p in presence of AKT inhibitor; the number of colonies was normalized over the colony counts in correspondent UNT condition. (**Figure 19 panel A**). Colony genotyping further showed that in untreated culture condition, triploid colonies maintained a higher frequency while the addition of AKTi led to a significant decrease in their growth (**Figure 19 panel B**). As regards the modulation of colonies' identity induced by AKTi, +9p samples showed a decrease in CFU-GEMM, BFU-E and CFU-M colonies compared to the homozygous control culture (**Figure 19 panel C**).

Taken together, these results suggest the dependency of +9p $CD34^+$ cells on AKT pathway to sustain clonogenicity and maintenance of most primitive stages of HSPCs differentiation, possibly linking 9p trisomy-dependent *CD274* upregulation to *POU5F1* and *NANOG* activity.

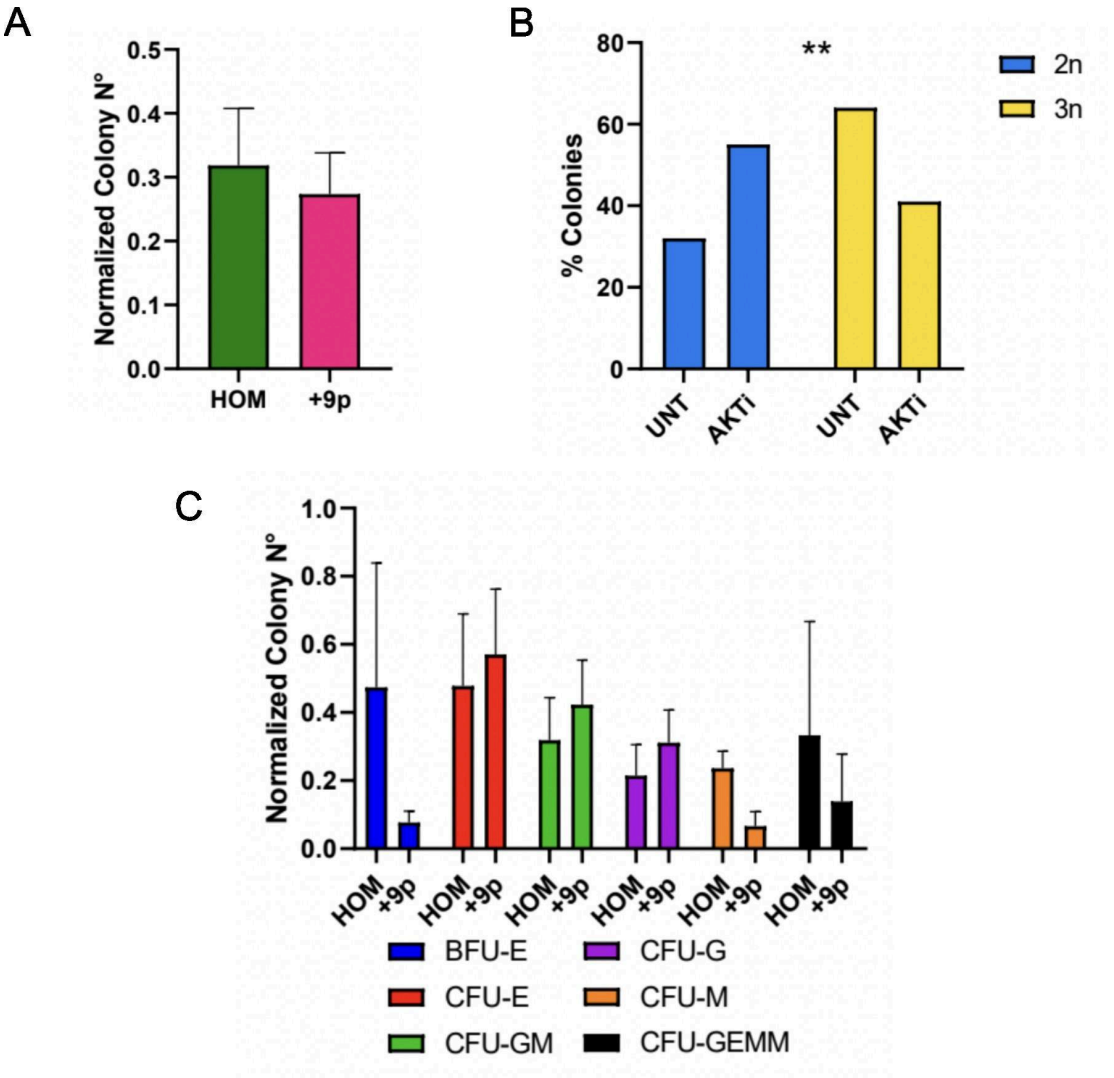

Figure 19. Response to AKT inhibitor treatment in CD34$^+$ cells from JAK2V617F-homozygous and +9p patients. (A) Ratio between the total number of colonies grown in methylcellulose-based clonogenic assays in AKTi and untreated samples, split between HOM (n=4) and +9p patients (n=6). Results are represented as mean + SEM. (B) Barplot depicting the frequency of 2n (diploid) colonies and 3n (+9p) colonies grown in methylcellulose from CD34$^+$ +9p patients (n=6), in untreated condition or with AKTi treatment. Statistical significance was assessed by Chi-square test. (C) Ratio between the number of colonies grown in methylcellulose assays with AKTi treatment or untreated conditions, grouped by different Colony-Forming Units (CFUs) in HOM and +9p patients. Results are represented as mean + SEM. Abbreviations: HOM, homozygous patients; +9p, 9p triploid patients; UNT, untreated culture condition; AKTi, AKT inhibitor culture condition; 2n, diploid colonies; 3n, +9p colonies; BFU-E, Burst-forming Unit-Erythroid; CFU-E, Colony-forming Unit-Erythroid; CFU-GM, Colony-forming Unit-Granulocyte/Macrophage; CFU-G, Colony-forming Unit-Granulocyte; CFU-M, Colony-forming Unit-Macrophage; CFU-GEMM, Colony-forming Unit-Granulocyte/Erythrocyte/Macrophage/Megakaryocyte. ** p <0.01.

Since patients' $CD34^+$ cells comprise heterogeneous genetic clones, we sought to determine whether the increased expression of *POU5F1* and *NANOG* observed in bulk population might be driven by +9p JAK2V617F-mutant cells. To this end, we plated +9p $CD34^+$ cells in methylcellulose medium and then picked the resulting $CD34^+$ single cell-derived colonies, which were simultaneously assessed by ddPCR for *CD274*, *POU5F1*, and *NANOG* expression as well as JAK2 genetic status and 9p copy number (**Figure 10**).

Firstly, we assessed the expression of *CD274* and of the two pluripotency factors *POU5F1* and *NANOG* in JAK2-diploid and -triploid colonies, showing overexpression of each inspected target associated with triploid colonies (**Figure 20 panel B, D, F**). More specifically, data split by JAK2 ploidy and mutational status highlighted that colonies with JAK2 trisomy and two mutated loci out of three drive the observed difference displaying the highest expression of *CD274*, *POU5F1* and *NANOG* genes (**Figure 20 panel A, C, E**).

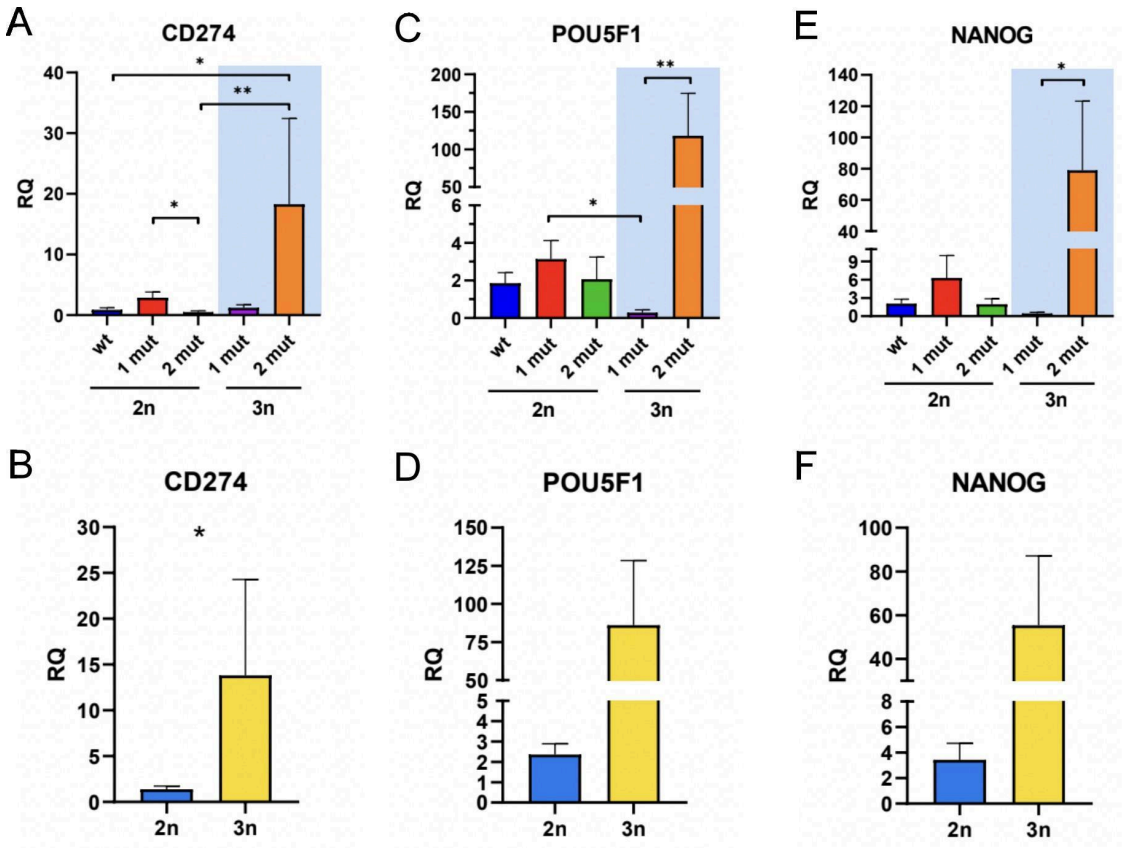

Figure 20. Expression at the transcriptional level of *CD274*, *POU5F1* and *NANOG* in single-cell derived colonies by ddPCR. Evaluation of *CD274* (A, B), *POU5F1* (C, D), and *NANOG* (E, F) expression at the transcriptional level in single-cell derived colonies by ddPCR. In panels A, C, and E, colonies (n = 54) were split according to the number of JAK2 mutated alleles and 9p ploidy status. Light blue area highlights +9p colonies. On the bottom plots, colonies were split according to 9p ploidy status in (B, D, and F). Results are represented as mean + SEM. Abbreviations: RQ, relative quantity; 2n, diploid colonies; 3n, +9p colonies.

Finally, to confirm that the observed clonogenicity effect was specifically ascribable to *POU5F1* and *NANOG* overexpression, a clonogenic assay was performed aftersiRNA-mediated silencing of these two stemness factors patients' $CD34^+$ cells. In the presence of simultaneous *POU5F1* and *NANOG* silencing, homozygous $CD34^+$ cells from JAK2 homozygous patients generated a greater number of colonies compared to those derived from +9p samples when seeded in methylcellulose medium; once again, colony number from silenced samples was normalized over the number of colonies generated by the corresponding control nucleofected with non-targeting siRNA (**Figure 21 panel A**). The assessment of colonies ploidy by ddPCR revealed that JAK2-triploid colonies were affected in their clonogenic potential by *POU5F1* and *NANOG* silencing, while JAK2-diploid colonies remained unaffected by their concomitant inhibition (**Figure 21 panel B**). Concerning then the influence of *POU5F1* and *NANOG* silencing on $CD34^+$ cells differentiation, a marked reduction in myeloid lineage colonies was observed upon siRNA nucleofection in +9p samples compared to the homozygous counterpart. Specifically, CFU-G and CFU-M normalised colony count significantly decreased upon genes expression silencing (**Figure 21 panel C**).

Collectively, these data showed that 9p gain positively impacts on *CD274, POU5F1* and *NANOG* expression levels in stem, progenitor, and myeloid lineage cells. Moreover, +9p $CD34^+$ cells displayed a dependency on PD-L1/AKT/NANOG-OCT4 axis, resulting sensitive to AKT inhibition and to *POU5F1* and *NANOG* double knockdown. Increased stemness features exhibited by +9p HSPCs can therefore be linked to *POU5F1* and *NANOG* pluripotency factors.

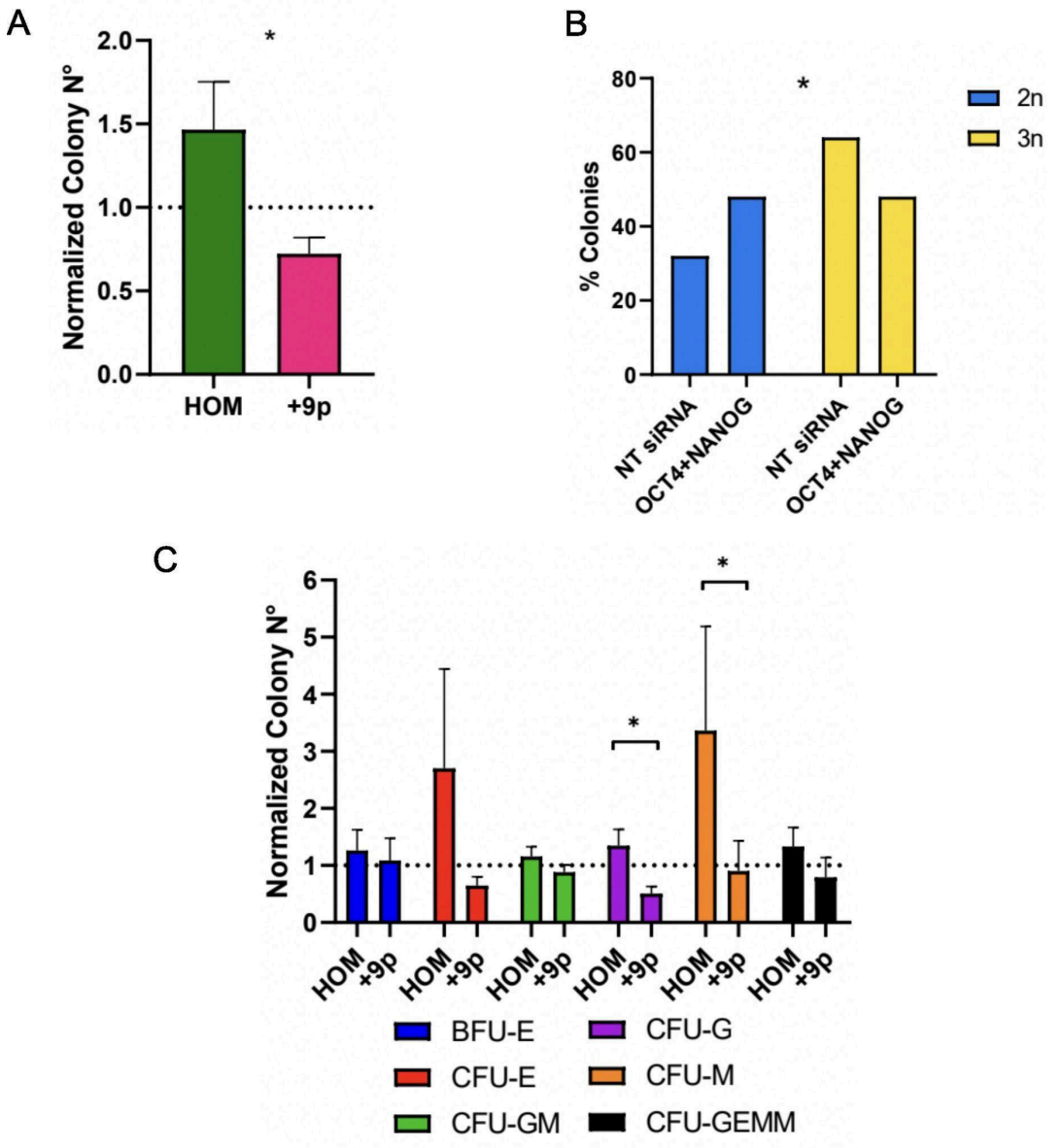

Figure 21. Clonogenic response to dual *POU5F1* and *NANOG* silencing of CD34^{+} cells from JAK2V617F-homozygous and +9p patients. (A) Ratio between the total number of colonies grown in methylcellulose-based clonogenic assays in *POU5F1* and *NANOG* dual silenced samples and control samples, split between HOM (n=4) and +9p patients (n=6). Results are represented as mean + SEM. (B) Barplot depicting the frequency of diploid and +9p colonies in +9p patients (n=6) in untreated samples or after *POU5F1* and *NANOG* silencing. Statistical significance was assessed by Chi-square test. (C) Ratio between the number of colonies grown in methylcellulose-based clonogenic assays in *POU5F1*- and *NANOG*-nucleofected samples and non-targeting siRNA-nucleofected samples, grouped according to the different Colony-Forming Units (CFUs) in HOM and +9p patients. Results are represented as mean + SEM. Abbreviations: HOM, homozygous patients; +9p, 9p triploid patients; NT siRNA, Non-targeting siRNA sample; OCT4+NANOG, *POU5F1* and *NANOG* double silenced samples; 2n, diploid colonies; 3n, +9p colonies; BFU-E, Burst-forming Unit-Erythroid; CFU-E, Colony-forming Unit-Erythroid; CFU-GM, Colony-forming Unit-Granulocyte/Macrophage; CFU-G, Colony-forming Unit-Granulocyte; CFU-M, Colony-forming Unit-Macrophage; CFU-GEMM, Colony-forming Unit-Granulocyte/Erythrocyte/Macrophage/Megakaryocyte. *$p < 0.05$.

7. PD-L1 protein relocalizes on plasma membrane in monocytes in +9p MPN patients

Given the upregulation of *CD274* expression in +9p myeloid cells and considering the relative decrease of monocyte colonies upon multiple PD-L1 pathway blockade strategies, we assessed PD-L1 protein expression in monocytes from HET, HOM, and +9p patients by means of flow cytometry (**Figure 22 panel A**). This analysis revealed a statistically significant increase in $CD14^+/PD\text{-}L1^+$ cells' frequency in peripheral blood samples of triploid MPN patients (**Figure 22 panel B, C**). Moving from these findings, we performed immunofluorescence staining of PD-L1 on patients' monocytes to delve into the observed differential PD-L1 levels. The technique highlighted variable localization of PD-L1 subcellular distribution among distinct patients' categories. Indeed, PD-L1 was more abundant in monocytes' cytoplasm in HET patients, while HOM patients exhibited a simultaneous cytoplasmic and membrane-bound localization of PD-L1. Most relevantly, +9p patients' monocytes presented instead a membrane PD-L1 distribution (**Figure 22 panel D**).

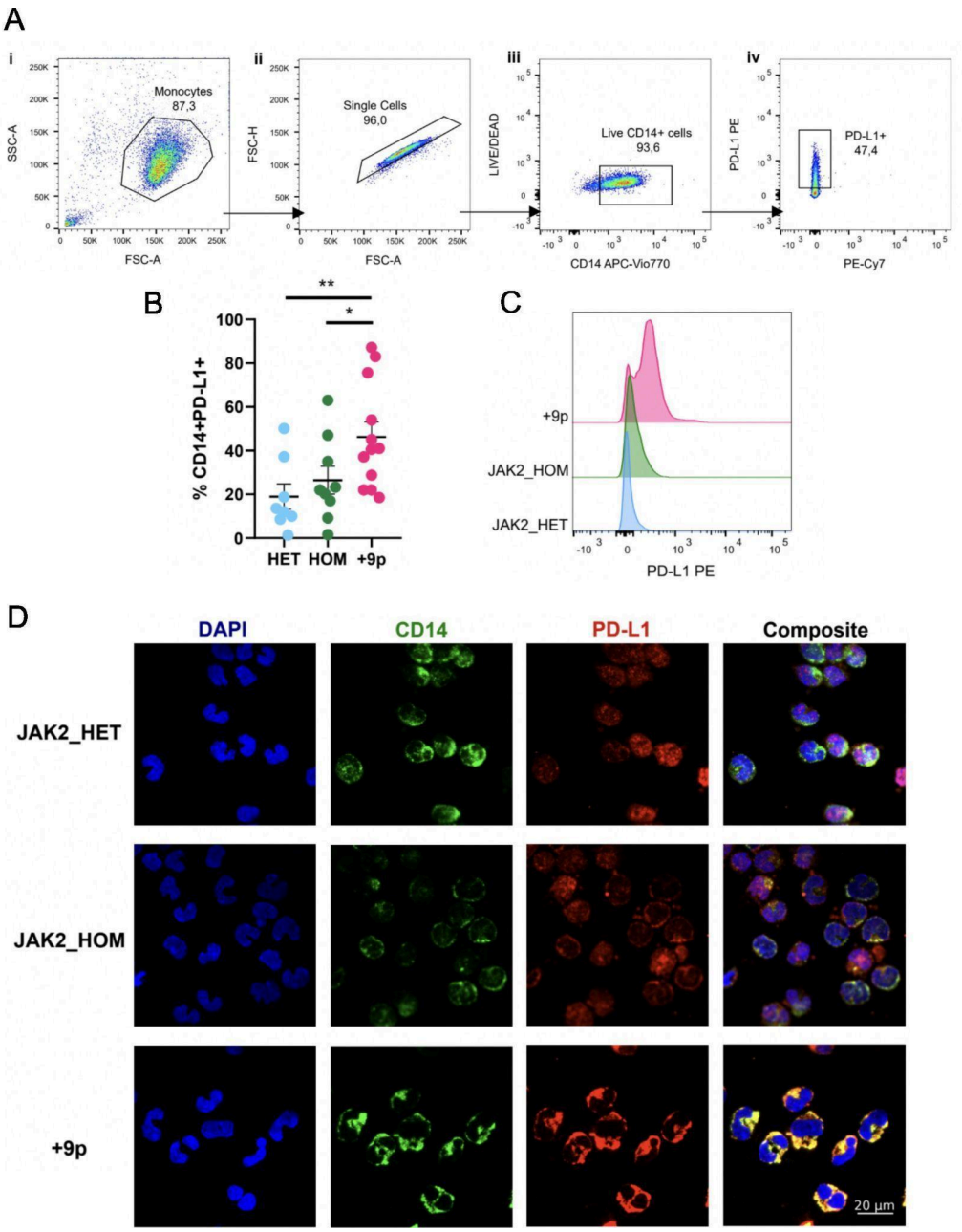

Figure 22. PD-L1 expression on monocytes of JAK2-mutated MF patients. (A - C) Flow cytometry analysis performed on patients' monocytes . (A) Representative gating strategy adopted to quantify $CD14^+/PD\text{-}L1^+$ cells. (i) Side scatter area (SSC-A) vs forward scatter area (FSC-A) plot, showing monocyte gate. (ii) Forward scatter height (FSC-H) vs forward scatter area (FSC-A) plot defining the single cell gate. (iii) LIVE/DEAD vs CD14 APC-Vio770 plot gating for live cells. (iv) PD-L1 PE vs PE-Cy7 plot depicting $PD\text{-}L1^+$ cell gate. (B) Percentage of circulating $CD14^+/PD\text{-}L1^+$ cells in patients. Results are represented as means ± SEM. (C) Representative histograms for flow cytometry detection of PD-L1 staining in $CD14^+$ cells from HET (n = 8), HOM (n = 9) and +9p (n = 12) patients. (D) PD-L1 cellular localization in monocytes of JAK2-mutated MPN patients, obtained through immunofluorescence staining on monocytes isolated from JAK2-heterozygous, -homozygous, and +9p patients. The figure displays representative confocal microscopy images. In every horizontal panel, the rightmost image represents a merge of the other 3 images on the left. Cells were labeled with anti-CD14 antibody (staining with green fluorescence) and with anti-PD-L1 antibody (in red fluorescence); nuclear counterstaining was performed with DAPI (blue fluorescence). HD: healthy donors; HET: JAK2-mutated heterozygous patients; HOM: JAK2-mutated homozygous patients; +9p: JAK2-mutated patients with 9p trisomy. *$p < 0.05$; **$p < 0.01$.

8. T cell exhaustion in +9p MPN patients

Starting from the recognition that elevated PD-L1 exposure could mediate immune surveillance impairment, and considering PD-L1 differential distribution observed in monocytes, we next examined the putative activation of the PD-1/PD-L1 axis in +9p MPN patients' T cells.

Among cytotoxic $CD8^+$ T-lymphocytes, we evaluated, by means of cytofluorimetric analysis, the frequency of $PD\text{-}1^+$ CD57- cells to identify T cells sensitive to PD-L1 stimulation and exhibiting an extrinsically-induced exhaustion phenotype in patients from our study cohort compared with HD samples. The adopted gating strategy is reported in **Figure 23 panel A**. This analysis revealed, in each group of MPN patients, an enrichment of $CD3^+/CD8^+/CD57^-/PD\text{-}1^+$ lymphocytes' frequency. Importantly, +9p patients displayed the highest percentage of the selected exhausted lymphocyte population compared to all the other groups (**Figure 23 panel B**). Moreover, the analysis of additional inhibitory receptors and markers (LAG3, CD244, CTLA4) showed higher abundance of exhausted cytotoxic T lymphocytes co-expressing multiple inhibitory receptors in +9p patients compared to HOM, HET, and healthy donor groups (**Figure 23 panel C, E, F**). Differently, HOM patients showed a more pronounced frequency of $TIM3^+/PD\text{-}1^+$ T cells compared to healthy donors (**Figure 23 panel D**).

Despite the absence of 9p duplication, an additional feature of $CD3^+$ lymphocytes in our cohort was the presence of JAK2V617F whose VAF detected using ddPCR was highly variable among patients (**Table 3**). As PD-L1 expression correlates with the JAK2V617F mutational burden in monocytes of MPN patients[108], we hypothesized a possible autocrine signaling of PD-L1 on PD-1 receptors in T cells, induced by JAK2 driver mutation and possibly related to JAK2V617F VAF. To study this correlation, we evaluated the frequency of $PD\text{-}1^+/PD\text{-}L1^+$ lymphocytes isolated from HOM and +9p patients, without detecting any difference in the frequency of T cells with simultaneous expression of both immune checkpoint molecules (**Figure 23 panel C**).

PATIENT	GROUP	JAK2V617F VAF (%) CD34+	JAK2V617F VAF (%) GN	JAK2V617F VAF (%) CD3+	JAK2V617F VAF (%) CD14+
1	+9p	39.6	65.2	2.2	64.2
2	+9p	N/A	57.0	N/A	N/A
3	+9p	56.2	55.1	0.6	24.3
4	+9p	N/A	47.1	N/A	N/A

5	+9p	100	91.7	16.1	86.0
6	+9p	41.2	3.9	10.5	4.6
7	+9p	100	66.9	15.8	80.6
8	+9p	84.4	85.8	26.6	89.3
9	+9p	N/A	25.9	N/A	N/A
10	+9p	65.5	63.8	34.2	69.4
11	+9p	N/A	25.9	N/A	N/A
12	+9p	100	88.1	8.4	77.2
23	JAK2_HOM	N/A	87.6	N/A	43.9
24	JAK2_HOM	N/A	86.0	N/A	90.1
25	JAK2_HOM	N/A	97.9	N/A	91.4
26	JAK2_HOM	92.2	99.0	3.2	97.8
27	JAK2_HOM	43.6	86.0	4.4	58.1
28	JAK2_HOM	25.0	88.7	5.6	61.8
29	JAK2_HOM	38.1	99.5	6.0	98.9
30	JAK2_HOM	21.1	64.6	2.4	40.5
31	JAK2_HOM	N/A	92.5	N/A	99.3
32	JAK2_HOM	84.5	97.5	9.4	96.2

Table 3. JAK2V617F allele frequency in cell fractions from JAK2-homozygous and +9p patients. Abbreviations: VAF, Variant Allele Frequency; N/A, not analyzed.

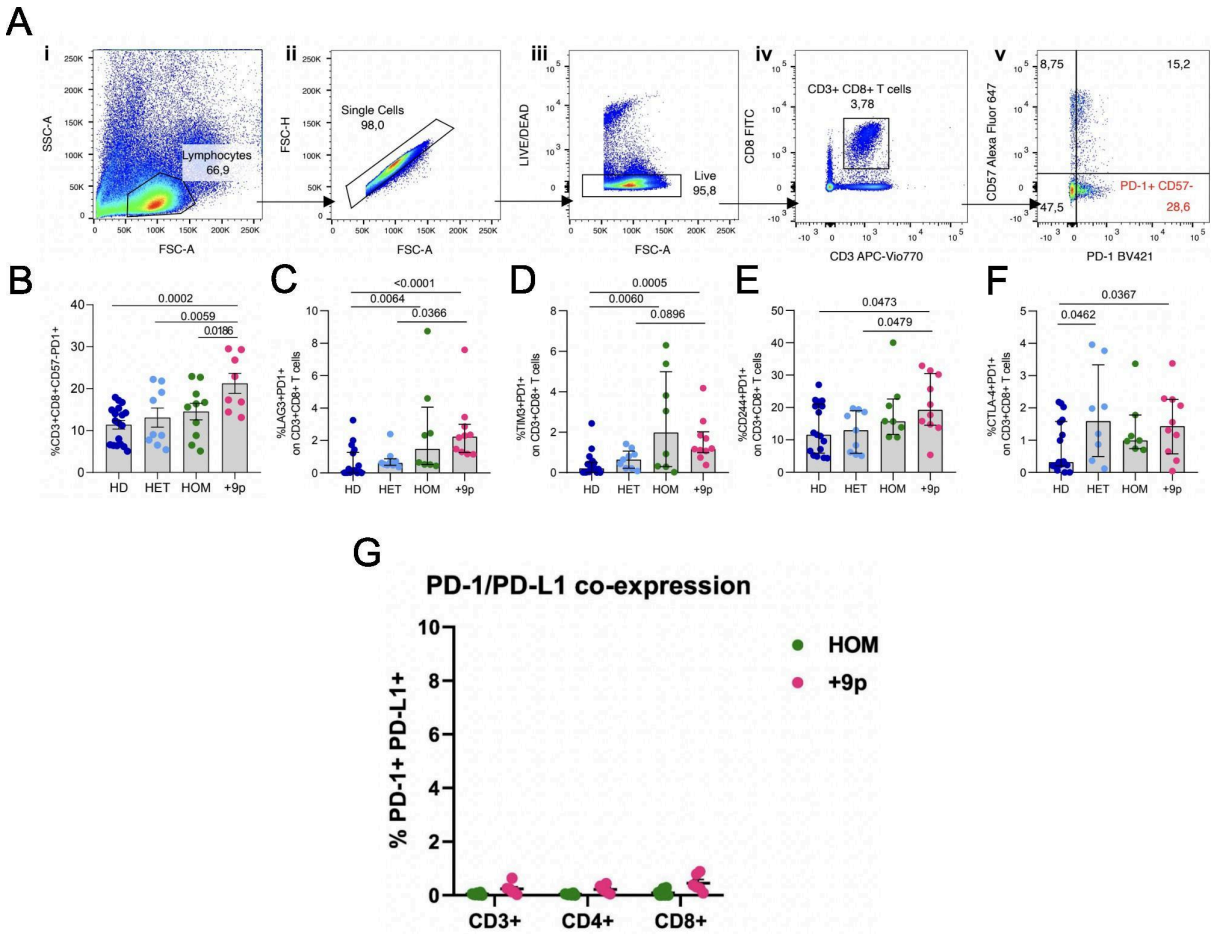

Figure 23. T-cell exhaustion in MPN patients and healthy donors. (A) Representative gating strategy used to quantify $CD3^+CD8^+$ $CD5^-$ $PD\text{-}1^+$ cells. (i) Side scatter area (SSC-A) vs forward scatter area (FSC-A) plot, showing the lymphocyte gate. (ii) Forward scatter height (FSC-H) vs forward scatter area (FSC-A) plot defining the single cell gate. (iii) LIVE/DEAD vs FSC-A plot gating for live cells. (iv) CD8-FITC vs CD3-APC Vio770 plot depicting $CD3^+$ $CD8^+$ cells. (v) CD57-Alexa Fluor 647 vs PD-1 BV421 plot, showing the percentage of PD-1 + CD57- cells.
(B-F) Flow-cytometric assessment of circulating exhausted $CD3^+$ $CD8^+$ $CD57^-$ $PD1^+$ (B), $CD3^+$ $CD8^+$ $PD1^+$ $LAG3^+$ (C), $CD3^+$ $CD8^+$ $PD1^+$ $TIM3^+$ (D), $CD3^+$ $CD8^+$ $PD1^+$ $CD244^+$ (E), $CD3^+$ $CD8^+$ $PD1^+$ $CTLA4^+$ (F) T cells in MPN patients and healthy donors. (G) Flow-cytometric assessment of PD-1/PD-L1 co-expression in $CD3^+$ T cells, $CD4^+$ T-helper cells and $CD8^+$ cytotoxic T-cells from patients (n=7 HOM, n=6 +9p) carrying JAK2V617F mutation in $CD3^+$ cells (VAF> 5%)
Results are represented as means ± SEM. HD: healthy donors; HET: JAK2-mutated heterozygous patients; HOM: JAK2-mutated homozygous patients; +9p: JAK2-mutated patients with 9p trisomy.

Overall, T lymphocytes exhaustion profiling suggests that +9p can mediate immune escape through membrane exposure of PD-L1 in mutated monocytes, favoring the evolution of the neoplastic clone.

DISCUSSION

Philadelphia-negative myeloproliferative neoplasms are clonal disorders characterized by single or multiple genetic lesions accumulating in hematopoietic stem and progenitor cells, leading to a deregulated overproduction of terminally differentiated myeloid cells. Three main clinical classes of MPNs have been extensively described, being PMF, ET and PV. The onset of these hematological malignancies is linked to three mutually exclusive "driver mutations" arising in *JAK2*, *CALR* or *MPL* genes, transducing a constitutive proliferative signal through STAT proteins[57]. Nonetheless, several additional mutations can emerge and concur to shape disease course. Among those, the most frequent involve genes pertaining chromatin remodeling, splicing regulation, cell cycle control and DNA repair[35]. Beside co-occurring mutations, also copy number variations can exert a role in disease progression[81].

Neoplastic clones in MPNs can display different chromosomal abnormalities, ranging from unbalanced chromosomal gains or losses, and balanced rearrangements. Literature reports that on average 50% of chronic-phase PMF patients carry chromosomal alterations at diagnosis[122].

Chromosome 9 alterations are among the most common cytogenetic lesions found in MPNs, yet their biological effects on cancer cells' phenotype have never been thoroughly explored[123]. More interestingly, chromosome 9 copy number variations have an impact on *JAK2* allele number, considering its locus localization on chromosome 9p24. Considering also JAK2V617F driver mutation, the most frequent MPN genetic lesion found in about 50% of ET and MF cases and up to 95% of PV diagnosis[59], the effects of chromosome 9 aneuploidies can become much more impactful in*JAK2*-mutated patients.

In this context, we identified a subset of MPN patients with a *JAK2* locus copy number gain, as detected by clinical NGS analysis. These patients also shared *JAK2* driver mutation, laying the basis for further investigation about the combination of these events. The validation through MLPA approach of *JAK2* gain in these patients enabled us to define that the observed amplification was not limited to *JAK2* locus but involved both entire chromosome 9 or 9p.

Starting from these considerations, we speculated whether chromosome 9 copy number abnormalities might represent a disease modifier in *JAK2*-mutant MPN patients. Since JAK2V617F allele frequency significantly impacts on MPN severity and phenotype, we sought to characterize the functional effects of +9p on *JAK2*-mutated cells, compared to diploid *JAK2*-heterozygous and -homozygous cells. We gathered a cohort of *JAK2*-mutated MPN patients including patients with +9p genotype, patients homozygous for JAK2V617F, and JAK2VF-heterozygous patients.

Firstly, we characterized how the chromosomal alteration was associated with different cell populations, identifying 9p trisomy in stem and progenitor cells, monocytes and granulocytes by means of MLPA technique. On the other hand, T cells were found diploid for chromosome 9, restricting the association of +9p with HSPCs and cells of myeloid lineage.
After the identification of the cell types carrying 9p aneuploidy in *JAK2*-mutated patients, we moved on to the understanding of how chromosomal and mutational alterations are associated in +9p patients and how this influences clonal evolution. Clonogenic assays enabled us to detect by ddPCR a higher frequency of triploid colonies with two *JAK2* mutated alleles out of three.

The next step was the unraveling of the molecular order of the events that in *JAK2* mutated patients lead to a predominant clone with such genotype. The reconstruction of the stepwise accumulation of mutations and +9p genomic alteration was achieved analyzing the relative frequency of the other detected colony genotypes. This approach revealed that the most probable dynamic leading to triploid cells with two *JAK2*-mutated alleles was the amplification of the chromosome carrying *JAK2*-mutant allele in heterozygous cells. This hypothesis was also confirmed by a peculiar +9p patient carrying an additional non-canonical *JAK2* mutation, specifically JAK2G571S. The genotyping of colonies derived from this patient confirmed the observed pattern of clonal evolution, with both *JAK2* mutations occurring as the first molecular events on the same allele, subsequently followed by 9p amplification of that specific mutated chromosome.

These findings were also replicated with a single-cell genomic approach by means of Tapestri single-cell genomic platform, through which *JAK2* copy number was inferred alongside its genotyping. We analyzed $CD34^+$ cells purified from one +9p patient, coupling the molecular information of *JAK2* mutational status with its ploidy at the single cell level. Normalized read counts associated with *JAK2*-mutant clone validated *JAK2* locus amplification, and the distribution of analyzed cells based on *JAK2* mutational status and copy number reflected the molecular order previously defined by colony analysis.
This inferred order of mutational events is also in agreement with literature suggesting that the enhanced replication rate induced by JAK2 hyperactivation can cause DNA damage, homologous recombination, and ultimately genomic instability[124,125].

The frequency of +9p HSPCs with two mutated *JAK2* alleles out of three, as observed in our colony-based and single-cell clonality studies, led us to investigate their biological and functional consequences. We set up clonogenic assays with $CD34^+$ cells from +9p, HET and HOM patients, revealing that HSPCs from duplicated patients generated a higher number of colonies in both assays. Moreover, +9p patients exhibited an increased frequency of colonies derived from primitive HSPCs when compared to heterozygous and homozygous controls, suggesting a correlation between chromosome 9 aneuploidy and the establishment of an altered self renewal/differentiation balance in stem and progenitor +9p cells.

Moving forward to the possible mechanisms underlying the increased potency phenotype of +9p HSPCs, we focused on additional genes involved in the duplication. We noticed that *CD274* gene, encoding PD-L1, was located just downstream of *JAK2* locus. Indeed, its mRNA levels were found upregulated in +9p patients' $CD34^+$ and myeloid cells. Interestingly, previous studies demonstrated the ability of PD-L1 to support stemness transcriptomic signature in other cancer types. This effect was exerted through the induction, mediated by AKT phosphorylation activity, of the pluripotency factors *POU5F1*, encoding OCT4, and *NANOG*[110,126]. These two genes are known regulators of the pluripotency transcriptional network of embryonic stem cells', yet *POU5F1* and *NANOG* expression has been reported also in hematopoietic $CD34^+$ cells and correlated with their in vitro maintenance[127–129]. Strikingly, we found an upregulation of *POU5F1* and *NANOG* mRNA levels in $CD34^+$ cells from +9p patients compared to other patients' groups, in line with previous observations of *CD274* expression.

To assess the effective correlation reported in literature between AKT signalling activation induced by PD-L1, we set up methylcellulose clonogenic assays supplemented with MK2206, an AKT inhibitor molecule. The analysis of these cultures reported a loss of clonogenic activity and primitive phenotype previously associated with +9p $CD34^+$ samples, compared to homozygous controls.

Next, we tried to discriminate the genotypes specifically associated with the increased expression of the two pluripotency factors. To do so, methylcellulose-grown colonies were subjected to a coupled genomic-transcriptomic characterization, which enabled the association of high levels of *CD274*, *POU5F1* and *NANOG* mRNAs with triploid cells carrying two mutant JAK2 copies out of three. Furthermore, the silencing of *POU5F1* and *NANOG* genes achieved by siRNA nucleofection in $CD34^+$ cells was shown to be sufficient to knock down the enhanced clonogenic potential and primitive phenotype already seen in methylcellulose assays of +9p patients.

The strong dependency of +9p $CD34^+$ cells on PD-L1 signalling led us to further evaluate its functional role in differentiated cell types with reported *CD274* upregulation. Specifically, +9p patients exhibited in flow cytometry a higher frequency of $PD\text{-}L1^+$ circulating monocytes. To further explore PD-L1 role, immunofluorescence staining of PD-L1 on monocytes samples revealed different subcellular localizations among patients groups: HET patients' monocytes showed mainly cytoplasmic PD-L1, while HOM patients exhibited both cytoplasmic and membrane PD-L1 compartmentalization. As regards +9p patients, PD-L1 mostly concentrated in monocytes' membrane, in line with observed flow cytometry data.

It is known that *CD274* transcriptional induction can be mediated by inflammatory cytokines, cell stressor, and oncogene signalling, while its subcellular trafficking is dependent on various post-translational modifications and recycling/degradation dynamics[130]. More specifically IL-6, through JAK/STAT signalling, has been shown to drive PD-L1 stabilization and cell surface translocation by STT3-mediated glycosylation[131]. These findings reinforce the rationale of the progressive cytoplasm-to-membrane PD-L1 shift observed in JAK2V617F-heterozygous, -homozygous, and +9p MPN patients.

The elevated PD-L1 expression and exposure in +9p myeloid cells, particularly monocytes, suggested a potential immune dysfunction exerted by these malignant cell types towards PD-1-expressing cells. We checked this possibility by flow cytometry through the analysis of immune exhaustion markers, identifying higher frequency of circulating exhausted $PD1^+$ lymphocytes in +9p patients samples compared to healthy donors, HET and HOM groups.

Cytofluorimetric analysis of the additional inhibitory receptors CTLA-4, LAG-3, CD244, and TIM-3 confirmed that T cells from +9p patients consistently expressed higher levels of most of the evaluated surface markers, compared with healthy donors and *JAK2*-mutated diploid controls.

Finally, since a minor fraction of T cells carrying JAK2V617F was detected in a subset of +9p patients, we proved by flow cytometry that the observed exhausted phenotype was not mediated by an autologous activation of PD-L1/PD-1 axis on different classes of lymphocytes.

This PhD project contributed to a more comprehensive characterization of the molecular interplay between JAK2V617F and +9p in MPNs. Through the assessment of Copy Number Variations and *JAK2* mutational status, we unveiled molecular and clonal evolution of triploid patients' HSPCs. Colony-based methods and single-cell analysis identified +9p cells with two out of three *JAK2*-mutated alleles as the most represented genotype, and indicated that *JAK2* mutation precedes 9p gain. Then, we determined the impact of concurrent JAK2V617F and somatic 9p trisomy on fostering clonogenic potential and skewing differentiation capacity of $CD34^+$ cells in clonogenic culture.

Since *JAK2* hyperactivation has been shown in literature to induce *CD274* expression[108,111], we confirmed a significant increment of PD-L1 mRNA and protein expression in +9p patients compared to either HET and HOM patients. Moreover, even considering only duplicated patients, +9p cells with two JAK2V617F alleles have shown higher *CD274* expression compared to JAK2-homozygous clones and other genetic assets. This evidence sets JAK2-mutant +9p patients in an independent MPN subclass, distinguished by JAK2-homozygous patients on the basis of the observed synergy between 9p amplification and JAK2V617F allele burden.

The role of PD-L1 altered expression in disease pathogenesis of +9p patients has been furtherly characterized by elucidating cell-intrinsic and cell-extrinsic mechanisms of action. We demonstrated a PD-L1 dependency within HSPCs in sustaining primitive and clonogenic behaviour through AKT/OCT4/NANOG axis, and a pivotal role in mediating immune escape and T cell exhaustion by $PD\text{-}L1^+$ monocytes.

Among the genes located on chromosome 9p, many other potential targets of the duplication could play a role in the observed biological features of +9p patients. Two representative examples are the transcription factor MLLT3, regulating stem cell division and hematopoietic stem cells differentiation, and IL-33, potentially favoring proliferation and differentiation of myeloid precursors. From this point of view, the genetic determinants of +9p MPNs pathogenesis still merit further studies.

Collectively, these findings gave insight into the synergistic effect of JAK2V617F and +9p, thereby distinguishing triploid patients from JAK2-homozygous patients and copy-neutral UPD. In conclusion, this project also provides evidence for the adoption of PD-L1-targeting therapies in +9p MPN patients, supporting the rationale for the development of personalized clinical approaches.

BIBLIOGRAPHY

1. Dameshek W. Some speculations on the myeloproliferative syndromes. Blood 1951;6(4):372–5.

2. Fialkow PJ. Cell lineages in hematopoietic neoplasia studied with glucose-6-phosphate dehydrogenase cell markers. J Cell Physiol 1982;113(S1):37–43.

3. Grabek J, Straube J, Bywater M, Lane SW. MPN: The Molecular Drivers of Disease Initiation, Progression and Transformation and their Effect on Treatment. Cells 2020;9(8):1901.

4. Brogan J, Kishtagari A, Corty RW, Pershad Y, Vlasschaert C, Sharber B, et al. Incident cytopenia and risk of subsequent myeloid neoplasm in age-related clonal hematopoiesis: a multi-biobank case-control study. EClinicalMedicine 2025;84:103283.

5. Khoury JD, Solary E, Abla O, Akkari Y, Alaggio R, Apperley JF, et al. The 5th edition of the World Health Organization Classification of Haematolymphoid Tumours: Myeloid and Histiocytic/Dendritic Neoplasms. Leukemia 2022;36(7):1703–19.

6. Titmarsh GJ, Duncombe AS, McMullin MF, O'Rorke M, Mesa R, De Vocht F, et al. How common are myeloproliferative neoplasms? A systematic review and meta-analysis. Am J Hematol 2014;89(6):581–7.

7. Tefferi A, Guglielmelli P, Larson DR, Finke C, Wassie EA, Pieri L, et al. Long-term survival and blast transformation in molecularly annotated essential thrombocythemia, polycythemia vera, and myelofibrosis. Blood 2014;124(16):2507–13; quiz 2615.

8. Kaifie A, Kirschner M, Wolf D, Maintz C, Hänel M, Gattermann N, et al. Bleeding, thrombosis, and anticoagulation in myeloproliferative neoplasms (MPN): analysis from the German SAL-MPN-registry. J Hematol OncolJ Hematol Oncol 2016;9:18.

9. Lussana F, Rambaldi A. Inflammation and myeloproliferative neoplasms. J Autoimmun 2017;85:58–63.

10. Cahu X, Constantinescu SN. Oncogenic Drivers in Myeloproliferative Neoplasms: From JAK2 to Calreticulin Mutations. Curr Hematol Malig Rep 2015;10(4):335–43.

11. Ng ZY, Fuller KA, Mazza-Parton A, Erber WN. Morphology of myeloproliferative neoplasms. Int J Lab Hematol 2023;45 Suppl 2:59–70.

12. Baxter EJ, Scott LM, Campbell PJ, East C, Fourouclas N, Swanton S, et al. Acquired mutation of the tyrosine kinase JAK2 in human myeloproliferative disorders. Lancet Lond Engl 2005;365(9464):1054–61.

13. Duan M, Bose P, Hunter AM, Qin A, Chang L, Li W, et al. Emerging Significance and Implications of a Durable Complete Molecular Remission in the Treatment of Polycythemia Vera. Curr Hematol Malig Rep 2025;20(1):13.

14. Prchal JF, Axelrad AA. Letter: Bone-marrow responses in polycythemia vera. N Engl J Med 1974;290(24):1382.

15. Green AR. Pathogenesis of polycythaemia vera. Lancet Lond Engl 1996;347(9005):844–5.

16. Gianelli U, Thiele J, Orazi A, Gangat N, Vannucchi AM, Tefferi A, et al. International Consensus Classification of myeloid and lymphoid neoplasms: myeloproliferative neoplasms. Virchows Arch 2023;482(1):53–68.

17. Cerquozzi S, Tefferi A. Blast transformation and fibrotic progression in polycythemia vera and essential thrombocythemia: a literature review of incidence and risk factors. Blood Cancer J 2015;5(11):e366.

18. Tefferi A, Gangat N, Loscocco GG, Guglielmelli P, Szuber N, Pardanani A, et al. Essential Thrombocythemia: A Review. JAMA 2025;333(8):701–14.

19. Tefferi A, Vannucchi AM, Barbui T. Essential thrombocythemia: 2024 update on diagnosis, risk stratification, and management. Am J Hematol 2024;99(4):697–718.

20. Vainchenker W, Yahmi N, Havelange V, Marty C, Plo I, Constantinescu SN. Recent advances in therapies for primary myelofibrosis. Fac Rev 2023;12:23.

21. Le Bousse-Kerdilès MC. Primary myelofibrosis and the ‘bad seeds in bad soil’ concept. Fibrogenesis Tissue Repair 2012;5(Suppl 1):S20.

22. Ruberti S, Bianchi E, Guglielmelli P, Rontauroli S, Barbieri G, Tavernari L, et al. Involvement of MAF/SPP1 axis in the development of bone marrow fibrosis in PMF patients. Leukemia 2018;32(2):438–49.

23. Bianchi E, Rontauroli S, Tavernari L, Mirabile M, Pedrazzi F, Genovese E, et al. Inhibition of ERK1/2 signaling prevents bone marrow fibrosis by reducing osteopontin plasma levels in a myelofibrosis mouse model. Leukemia 2023;37(5):1068–79.

24. Decker M, Martinez-Morentin L, Wang G, Lee Y, Liu Q, Leslie J, et al. Leptin-receptor-expressing bone marrow stromal cells are myofibroblasts in primary

myelofibrosis. Nat Cell Biol 2017;19(6):677–88.

25. Schneider RK, Mullally A, Dugourd A, Peisker F, Hoogenboezem R, Van Strien PMH, et al. Gli1+ Mesenchymal Stromal Cells Are a Key Driver of Bone Marrow Fibrosis and an Important Cellular Therapeutic Target. Cell Stem Cell 2017;20(6):785-800.e8.

26. Li R, Colombo M, Wang G, Rodriguez-Romera A, Benlabiod C, Jooss NJ, et al. A proinflammatory stem cell niche drives myelofibrosis through a targetable galectin-1 axis. Sci Transl Med 2024;16(768):eadj7552.

27. Verstovsek S, Manshouri T, Pilling D, Bueso-Ramos CE, Newberry KJ, Prijic S, et al. Role of neoplastic monocyte-derived fibrocytes in primary myelofibrosis. J Exp Med 2016;213(9):1723–40.

28. Gianelli U, Vener C, Bossi A, Cortinovis I, Iurlo A, Fracchiolla NS, et al. The European Consensus on grading of bone marrow fibrosis allows a better prognostication of patients with primary myelofibrosis. Mod Pathol Off J U S Can Acad Pathol Inc 2012;25(9):1193–202.

29. Tefferi A. Primary myelofibrosis: 2017 update on diagnosis, risk-stratification, and management. Am J Hematol 2016;91(12):1262–71.

30. Orvain C, Luque Paz D, Dobo I, Cottin L, Le Calvez G, Chauveau A, et al. Circulating Cd34+ cell count differentiates primary myelofibrosis from other Philadelphia-negative myeloproliferative neoplasms: a pragmatic study. Ann Hematol 2016;95(11):1819–23.

31. Barosi G, Viarengo G, Pecci A, Rosti V, Piaggio G, Marchetti M, et al. Diagnostic and clinical relevance of the number of circulating CD34(+) cells in myelofibrosis with myeloid metaplasia. Blood 2001;98(12):3249–55.

32. Passamonti F, Vanelli L, Malabarba L, Rumi E, Pungolino E, Malcovati L, et al. Clinical utility of the absolute number of circulating CD34-positive cells in patients with chronic myeloproliferative disorders. Haematologica 2003;88(10):1123–9.

33. Arora B, Sirhan S, Hoyer JD, Mesa RA, Tefferi A. Peripheral blood CD34 count in myelofibrosis with myeloid metaplasia: a prospective evaluation of prognostic value in 94 patients. Br J Haematol 2005;128(1):42–8.

34. Auerbach S, Puka B, Golla U, Chachoua I. Recent Advances towards the Understanding of Secondary Acute Myeloid Leukemia Progression. Life Basel Switz 2024;14(3):309.

35. Rontauroli S, Carretta C, Parenti S, Bertesi M, Manfredini R. Novel Molecular Insights into Leukemic Evolution of Myeloproliferative Neoplasms: A Single Cell Perspective. Int J Mol Sci 2022;23(23):15256.

36. Milosevic JD, Puda A, Malcovati L, Berg T, Hofbauer M, Stukalov A, et al. Clinical significance of genetic aberrations in secondary acute myeloid leukemia. Am J Hematol 2012;87(11):1010–6.

37. Dunbar AJ, Rampal RK, Levine R. Leukemia secondary to myeloproliferative

neoplasms. Blood 2020;136(1):61–70.

38. Morton LM, Dores GM, Schonfeld SJ, Linet MS, Sigel BS, Lam CJK, et al. Association of Chemotherapy for Solid Tumors With Development of Therapy-Related Myelodysplastic Syndrome or Acute Myeloid Leukemia in the Modern Era. JAMA Oncol 2019;5(3):318–25.

39. Cervantes F, Dupriez B, Pereira A, Passamonti F, Reilly JT, Morra E, et al. New prognostic scoring system for primary myelofibrosis based on a study of the International Working Group for Myelofibrosis Research and Treatment. Blood 2009;113(13):2895–901.

40. Hussein K, Pardanani AD, Van Dyke DL, Hanson CA, Tefferi A. International Prognostic Scoring System-independent cytogenetic risk categorization in primary myelofibrosis. Blood 2010;115(3):496–9.

41. Passamonti F, Cervantes F, Vannucchi AM, Morra E, Rumi E, Pereira A, et al. A dynamic prognostic model to predict survival in primary myelofibrosis: a study by the IWG-MRT (International Working Group for Myeloproliferative Neoplasms Research and Treatment). Blood 2010;115(9):1703–8.

42. Rotunno G, Pacilli A, Artusi V, Rumi E, Maffioli M, Delaini F, et al. Epidemiology and clinical relevance of mutations in postpolycythemia vera and postessential thrombocythemia myelofibrosis: A study on 359 patients of the AGIMM group. Am J Hematol 2016;91(7):681–6.

43. Loscocco GG, Coltro G, Guglielmelli P, Vannucchi AM. Integration of Molecular Information in Risk Assessment of Patients with Myeloproliferative Neoplasms. Cells 2021;10(8):1962.

44. Guglielmelli P, Lasho TL, Rotunno G, Mudireddy M, Mannarelli C, Nicolosi M, et al. MIPSS70: Mutation-Enhanced International Prognostic Score System for Transplantation-Age Patients With Primary Myelofibrosis. J Clin Oncol Off J Am Soc Clin Oncol 2018;36(4):310–8.

45. Passamonti F, Giorgino T, Mora B, Guglielmelli P, Rumi E, Maffioli M, et al. A clinical-molecular prognostic model to predict survival in patients with post polycythemia vera and post essential thrombocythemia myelofibrosis. Leukemia 2017;31(12):2726–31.

46. Tefferi A, Guglielmelli P, Nicolosi M, Mannelli F, Mudireddy M, Bartalucci N, et al. GIPSS: genetically inspired prognostic scoring system for primary myelofibrosis. Leukemia 2018;32(7):1631–42.

47. Gagelmann N, Ditschkowski M, Bogdanov R, Bredin S, Robin M, Cassinat B, et al. Comprehensive clinical-molecular transplant scoring system for myelofibrosis undergoing stem cell transplantation. Blood 2019;133(20):2233–42.

48. Passamonti F. Prognostic factors and models in polycythemia vera, essential thrombocythemia, and primary myelofibrosis. Clin Lymphoma Myeloma Leuk 2011;11 Suppl 1:S25-27.

49. Tefferi A, Guglielmelli P, Lasho TL, Coltro G, Finke CM, Loscocco GG, et al. Mutation-enhanced international prognostic systems for essential thrombocythaemia and polycythaemia vera. Br J Haematol 2020;189(2):291–302.

50. Hong J. Prognostication in myeloproliferative neoplasms, including mutational abnormalities. Blood Res 2023;58(S1):S37–45.

51. Cazzola M. Risk stratifying MDS in the time of precision medicine. Hematol Am Soc Hematol Educ Program 2022;2022(1):375–81.

52. Parenti S, Rontauroli S, Carretta C, Mallia S, Genovese E, Chiereghin C, et al. Mutated clones driving leukemic transformation are already detectable at the single-cell level in CD34-positive cells in the chronic phase of primary myelofibrosis. NPJ Precis Oncol 2021;5(1):4.

53. Calabresi L, Carretta C, Romagnoli S, Rotunno G, Parenti S, Bertesi M, et al. Clonal dynamics and copy number variants by single-cell analysis in leukemic evolution of myeloproliferative neoplasms. Am J Hematol 2023;98(10):1520–31.

54. Nangalia J, Green AR. Myeloproliferative neoplasms: from origins to outcomes. Blood 2017;130(23):2475–83.

55. Ungureanu D, Wu J, Pekkala T, Niranjan Y, Young C, Jensen ON, et al. The pseudokinase domain of JAK2 is a dual-specificity protein kinase that negatively regulates cytokine signaling. Nat Struct Mol Biol 2011;18(9):971–6.

56. Vainchenker W, Kralovics R. Genetic basis and molecular pathophysiology of classical myeloproliferative neoplasms. Blood 2017;129(6):667–79.

57. Vainchenker W, Constantinescu SN. JAK/STAT signaling in hematological malignancies. Oncogene 2013;32(21):2601–13.

58. James C, Ugo V, Le Couédic JP, Staerk J, Delhommeau F, Lacout C, et al. A unique clonal JAK2 mutation leading to constitutive signalling causes polycythaemia vera. Nature 2005;434(7037):1144–8.

59. Kralovics R, Passamonti F, Buser AS, Teo SS, Tiedt R, Passweg JR, et al. A gain-of-function mutation of JAK2 in myeloproliferative disorders. N Engl J Med 2005;352(17):1779–90.

60. Levine RL, Wadleigh M, Cools J, Ebert BL, Wernig G, Huntly BJP, et al. Activating mutation in the tyrosine kinase JAK2 in polycythemia vera, essential thrombocythemia, and myeloid metaplasia with myelofibrosis. Cancer Cell 2005;7(4):387–97.

61. Williams N, Lee J, Mitchell E, Moore L, Baxter EJ, Hewinson J, et al. Life histories of myeloproliferative neoplasms inferred from phylogenies. Nature 2022;602(7895):162–8.

62. Dawson MA, Bannister AJ, Göttgens B, Foster SD, Bartke T, Green AR, et al. JAK2 phosphorylates histone H3Y41 and excludes HP1alpha from chromatin. Nature 2009;461(7265):819–22.

63. Liu F, Zhao X, Perna F, Wang L, Koppikar P, Abdel-Wahab O, et al. JAK2V617F-mediated phosphorylation of PRMT5 downregulates its methyltransferase activity and promotes myeloproliferation. Cancer Cell 2011;19(2):283–94.

64. Tiedt R, Hao-Shen H, Sobas MA, Looser R, Dirnhofer S, Schwaller J, et al. Ratio of mutant JAK2-V617F to wild-type Jak2 determines the MPD phenotypes in transgenic mice. Blood 2008;111(8):3931–40.

65. Mullally A, Lane SW, Ball B, Megerdichian C, Okabe R, Al-Shahrour F, et al. Physiological Jak2V617F Expression Causes a Lethal Myeloproliferative Neoplasm with Differential Effects on Hematopoietic Stem and Progenitor Cells. Cancer Cell 2010;17(6):584–96.

66. Guglielmelli P, Mora B, Gesullo F, Mannelli F, Loscocco GG, Signori L, et al. Clinical impact of mutated JAK2 allele burden reduction in polycythemia vera and essential thrombocythemia. Am J Hematol 2024;99(8):1550–9.

67. Pikman Y, Lee BH, Mercher T, McDowell E, Ebert BL, Gozo M, et al. MPLW515L is a novel somatic activating mutation in myelofibrosis with myeloid metaplasia. PLoS Med 2006;3(7):e270.

68. Pardanani AD, Levine RL, Lasho T, Pikman Y, Mesa RA, Wadleigh M, et al. MPL515 mutations in myeloproliferative and other myeloid disorders: a study of 1182 patients. Blood 2006;108(10):3472–6.

69. Akpınar TS, Hançer VS, Nalçacı M, Diz-Küçükkaya R. MPL W515L/K Mutations in Chronic Myeloproliferative Neoplasms. Turk J Haematol Off J Turk Soc Haematol 2013;30(1):8–12.

70. Michalak M, Groenendyk J, Szabo E, Gold LI, Opas M. Calreticulin, a multi-process calcium-buffering chaperone of the endoplasmic reticulum. Biochem J 2009;417(3):651–66.

71. Chachoua I, Pecquet C, El-Khoury M, Nivarthi H, Albu RI, Marty C, et al. Thrombopoietin receptor activation by myeloproliferative neoplasm associated calreticulin mutants. Blood 2016;127(10):1325–35.

72. Araki M, Yang Y, Masubuchi N, Hironaka Y, Takei H, Morishita S, et al. Activation of the thrombopoietin receptor by mutant calreticulin in CALR-mutant myeloproliferative neoplasms. Blood 2016;127(10):1307–16.

73. Elf S, Abdelfattah NS, Chen E, Perales-Patón J, Rosen EA, Ko A, et al. Mutant Calreticulin Requires Both Its Mutant C-terminus and the Thrombopoietin Receptor for Oncogenic Transformation. Cancer Discov 2016;6(4):368–81.

74. Araki M, Yang Y, Imai M, Mizukami Y, Kihara Y, Sunami Y, et al. Homomultimerization of mutant calreticulin is a prerequisite for MPL binding and activation. Leukemia 2019;33(1):122–31.

75. Rivera JF, Baral AJ, Nadat F, Boyd G, Smyth R, Patel H, et al. Zinc-dependent multimerization of mutant calreticulin is required for MPL binding and MPN

pathogenesis. Blood Adv 2021;5(7):1922–32.

76. Nangalia J, Massie CE, Baxter EJ, Nice FL, Gundem G, Wedge DC, et al. Somatic CALR mutations in myeloproliferative neoplasms with nonmutated JAK2. N Engl J Med 2013;369(25):2391–405.

77. Klampfl T, Gisslinger H, Harutyunyan AS, Nivarthi H, Rumi E, Milosevic JD, et al. Somatic mutations of calreticulin in myeloproliferative neoplasms. N Engl J Med 2013;369(25):2379–90.

78. Pietra D, Rumi E, Ferretti VV, Di Buduo CA, Milanesi C, Cavalloni C, et al. Differential clinical effects of different mutation subtypes in CALR-mutant myeloproliferative neoplasms. Leukemia 2016;30(2):431–8.

79. Marty C, Pecquet C, Nivarthi H, El-Khoury M, Chachoua I, Tulliez M, et al. Calreticulin mutants in mice induce an MPL-dependent thrombocytosis with frequent progression to myelofibrosis. Blood 2016;127(10):1317–24.

80. Jones AV, Chase A, Silver RT, Oscier D, Zoi K, Wang YL, et al. JAK2 haplotype is a major risk factor for the development of myeloproliferative neoplasms. Nat Genet 2009;41(4):446–9.

81. Molina O, Abad MA, Solé F, Menéndez P. Aneuploidy in Cancer: Lessons from Acute Lymphoblastic Leukemia. Trends Cancer 2021;7(1):37–47.

82. Hussein K, Van Dyke DL, Tefferi A. Conventional cytogenetics in myelofibrosis: literature review and discussion. Eur J Haematol 2009;82(5):329–38.

83. Tefferi A, Mesa RA, Schroeder G, Hanson CA, Li CY, Dewald GW. Cytogenetic findings and their clinical relevance in myelofibrosis with myeloid metaplasia. Br J Haematol 2001;113(3):763–71.

84. Klampfl T, Harutyunyan A, Berg T, Gisslinger B, Schalling M, Bagienski K, et al. Genome integrity of myeloproliferative neoplasms in chronic phase and during disease progression. Blood 2011;118(1):167–76.

85. Patnaik MM, Knudson RA, Gangat N, Hanson CA, Pardanani A, Tefferi A, et al. Chromosome 9p24 abnormalities: prevalence, description of novel JAK2 translocations, JAK2V617F mutation analysis and clinicopathologic correlates. Eur J Haematol 2010;84(6):518–24.

86. Hahm C, Huh HJ, Mun YC, Seong CM, Chung WS, Huh J. Genomic aberrations of myeloproliferative and myelodysplastic/myeloproliferative neoplasms in chronic phase and during disease progression. Int J Lab Hematol 2015;37(2):181–9.

87. Pizzi M, Silver RT, Barel A, Orazi A. Recombinant interferon-α in myelofibrosis reduces bone marrow fibrosis, improves its morphology and is associated with clinical response. Mod Pathol Off J U S Can Acad Pathol Inc 2015;28(10):1315–23.

88. Cortelazzo S, Finazzi G, Ruggeri M, Vestri O, Galli M, Rodeghiero F, et al. Hydroxyurea for patients with essential thrombocythemia and a high risk of thrombosis. N Engl J Med 1995;332(17):1132–6.

89. Landolfi R, Marchioli R, Kutti J, Gisslinger H, Tognoni G, Patrono C, et al. Efficacy and safety of low-dose aspirin in polycythemia vera. N Engl J Med 2004;350(2):114–24.

90. Pandey G, Kuykendall AT, Reuther GW. JAK2 inhibitor persistence in MPN: uncovering a central role of ERK activation. Blood Cancer J 2022;12(1):13.

91. Codilupi T, Szybinski J, Arunasalam S, Jungius S, Dunbar AC, Stivala S, et al. Development of Resistance to Type II JAK2 Inhibitors in MPN Depends on AXL Kinase and Is Targetable. Clin Cancer Res Off J Am Assoc Cancer Res 2024;30(3):586–99.

92. Levy G, Mambet C, Pecquet C, Bailly S, Havelange V, Diaconu CC, et al. Targets in MPNs and potential therapeutics. Int Rev Cell Mol Biol 2022;366:41–81.

93. Quintás-Cardama A, Vaddi K, Liu P, Manshouri T, Li J, Scherle PA, et al. Preclinical characterization of the selective JAK1/2 inhibitor INCB018424: therapeutic implications for the treatment of myeloproliferative neoplasms. Blood 2010;115(15):3109–17.

94. Arana Yi C, Tam CS, Verstovsek S. Efficacy and safety of ruxolitinib in the treatment of patients with myelofibrosis. Future Oncol Lond Engl 2015;11(5):719–33.

95. Ortmann CA, Kent DG, Nangalia J, Silber Y, Wedge DC, Grinfeld J, et al. Effect of mutation order on myeloproliferative neoplasms. N Engl J Med 2015;372(7):601–12.

96. Vannucchi AM, Guglielmelli P, Rambaldi A, Bogani C, Barbui T. Epigenetic therapy in myeloproliferative neoplasms: evidence and perspectives. J Cell Mol Med 2009;13(8A):1437–50.

97. Li S, Jin Y, Wu H, Yuan H, Zhao J. Recent advances in targeting protein degradation for tumor immunotherapy. J Hematol OncolJ Hematol Oncol 2025;19(1):5.

98. Chifotides HT, Bose P, Masarova L, Pemmaraju N, Verstovsek S. SOHO State of the Art Updates and Next Questions: Novel Therapies in Development for Myelofibrosis. Clin Lymphoma Myeloma Leuk 2022;22(4):210–23.

99. Dong H, Zhu G, Tamada K, Chen L. B7-H1, a third member of the B7 family, co-stimulates T-cell proliferation and interleukin-10 secretion. Nat Med 1999;5(12):1365–9.

100. Kornepati AVR, Vadlamudi RK, Curiel TJ. Programmed death ligand 1 signals in cancer cells. Nat Rev Cancer 2022;22(3):174–89.

101. Patsoukis N, Wang Q, Strauss L, Boussiotis VA. Revisiting the PD-1 pathway. Sci Adv 2020;6(38):eabd2712.

102. Curiel TJ, Wei S, Dong H, Alvarez X, Cheng P, Mottram P, et al. Blockade of B7-H1 improves myeloid dendritic cell-mediated antitumor immunity. Nat Med 2003;9(5):562–7.

103. Jalali S, Price-Troska T, Bothun C, Villasboas J, Kim HJ, Yang ZZ, et al. Reverse

signaling via PD-L1 supports malignant cell growth and survival in classical Hodgkin lymphoma. Blood Cancer J 2019;9(3):22.

104. Zhang X, Huang X, Xu J, Li E, Lao M, Tang T, et al. NEK2 inhibition triggers anti-pancreatic cancer immunity by targeting PD-L1. Nat Commun 2021;12(1):4536.

105. Kleffel S, Posch C, Barthel SR, Mueller H, Schlapbach C, Guenova E, et al. Melanoma Cell-Intrinsic PD-1 Receptor Functions Promote Tumor Growth. Cell 2015;162(6):1242–56.

106. Gao Y, Nihira NT, Bu X, Chu C, Zhang J, Kolodziejczyk A, et al. Acetylation-dependent regulation of PD-L1 nuclear translocation dictates the efficacy of anti-PD-1 immunotherapy. Nat Cell Biol 2020;22(9):1064–75.

107. Du W, Zhu J, Zeng Y, Liu T, Zhang Y, Cai T, et al. KPNB1-mediated nuclear translocation of PD-L1 promotes non-small cell lung cancer cell proliferation via the Gas6/MerTK signaling pathway. Cell Death Differ 2021;28(4):1284–300.

108. Milosevic Feenstra JD, Jäger R, Schischlik F, Ivanov D, Eisenwort G, Rumi E, et al. PD-L1 overexpression correlates with JAK2-V617F mutational burden and is associated with 9p uniparental disomy in myeloproliferative neoplasms. Am J Hematol 2022;97(4):390–400.

109. Mascarenhas J, Gleitz HFE, Chifotides HT, Harrison CN, Verstovsek S, Vannucchi AM, et al. Biological drivers of clinical phenotype in myelofibrosis. Leukemia 2023;37(2):255–64.

110. Almozyan S, Colak D, Mansour F, Alaiya A, Al-Harazi O, Qattan A, et al. PD-L1 promotes OCT4 and Nanog expression in breast cancer stem cells by sustaining PI3K/AKT pathway activation. Int J Cancer 2017;141(7):1402–12.

111. Prestipino A, Emhardt AJ, Aumann K, O'Sullivan D, Gorantla SP, Duquesne S, et al. Oncogenic JAK2V617F causes PD-L1 expression, mediating immune escape in myeloproliferative neoplasms. Sci Transl Med 2018;10(429):eaam7729.

112. Barbui T, Thiele J, Gisslinger H, Kvasnicka HM, Vannucchi AM, Guglielmelli P, et al. The 2016 WHO classification and diagnostic criteria for myeloproliferative neoplasms: document summary and in-depth discussion. Blood Cancer J 2018;8(2):15.

113. Barosi G, Mesa RA, Thiele J, Cervantes F, Campbell PJ, Verstovsek S, et al. Proposed criteria for the diagnosis of post-polycythemia vera and post-essential thrombocythemia myelofibrosis: a consensus statement from the International Working Group for Myelofibrosis Research and Treatment. Leukemia 2008;22(2):437–8.

114. Carretta C, Mallia S, Genovese E, Parenti S, Rontauroli S, Bianchi E, et al. Genomic Analysis of Hematopoietic Stem Cell at the Single-Cell Level: Optimization of Cell Fixation and Whole Genome Amplification (WGA) Protocol. Int J Mol Sci 2020;21(19):7366.

115. Rontauroli S, Castellano S, Guglielmelli P, Zini R, Bianchi E, Genovese E, et al. Gene expression profile correlates with molecular and clinical features in patients with myelofibrosis. Blood Adv 2021;5(5):1452–62.

116. Parenti S, Rabacchi C, Marino M, Tenedini E, Artuso L, Castellano S, et al. Characterization of New ATM Deletion Associated with Hereditary Breast Cancer. Genes 2021;12(2):136.

117. Salati S, Lisignoli G, Manferdini C, Pennucci V, Zini R, Bianchi E, et al. Co-culture of hematopoietic stem/progenitor cells with human osteblasts favours mono/macrophage differentiation at the expense of the erythroid lineage. PloS One 2013;8(1):e53496.

118. Zini R, Norfo R, Ferrari F, Bianchi E, Salati S, Pennucci V, et al. Valproic acid triggers erythro/megakaryocyte lineage decision through induction of GFI1B and MLLT3 expression. Exp Hematol 2012;40(12):1043-1054.e6.

119. Fantini S, Rontauroli S, Sartini S, Mirabile M, Bianchi E, Badii F, et al. Increased Plasma Levels of lncRNAs LINC01268, GAS5 and MALAT1 Correlate with Negative Prognostic Factors in Myelofibrosis. Cancers 2021;13(19):4744.

120. Bertesi M, Fantini S, Alecci C, Lotti R, Martello A, Parenti S, et al. Promoter Methylation Leads to Decreased ZFP36 Expression and Deregulated NLRP3 Inflammasome Activation in Psoriatic Fibroblasts. Front Med 2020;7:579383.

121. Genovese E, Mirabile M, Rontauroli S, Sartini S, Fantini S, Tavernari L, et al. The Response to Oxidative Damage Correlates with Driver Mutations and Clinical Outcome in Patients with Myelofibrosis. Antioxid Basel Switz 2022;11(1):113.

122. Reilly JT, Wilson G, Barnett D, Watmore A, Potter A. Karyotypic and ras gene mutational analysis in idiopathic myelofibrosis. Br J Haematol 1994;88(3):575–81.

123. Díaz-González Á, Mora E, Avetisyan G, Furió S, De la Puerta R, Gil JV, et al. Cytogenetic Assessment and Risk Stratification in Myelofibrosis with Optical Genome Mapping. Cancers 2023;15(11):3039.

124. Karantanos T, Moliterno AR. The roles of JAK2 in DNA damage and repair in the myeloproliferative neoplasms: Opportunities for targeted therapy. Blood Rev 2018;32(5):426–32.

125. Plo I, Nakatake M, Malivert L, de Villartay JP, Giraudier S, Villeval JL, et al. JAK2 stimulates homologous recombination and genetic instability: potential implication in the heterogeneity of myeloproliferative disorders. Blood 2008;112(4):1402–12.

126. Liao TT, Lin CC, Jiang JK, Yang SH, Teng HW, Yang MH. Harnessing stemness and PD-L1 expression by AT-rich interaction domain-containing protein 3B in colorectal cancer. Theranostics 2020;10(14):6095–112.

127. Świstowska M, Gil-Kulik P, Czop M, Wieczorek K, Macheta A, Petniak A, et al. Comparison of SOX2 and POU5F1 Gene Expression in Leukapheresis-Derived CD34+ Cells before and during Cell Culture. Int J Mol Sci 2023;24(4):4186.

128. Mintz PJ, Huang KW, Reebye V, Nteliopoulos G, Lai HS, Sætrom P, et al. Exploiting human CD34+ stem cell-conditioned medium for tissue repair. Mol Ther J Am Soc Gene Ther 2014;22(1):149–59.

129. Chaurasia P, Gajzer DC, Schaniel C, D'Souza S, Hoffman R. Epigenetic

reprogramming induces the expansion of cord blood stem cells. J Clin Invest 2014;124(6):2378–95.

130. Lemma EY, Letian A, Altorki NK, McGraw TE. Regulation of PD-L1 Trafficking from Synthesis to Degradation. Cancer Immunol Res 2023;11(7):866–74.

131. Li J, Xiao Y, Yu H, Jin X, Fan S, Liu W. Mutual connected IL-6, EGFR and LIN28/Let7-related mechanisms modulate PD-L1 and IGF upregulation in HNSCC using immunotherapy. Front Oncol 2023;13:1140133.